Aircraft Empennage Structural Detail Design

421S9303B2R2
19 April, 1993

AE421/03/Bravo
Lead Engineer: Greg Meholic
Team Members: Ronda Brown
Melissa Hall
Robert Harvey
Michael Singer
Gustavo Tella

Submitted To:
Dr. J.G. Ladesic

Table of Contents

Table of Contents (con't)

List of Figures and Tables

1. Project Summary

1.1 Design Goals

This project involved the detailed design of the aft fuselage and empennage structure, vertical stabilizer, rudder, horizontal stabilizer, and elevator for the Triton primary flight trainer. The main design goals under consideration were to illustrate the integration of the control systems devices used in the tail surfaces and their necessary structural supports as well as the elevator trim, navigational lighting system, electrical systems, tail-located ground tie, and fuselage/cabin interface structure. Accommodations for maintenance, lubrication, adjustment, and repairability were devised. Weight, fabrication, and (sub)assembly goals were addressed. All designs were in accordance with the FAR Part 23 stipulations for a normal category aircraft.

1.2 Statement of Work Requirements

The Statement of Work for the cockpit set forth several design requirements. The structural designs are required to sustain anticipated loading conditions which can occur in normal flight training operations. Easy removal or re-installation of the tail portions from/to the fuselage must be provided by means of interface structures which safely carry the applicable loads defined in FAR Part 23 and the Statement of Work. Adverse effects due to varying environmental conditions must be addressed, including sand or dust, rain, ice or snow, and salt or fog. The aircraft must have a service life of 20 years. The critical design components are required to provide a safe life of 10^7 load cycles and 10,000 operational mission cycles.

Table 1 Summary of Critical Detail Parts

Part No. (Dwg #)	Title	Load(s) (psi)	Load Source	M.S./type (part)	Page No.
1 (02)	Front Spar (HS)	29,511	Cruise Flt	0.017/fatigue	19
2 (02)	Rear Spar (HS)	29,169	Maneuv. Flt	0.028/fatigue	19-20
5 (04)	Front Fuselage Interface (VS)	30,800	Cruise Flt	0.006/fatigue	24
6 (04)	Rear Fuselage Interface (VS)	29,800	Maneuv. Flt	0.039/fatigue	24
1 (06)	Skin Panel E (Tail Cone)	3,564	Torsion	0.075/U buckle	26-27

2. Description of Design

2.1 Horizontal Stabilizer

Both the maneuvering and cruise load cases were used to size this surface. The front spar is located at 6.25" from the leading edge. There are three reasons for this placement: it is near the position of maximum thickness of the airfoil, it divides the skin panels into approximately equal sizes, and it is near the location of the cruise loading. The thickness of the front spar is 0.072" of which 0.04" is a doubler that spans to the 37.0" butt line. The width of the flanges is 0.9". To meet fatigue requirements, two L-shaped triplers which fit inside the C-channel with thicknesses of 0.04" and 0.8" legs are included up to the 22.0" butt line along the half-span (Refer to Formal Drawing 421S9303B202). The rear spar is located at the trailing edge (15.5" with respect to the leading edge) of the horizontal stabilizer, as is customary. The rear spar has characteristics identical to the front spar except that the L-shaped triplers are only 0.032" thick. Five ribs are situated along the half-span at intervals of 15.0" with the first spar located at 7.0" from the centerline of the aircraft. All ribs as well as the skin have a thickness of 0.02". There are three hinges on which the elevator rotates. These are located at (with respect to the center line of the empennage) the 5.0", 36.0", and 67.0" butt lines (See Figure 01 for a detail view of a hinge). The fuselage interface structures are C-channels which are riveted to the

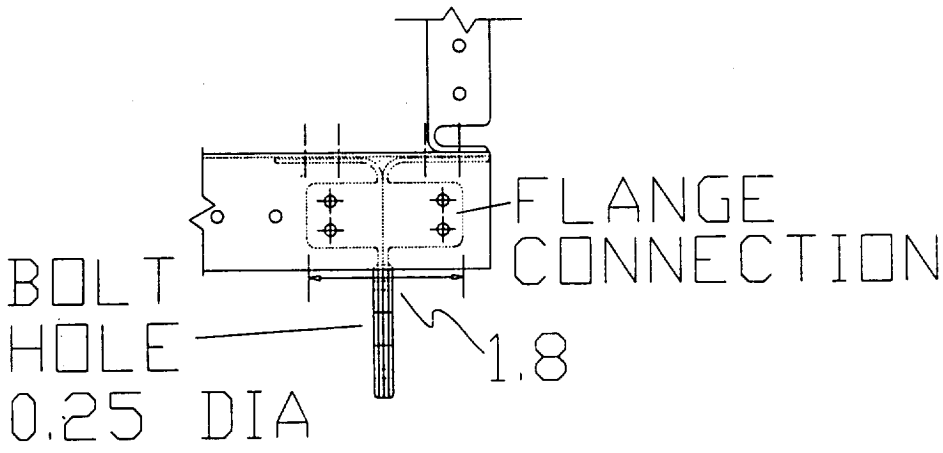

Figure 01 Horizontal Stabilizer Hinge Detail

inside of either spar and bolted to a former inside the aft fuselage (See Figure 02). The front interface channel has a height of 2.536", flange width of 1.00", and thickness of 0.082". The rear interface channel has the same properties as the front interface with the exception that the height is 2.046". Both interface structures are joined to a former in the aft empennage by eight 0.25" bolts, four in the flanges and four in the web.

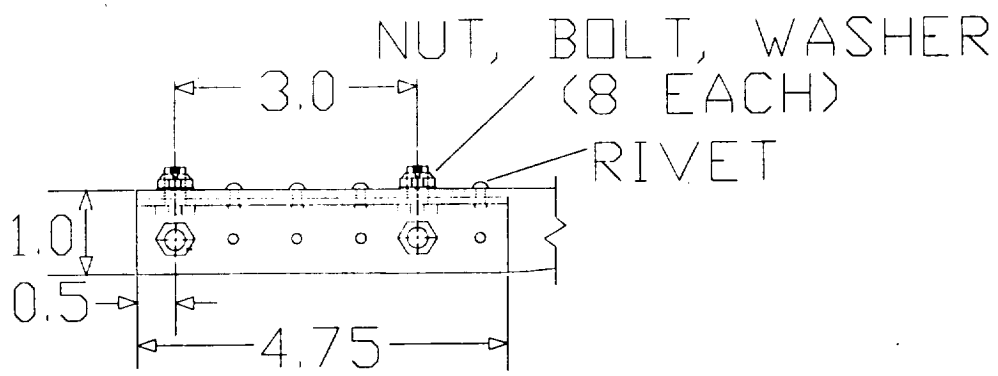

Figure 02 Horizontal Stabilizer Front Interface Bracket Detail

2.2 Elevator

The maneuvering load distribution was used to size the elevator. The front spar is located at the leading edge of the elevator as is historically done for attachment of the hinges. The C-channel front spar has a thickness of 0.02" with a flange width of 0.5". The rear spar is positioned 7.0" behind the front spar and serves to prevent buckling of the skin panels. It has the same thickness and flange width as the front spar. The elevator has three ribs behind the front spar on each half span: one at both the root and tip and the third in the middle (Refer to Formal Drawing 421S9303B203). The are four additional ribs in the leading edge portion of the elevator, two at each position previously stated surround the hinges whose locations are described in Section 2.1 (See Figure 03 on the next page). The thickness of the ribs and skin is 0.02" thick.

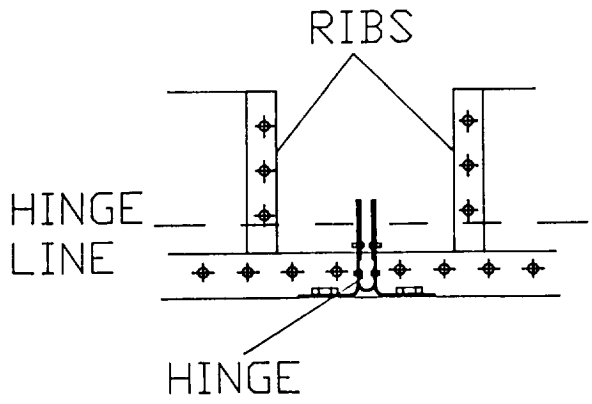

Figure 03 Elevator Leading Edge Rib Detail

2.3 Vertical Stabilizer

The design criterion for this surface was the cruise loading case. The C-channel front spar of the vertical stabilizer is positioned just behind the quarter chord at the root and angles forward until it is directly in front of the quarter chord at the tip. It has a thickness of 0.05" and a flange width of 0.7". Two L-shaped doublers are placed opposite the flanges for a length of 23.0" in order to meet fatigue requirements. These doublers have legs which are 0.5" long and 0.032" thick (Refer to Formal Drawing 421S9303B204). The rear spar is located in the standard position at the trailing edge of the stabilizer. It has characteristics which are identical to the front spar with the exception that it does not require doublers. Stringers are located between the front and rear spars to prevent buckling of the skin; this stringer extends 34.0" from the root of the stabilizer. There are four ribs: one at the root chord, one at the tip chord, and the other two at 8.0" and 28.0" from the root. Due to the sweep of the vertical stabilizer, each rib runs in two directions (See Figure 04 on next page). The ribs ahead of the front spar are perpendicular to

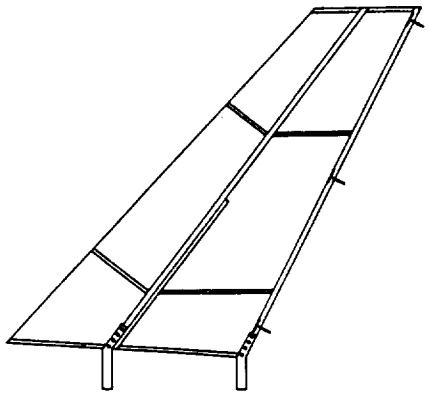

Figure 04 Vertical Stabilizer Rib Diagram

the spar. Both the ribs and the skin are 0.02" in thickness. There are three hinges about which the rudder rotates; these are located at the root and tip chord and at 24.0" from the stabilizer root chord. The fuselage interface structures are C-channels which attach to the either the front or rear spar by means of rivets. Eight 0.3125" bolts attach each interface structure to formers inside the aft empennage. The front interface extends 5.0" into the fuselage, is 4.1" wide and has a flange width of 1.50". The flange widths of the spars are gradually increased to meet those of the interface pieces (See Figure 05). The rear interface piece is identical to the front with the exception that it has a thinner width of 2.7". There are two navigational lights at the top of the stabilizer. The lightening holes provide space to run the electrical systems for these lights.

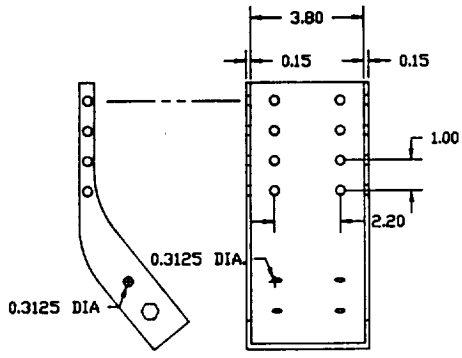

Figure 05 Vertical Stabilizer Front Interface Bracket Detail

2.4 Rudder

The maneuvering case was used to size this control surface. The front spar of the rudder is located at the leading edge of the rudder for attachment of the hinges. Both the front and rear spars are C-channels with a thickness of 0.02" and flange width of 0.5". The rear spar is located 7.0" behind the front spar and facilitates the prevention of buckling in the skin panels (Refer to Formal Drawing 421S9303B205). Because the rudder extends below the vertical stabilizer, its rib positions are different. There is a rib at the bottom of the rudder to provide a partially closed cavity. The other three ribs are at the hinge locations; the ribs in the leading edge portion are configured similarly to those described in the Section 2.2. The thickness of the ribs and skin is 0.02".

2.5 Tail Cone

The empennage is designed to transmit the loads and moments imposed by the control surfaces into the fuselage structure. The structure is a slightly elliptical cone constructed of stringers and formers and wrapped in a 0.025" aluminum skin. All of the torsional loads are absorbed by the skin; while the bending loads are transmitted through four stringers each at 45° to the aircraft's longitudinal axis (See Figure 06). Stringer buckling is prevented by internal

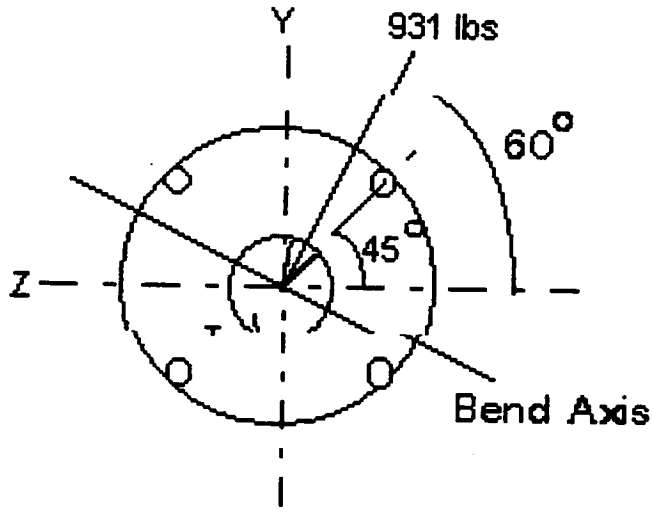

Figure 06 Empennage Stringer Diagram

formers spaces every 20 inches. The formers at the control surface interface locations are modified since they are the first components inside the empennage to receive the loads. These formers are designed to transmit the control surface loads through rivet shear from attachment brackets riveted to the former and bolted to the interface structures (See Figure 07). Except for the interface brackets, each component of the structure is made from 0.025" sheet and assembled with rivets.

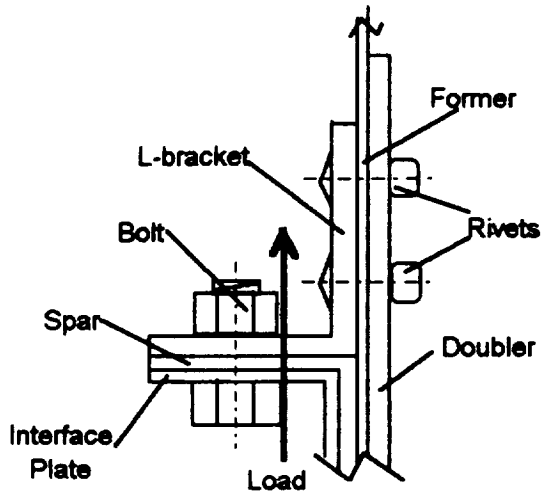

Figure 07 Interface Former Diagram

3. Loads and Loading

3.1 Horizontal Stabilizer

Bending in the horizontal stabilizer is carried by the spars. The bending induced during cruise mainly affects the flanges in the C-channel, front spar due to the cruise load's peaked distribution near the leading edge. The rear spar caps carry the majority of the bending caused by the maneuvering load distribution which peaks at the leading edge of the elevator. The skin carries the shear flow and is sized by the maneuvering shear force because of its greater moment arm with respect to the spars. The largest loads are carried by the front and rear spars at the root of the stabilizer. These loads are 29,508 psi and 29,169 psi of bending stress induced during cruise flight on the front and rear spars, respectively.

3.2 Elevator

The leading edge front spar of the elevator carries bending. Due to the locations of the resultant loads, only a small amount of torsion exists in the structure. The rear spar is auxiliary and serves only the purpose of preventing the skin panels from buckling. The loads are small enough that only a unit cell analysis was necessary to size the skin thickness.

3.3 Calculations on the Horizontal Stabilizer and Elevator

Loading On The Horizontal Tail Surfaces Due to Maneuvering

w is the load according to FAR Part 23 App. A, Figure A5 and Table 2 Figure (A) *See Appendix 2*
c is the mean aerodynamic chord of the horizontal stabilizer and elevator

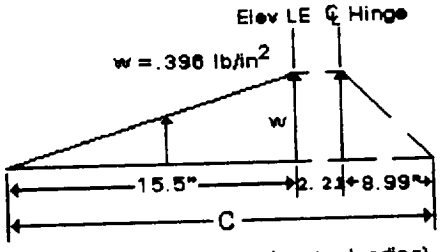

Chordwise Maneuvering Load Distribution (Case A) Per FAR Part 23 Appendix A

Note
The only portion of the elevator loading which will be used in this section is that which determines the hinge loads on the horizontal stabilizer.

Loading On the Horizontal Stabilizer Due to Elevator Deflection

mac_{hs} is the mean aerodynamic chord of the horizontal stabilizer
w_{hs} is the chordwise load on the horizontal stabilizer per FAR Appendix A
F_r is the resultant force of the chordwise triangular distributed load shown below

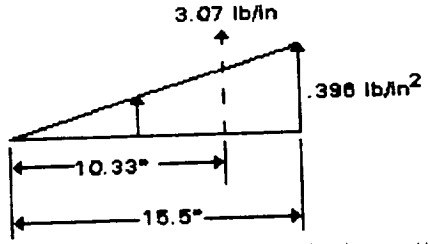

Chordwise Maneuvering Load Distribution on H. Stabilizer

$w_{hs} := .396 \cdot lb \cdot in^{-1}$ $mac_{hs} := 15.5 \cdot in$

$F_r := 0.5 \cdot mac_{hs} \cdot w_{hs}$ $F_r = 3.07 \cdot lb \cdot in^{-1}$

The resultant force, F_r, is shown in phanton.

When this resultant force is applied spanwise across the horizontal stabilizer, it can be represented by the following free body diagram.

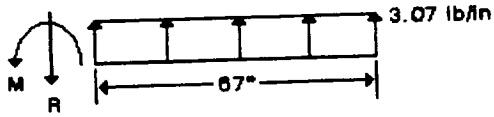

Free Body Diagram of Spanwise Maneuvering Load

Loading On the Elevator Due to Deflection

w_e is the chordwise load on the elevator per FAR Part 23 Appendix A

d_{hl} is the distance from the leading edge of the elevator to its hinge line

d_a is the distance from the hinge line to the trailing edge of the elevator

F_r is the resultant force of the distributed load

x is the position of the resultant force with respect to the leading edge of the elevator

The chordwise loading at the root chord is shown in the following free body diagram.

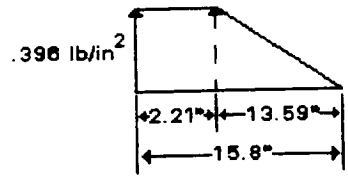

Chordwise Maneuvering Load On Elevator At Root

The resultant of the chordwise force at the root is:

$w_e := .396 \cdot lb \cdot in^{-2}$ $d_{hl} := 2.21 \cdot in$ $d_a := 13.59 \cdot in$

$F_r := w_e \cdot d_{hl} + 0.5 \cdot w_e \cdot d_a$ (Equation 1)

$F_r := 3.57 \cdot lb \cdot in^{-1}$

The position of this resultant force is located:

$$x := \frac{w_e \cdot \frac{d_{hl}^2}{2} + 0.5 \cdot w_e \cdot d_a \cdot \left(\frac{d_a}{3} + d_{hl}\right)}{F_r} \qquad x := 5.36 \cdot in \quad \text{(Equation 2)}$$

The same analysis was used at the mean aerodynamic chord and tip chord. The results of the calculations are: From Equations 1 and 2 above,

M.A.C. : $F_r := 2.66 \cdot lb \cdot in^{-1}$ $x := 3.85 \cdot in$ *Tip Chord* : $F_r := 1.31 \cdot lb \cdot in^{-1}$ $x := 1.71 \cdot in$

Therefore, the spanwise load distribution on the elevator can be shown by the following free body diagram. The resultant force is shown in phantom.

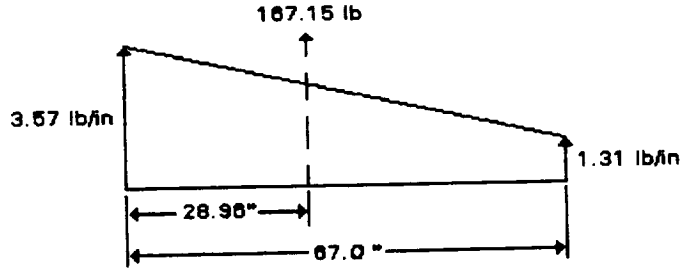

Spanwise Maneuvering Load On The Elevator

The Reactions on the Horizontal Stabilizer Due to the Hinges

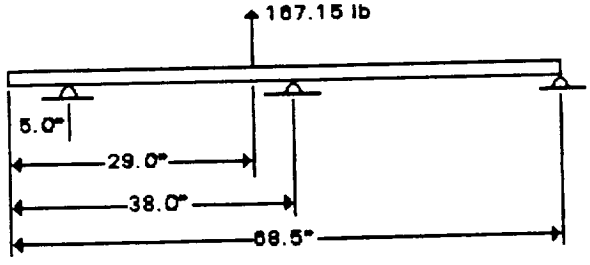

Diagram of Elevator Hinge Placements

The above sketch can be represented by the following free body diagram.
The middle hinge can be removed to simplify the initial analysis and later replaced.

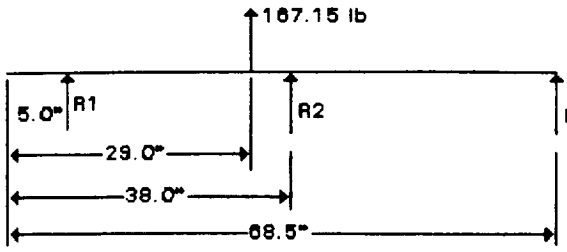

Therefore, the hinge reactions are:

$$\Sigma F_y = R_1 + R_3 + 167.15\cdot lb = 0$$

$$\Sigma M_A = 167.15\cdot lb\cdot 22.5\cdot in + R_3\cdot 68.5\cdot in = 0$$

$$R_3 = -54.9\cdot lb$$

$$R_1 = -112.5\cdot lb$$

Free Body Diagram of the Elevator With Unknown Hinge Point Loads

After replacing the middle hinge, the reactions due to the three hinges can be estimated as:

$R_1 = -56.13\cdot lb$ $\quad R_2 = -83.58\cdot lb$ $\quad R_3 = -27.45\cdot lb$

By combining the original load distribution on the horizontal stabilizer due to elevator deflection with the point loads due to the hinge reactions, the final load distribution can be determined. The following free body diagram represents this load distribution.

Using static equilibrium, the reaction forces can be calculated.

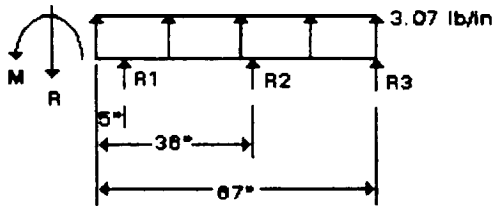

$$\Sigma F_y : R = 372.85\cdot lb$$

$$\Sigma M : M = -12019.3\cdot lb\cdot in$$

Free Body Diagram of the Stabilizer With Hinge Point Loads

Now the equations of the shear and bending moment diagrams can be determined. ***The following method will be used in determining all subsequenct shear and bending moment diagrams. However, the mechanics of this method will not be presented again.***

The first cut is made from $0 < x < 5$ inches

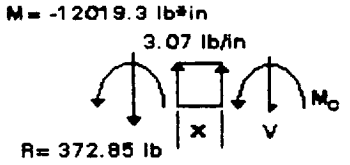

$$\Sigma F_y : V = 3.07\cdot lb\cdot in^{-1}\cdot x - 372.85\cdot lb$$

$$\Sigma M_c : M_c = 1.535\cdot lb\cdot in^{-1}\cdot x^2 - 372.85\cdot lb\cdot x + 12019.3\cdot lb\cdot in$$

First Cut of the Stabilizer Free Body Diagram

The second cut is made from $5 < x < 36$ inches

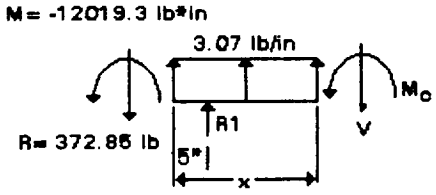

$$\Sigma F_y : V = 3.07\cdot lb\cdot in^{-1}\cdot x - 316.72\cdot lb$$

$$\Sigma M_c : M_c = 1.535\cdot lb\cdot in^{-1}\cdot x^2 - 316.72\cdot lb\cdot x + 12019.3\cdot lb\cdot in$$

Second Cut of the Stabilizer Free Body Diagram

The third cut is made from $36 < x < 67$ inches

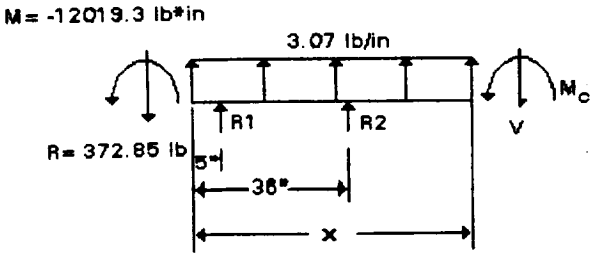

Third Cut of the Stabilizer Free Body Diagram

$$\Sigma F_y : V = 3.07 \cdot lb \cdot in^{-1} \cdot x - 233.14 \cdot lb$$

$$\Sigma M_c : M_c = \left(1.535 \cdot lb \cdot in^{-1} \cdot x^2 - 233.14 \cdot lb \cdot x\right) + 8449.05 \cdot lb \cdot in$$

The shear and bending moment diagrams appear as follows:

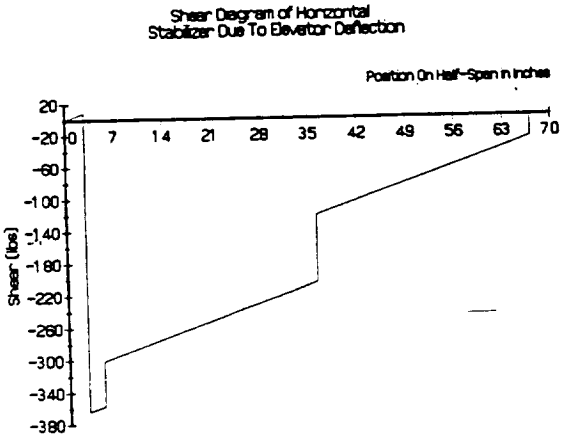

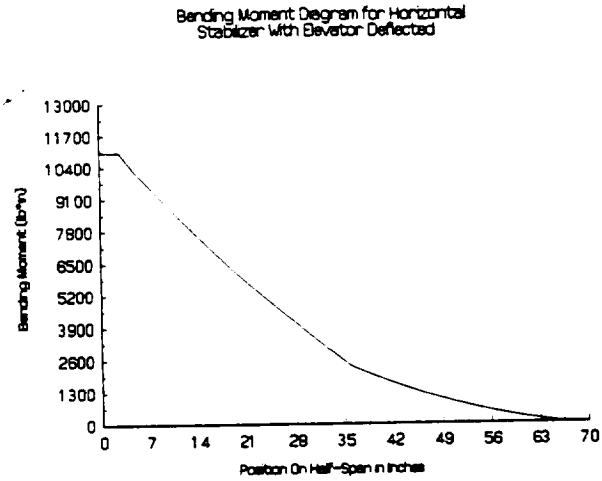

Loading at Level Cruise

w is the aerodynamic load at cruise condition from FAR Appendix A, Figure 5A *See Appendix 2*

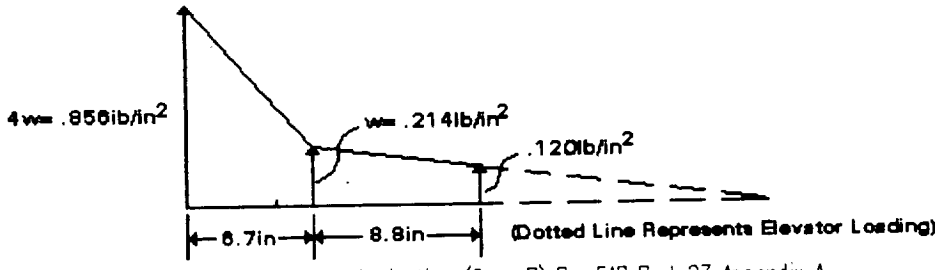

Chordwise Cruise Load Distribution (Case B) Per FAR Part 23 Appendix A

The resultant force, F_r, of the chordwise cruise load on the horizontal stabilizer can be represented by the sketch on the left. When this resultant force is applied spanwise across the horizontal stabilizer it can be represented by the free body diagram on the right.

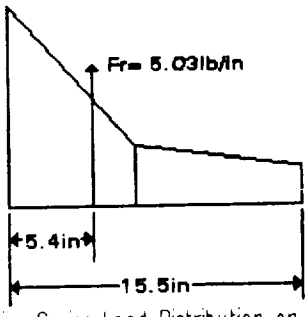

Chordwise Cruise Load Distribution on H. Stabilizer

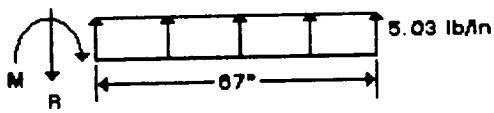

Free Body Diagram of Spanwise Cruise Load

Elevator Hinge Loads Acting on Horizontal Stabilizer at Cruise

From the aerodynamic loading given in FAR part 23 Appendix A, the chordwise load distributions on the elevator are shown in the sketches below on the left. The spanwise load distribution on the elevator is shown by the free body diagram on the right. The resultant force is shown in phantom.

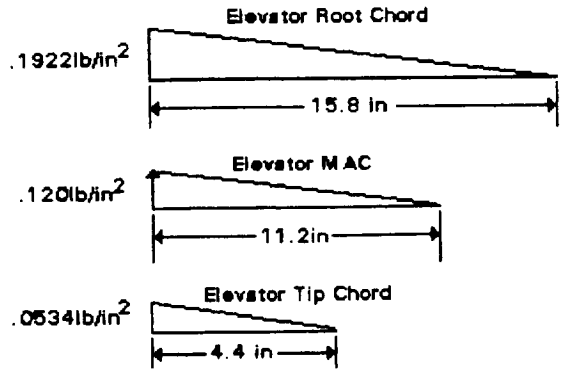

Chordwise Cruise Load on Elevator At Root, MAC, & Tip

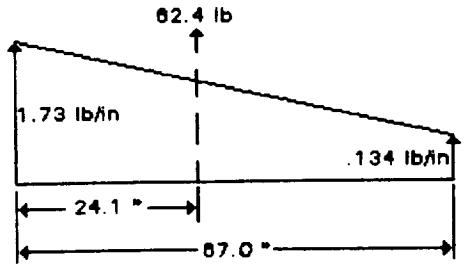

Spanwise Cruise Load On The Elevator

The hinge loads were determined using the same analysis shown for the maneuvering load distribution. The hinge loads were determined to be the following:

$R_1 = 24.5 \cdot lb$ $R_2 = 30.84 \cdot lb$ $R_3 = 7.16 \cdot lb$

By combining the original load distribution on the horizontal stabilizer during cruise with the point loads due to the hinge reactions, the final load distribution can be determined. The following free body diagram represents this load distribution.

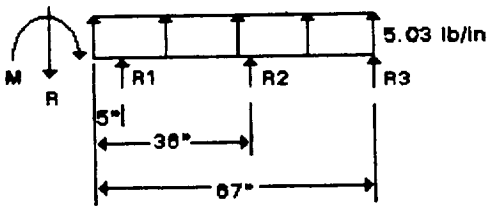

Free Body Diagram of the Stabilizer With Hinge Point Loads

Using static equilibrium, the reaction forces can be calculated:

$\Sigma F_y: \quad R = 400.0 \cdot lb$

$\Sigma M_c: \quad M = 13002 \cdot lb \cdot in$

The shear and bending moment diagrams appear as follows:

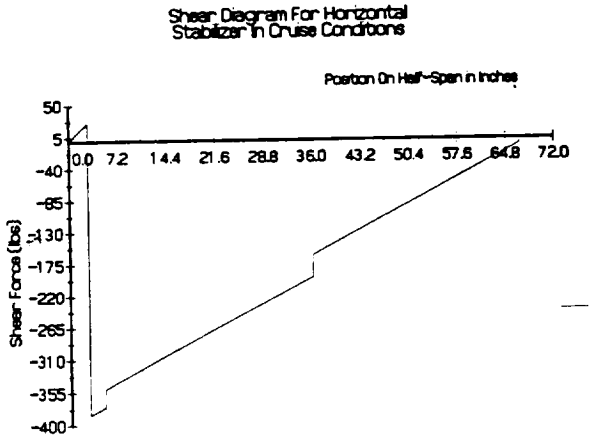

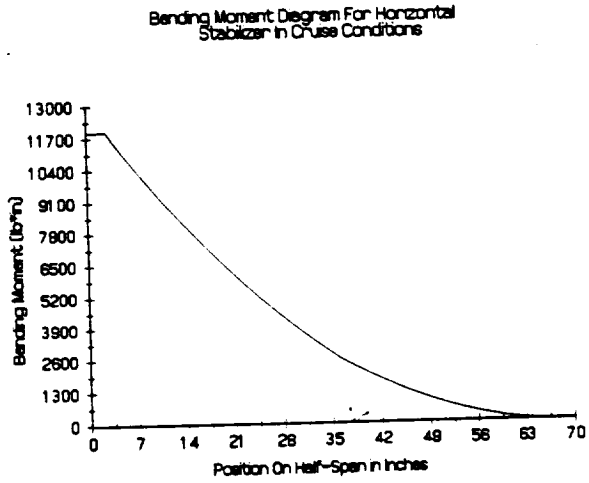

Loading Due to Snow

The statement of work requires that the horizontal stabilizer be able to withstand 8.0 inches of wet snow. The following is a determination of the loading that occurs due to this accumulation of snow.

ρ_s is the weight density of wet snow

d_s is the depth of the accumulated snow

A_{hs} is the area of half of the horizontal stabilizer (not including the elevator)

W_s is the weight of the snow

d_{ls} is the distributed loading due to the snow

s is the half span of the horizontal stabilizer including the fairing

Therefore, the distributed loading appears as the following sketch:

$\rho_s := 12 \cdot lb \cdot ft^{-3}$ $A_{hs} := 7.34 \cdot ft^2$ $d_s := .667 \cdot ft$

$W_s := A_{hs} \cdot d_s \cdot \rho_s$ $W_s = 58.72 \cdot lb$ $s := 73.5 \cdot in$

$$d_{ls} := \frac{W_s}{s} \qquad d_{ls} = .799 \cdot lb \cdot in^{-1}$$

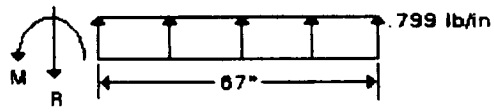

Free Body Diagram of the Spanwise Snow Load Distribution

Using the equations of static equilibrium, the reaction loads can be calculated.

$\Sigma F_y: \quad R = 53.53 \cdot lb$ $\qquad \Sigma M: \quad M = -1793.4 \cdot lb \cdot in$

Because this was not a critical design case, the shear and moment diagrams will not be shown.

3.4 Vertical Stabilizer

Bending in the vertical stabilizer is carried principally by the front spar. The cruise loading condition was used to size both the front and rear spars of the vertical stabilizer. The skin carries the shear flow. The largest loads produced by the vertical stabilizer will be carried by the fuselage interface structures which are attached to the spars. These loads are 30,800 psi and 29,800 psi on the front and rear interface brackets, respectively.

3.5 Rudder

The leading edge front spar of the rudder was designed to carry bending induced during maneuvers. The rear spar facilitates the prevention of buckling in the skin panels but is otherwise auxiliary. As with the elevator, only a unit cell analysis was required to size the skin thickness.

3.6 CALCULATIONS ON VERTICAL STABILIZER AND RUDDER

Loading on Stabilizer Due to Rudder Deflection (Case A in FAR Part 23 Appendix A)

mac_{vs} is the mean aerodynamic chord of the vertical stabilizer (minus the rudder)
w_{vs} is the chordwise load on the vertical stabilizer per FAR Appendix A
F_r is the resultant force of the triangular distributed load shown below on the left

mac_{vs} = 3.33 ft w_{vs} = 51.18 lb/ft²
$F_r = 0.5 mac_{vs} w_{vs}$ = 56.55 lb/ft

The chordwise distribution as well as the magnitude and location of F_r are shown in the sketch on the left.
When this resultant force is applied spanwise across the vertical stabilizer, it can be represented by the diagram to the right.

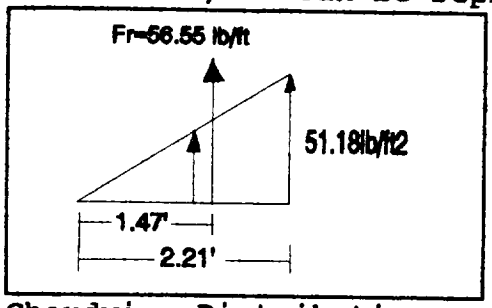

Chordwise Distribution

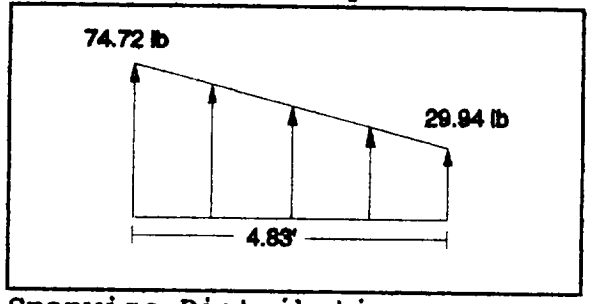

Spanwise Distribution

Loading on Rudder Due to Deflection

*Note: the rudder is hinged at the leading edge
c_r is the rudder chord at the mac of the vertical stabilizer
w_r is the chordwise load on the rudder per FAR Appendix A
F_r is the resultant force of the distributed load

c_r = 1.12 ft w_r = 51.18 lb/ft²
$F_r = 0.5 c_r w_r$ = 28.66 lb/ft

The chordwise distribution as well as the magnitude and location of F_r are shown in the sketch on the left.
When this resultant force is applied spanwise across the vertical stabilizer, it can be represented by the diagram to the right.

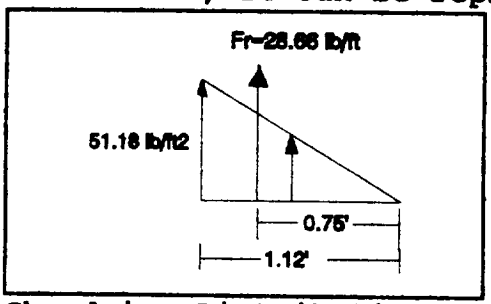

Chordwise Distribution

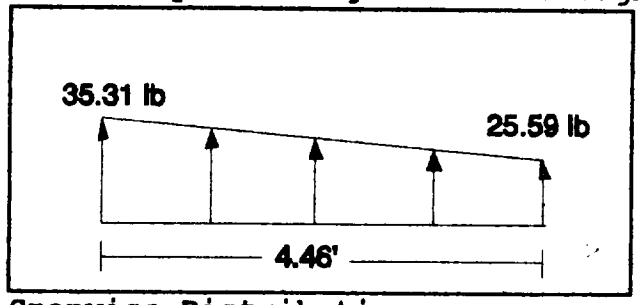

Spanwise Distribution

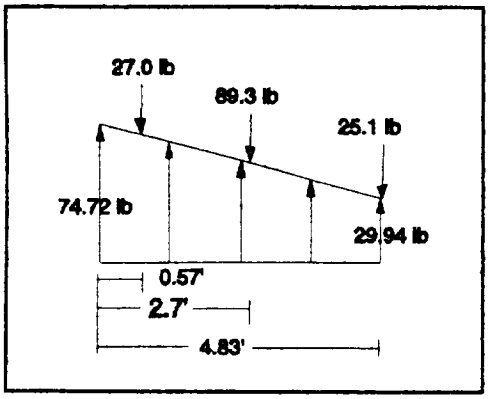

The loading on rudder is transferred to the stabilizer through the three hinges. Therefore, the loads from the rudder are resolved into three point loads and added to the loading on the stabilizer.

From this distribution, the shear and moment diagrams for the vertical stabilizer due to deflection of the rudder can be drawn.

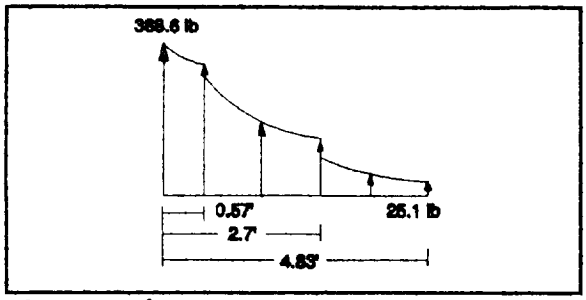

Shear Diagram

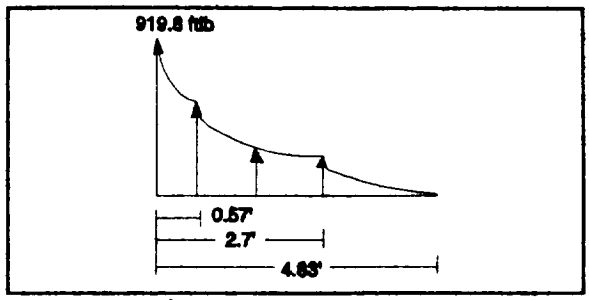

Moment Diagram

The shear and moment diagrams for the rudder are shown below.

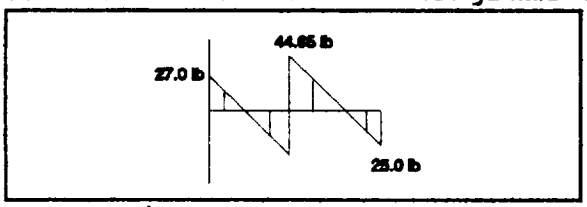

Shear Diagram

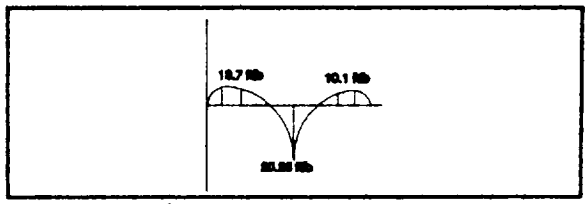

Moment Diagram

Unsymmetrical Loading on Stabilizer (Case B in FAR Part 23 Appendix A)

mac_{vs} as defined previously (minus the rudder)
w_{vs} as defined previously
x is the quarter chord distance (if rudder is included)
c_r as defined previously
y_r is the chordwise load at the leading edge of the rudder
F_r is the resultant force of the distributed load

$F_r = 0.5(3w_{vs})(x) + w_{vs}(x) + 0.5(w_{vs})(mac_{vs}-x) - 0.5(c_r)(y_r)$
$F_r = 78.77$ lb/ft

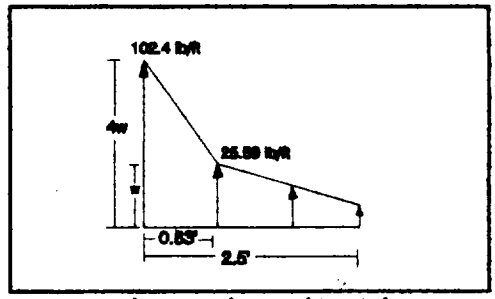

Chordwise Distribution

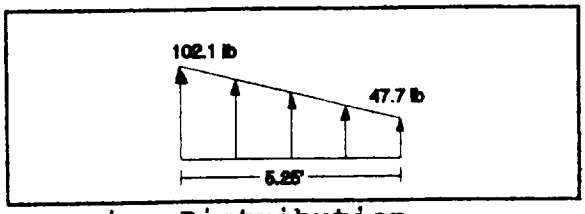

Spanwise Distribution

When the resultant force is applied spanwise across the stabilizer, it can be represented by the diagram to the left.

Unsymmetrical Loading on Rudder

c_r as defined previously
y_r is the chordwise load at the leading edge of the rudder
F_r is the resultant force of the distributed load

$c_r = 1.12$ ft $\qquad y_r = 11.5$ lb/ft^2
$F_r = 0.5 c_r y_r = 6.44$ lb/ft

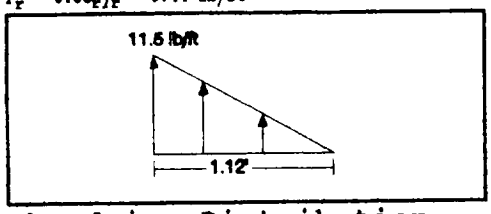

Chordwise Distribution

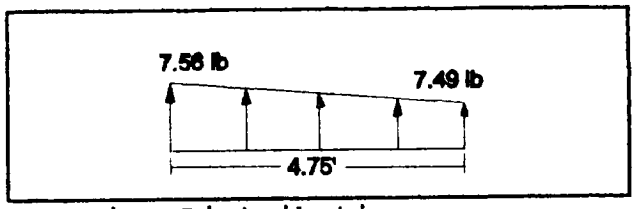

Spanwise Distribution

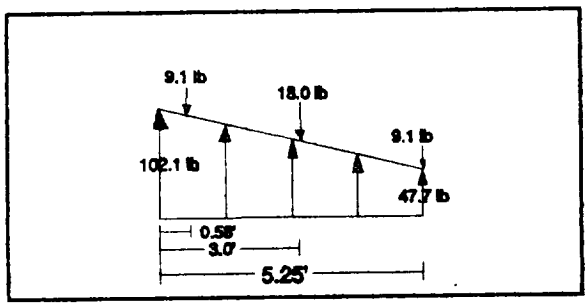

As shown in the previous analysis, the loading on the rudder is transferred to the stabilizer through the three hinges. The loads on the rudder are resolved into three point loads and added to the loading on the stabilizer as shown.

From this distribution, the shear and moment diagrams for the stabilizer in the unsymmetrical loading case can be drawn.

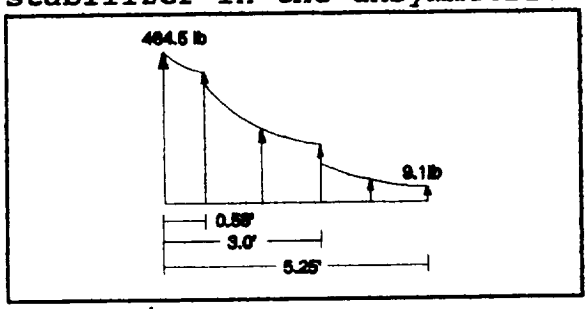

Shear Diagram

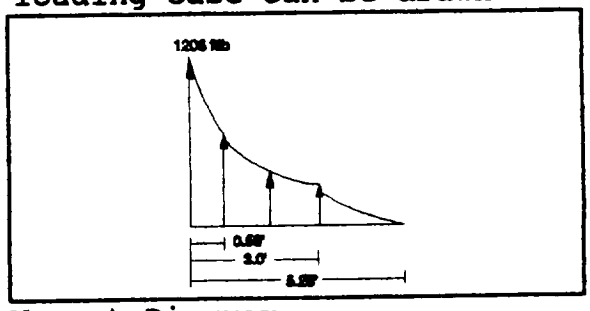

Moment Diagram

Analysis shows that the critical case for stabilizer design is Case B while the critical case for rudder design is Case A.

3.7 Tail Cone

The loads transmitted into the aft fuselage section of the aircraft (tail cone) are generated by the control surfaces, the tie down force, and snow blanketing. The worst case loads from the control surfaces were the highest of the three conditions and were used for the structural design of the empennage.

These loads satisfied the FAR23 required limit loads for the surfaces. Design of the empennage accounted for the torsion developed by both rudder deflection and unsymmetrical lift on the horizontal stabilizer resulting from maneuvering flight conditions. The bending and shear stresses were calculated using the resultant force created from both the stabilizer and fin. This resultant was treated as a point load at STA 269 at 60° to the horizontal. STA 269 was chosen as a mean distance between the fin and stabilizer loads. The loading conditions are shown below.

3.8 Calculations on the Tail Cone

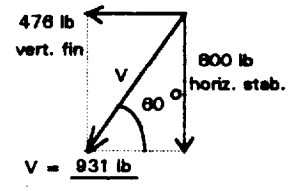

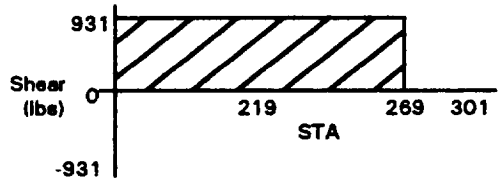

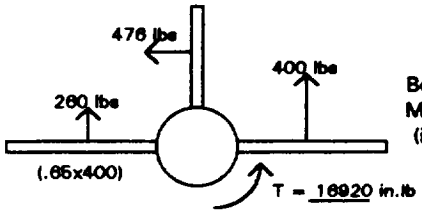

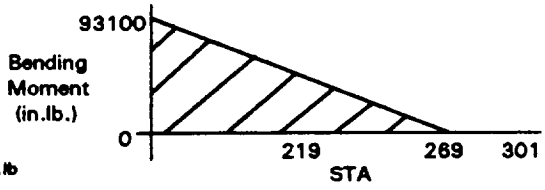

Snow Load

The snow load was determined through geometrical analysis of the empennage and the surfaces:

Volume of empennage top surface area + Volume of horiz. stabilizer area:

$$(8 \text{ in snow})\,[0.5\,(23 \text{ in} + 9 \text{ in})\,(132 \text{ in}) + (3600 \text{ in}^2)] = 45696 \text{ in}^3 = 26.44 \text{ ft}^3$$

Density of wet snow = 12 lbs/ft^3, so:

$$(26.44 \text{ ft}^3)\,(12 \text{ lbs/ft}^3) = 317.33 \text{ lbs snow}$$

The tie down force was determined by calculating the lift on the horizontal tail per the conditions in the statement of work. The standard lift equation was used in conjunction with the 3-D lift curve slope equation as shown below:

$$L = \left[\frac{a_o}{1 + \frac{57.3 a_o r}{\pi AR}}\right] \alpha \tfrac{1}{2} \rho V^2 S \quad = \quad 755 \text{ lbs}$$

Where: a_0 = 0.11 per ° (2-D lift curve slope of NACA 0009)
r = 0.85 (from Perkins and Hage for the horiz. stabilizer)
α = 10° (angle of attack at +10° tie down angle)
ρ = density at sea level
V = 176 fps (gust velocity equal to 120 mph)
S = 25 ft^2 (horizontal tail area)

In short, the skin was designed to absorb torsion while the stringers and formers were sized to transmit bending. Fatigue analysis is analyzed throughout the structural substantiation section for cyclically loaded components.

4. Structural Substantiation

4.1 Sizing the Horizontal Stabilizer

Sizing the Front and Rear Spars of the Horizontal Stabilizer

Note: The material chosen for all structures in the horizontal stabilizer was 2024-T3 aluminum. This material has a axial yield strength of 42 ksi, ultimate shear strength of 39 ksi, and a bearing yield strength of 88 ksi. The values were taken from MIL-HDBK-5E (See Appendix 3).

Front Spar: The front spar was placed at 6.25 inches from the leading edge of the stabilizer. This was done for three reasons: it is near the location of the cruise loading at 7.0 inches as well as the maximum thickness of the airfoil and separates the skin into evenly sized panels. From the Theory of Wing Sections, the height of the front spar along the span is known (See Appendix 4).

The front spar was sized at 5.0 inches from the centerline of the airplane, the initial position of the first rib. This rib was later moved to 7.0" inches due to an error in estimating the width of the fairing. The lever rule was used to determine the portion of the moments carried by the spar due to each type of loading, cruise and maneuvering. The moment produced during cruise is carried mainly (91.9%) by the front spar. The torsional stresses caused by the cruise and maneuvering loads were negligible when compared to the magnitude of the bending stress produced during cruise. Therefore, this cruise moment is the design criterion.

$h := 2.68 \cdot in \quad A := 0.90 \cdot t \cdot in \quad d := 1.34 \cdot in$

$I_1 := \frac{1}{12} \cdot t \cdot h^3 + 2 \cdot A \cdot d^2 \quad I_1 = 5.13 \cdot t \cdot in^3$

$M := 11063 \cdot lb \cdot in \quad c := 1.34 \cdot in \quad \sigma_y := 42000 \cdot lb \cdot in^{-2}$

$\sigma_y := \frac{.919 \cdot M \cdot c}{I_1} \quad t = .0632 \cdot in$

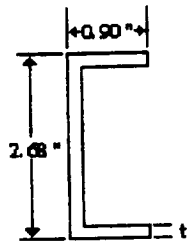

Initial Design of the Front Spar

Therefore, a 0.032" sheet was chosen with a 0.04" doubler. After performing this same analysis at several points down the span, it was determined that the doubler could be removed at 37.0 inches outboard on the span.

Fatigue Analysis: In order to meet the design specification of 10^7 cycles, the maximum loading could not exceed a thirty thousand psi limit load at a mean stress of ten thousand psi (See Appendix 5). Therefore, the added moment of inertia needed to produce these results was determined.

$\sigma_f := 30000 \cdot lb \cdot in^{-2} \quad \sigma_f := \frac{.919 \cdot M \cdot c}{I_2} \quad I_2 := .4541 \cdot in^4$

$I_{add} := I_2 - I_1 \quad I_{add} = .1358 \cdot in^4 \quad MS_{fatigue} = 0.017$

To increase the moment of inertia, two L- shaped pieces were added to the center of the C channel as shown. These produce a moment of inertia of .1434 in^4. Similar fatigue analyses were performed along the span to determine where the additions could be removed. It was determined that they were only necessary up to 22.0 inches along the span.

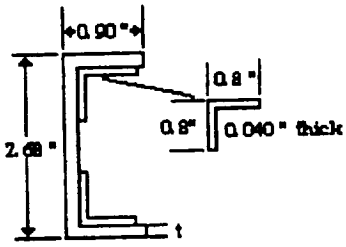

Front Spar After Fatigue Analysis

Rear Spar: The rear spar was analyzed in an indentical manner. The design criterion for this spar was the maneuvering moment of which 69.7% is carried by the rear spar.

$h := 2.19 \cdot in \quad A := 0.90 \cdot t \cdot in \quad d := 1.095 \cdot in \quad I_3 := 3.04 \cdot t \cdot in^3$

$M := 10193 \cdot lb \cdot in \quad c := 1.095 \cdot in \quad \sigma_y := \frac{.697 \cdot M \cdot c}{I} \quad t := .0609 \cdot in$

Therefore, with a thickness of 0.0609 inches, a sheet of 0.032 inches and doubler of 0.040 inches were chosen as with the front spar. Again, this doubler ends at 37.0 inches outboard along the spar.

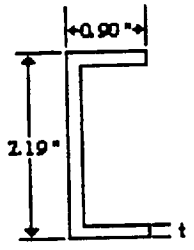

Initial Design of the Rear Spar

Fatigue Analysis:

$\sigma_f = \frac{.697 \cdot M \cdot c}{I_4}$ $I_4 = .2593 \cdot in^4$ $I_{add} = I_4 - I_3$

$I_{add} = .0626$ $MS_{fatigue} = 0.028$

The L-shaped pieces which were added give an added moment of inertia of .070 in^4. These pieces will extend to 22.0 inches along the spar where they are no longer needed.

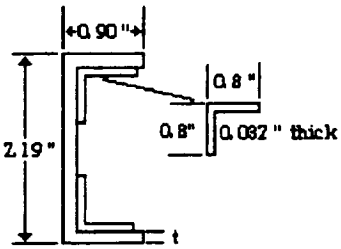

Rear Spar After Fatigue Analysis

Sizing the Skin Thickness On The Horizontal Stabilizer

A multi-cell analysis was used to size this portion of the horizontal stabilizer. After determing the shear flow on the skin, the shear stress was set equal to the equation derived from the sheet buckling criterion to determine the proper skin thickness. Each flange area was determined by summing the flange area from the C channel, the area of the web one characteristic distance from the flange, and the area of the skin one characteristic distance in each direction from the flange.

$A_f = 0.1602 \cdot in^2$ $V_y = -273.0 \cdot lb$ $I_z = \Sigma A_i y_i^2 = .7667\ in^4$

$P_f = \frac{V_y \cdot y \cdot A_f}{I_z}$ $P_f = -49.1 \cdot y \cdot in^3$ $P_1 = 65.3 \cdot lb \cdot in^{-1}$

$P_2 = 59.3 \cdot lb \cdot in^{-1}$ $P_4 = -P_1$ $P_3 = -P_2$

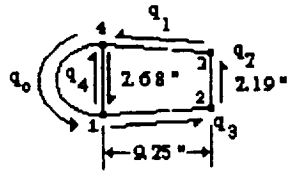

$A_f = .1602\ in^2$

Multi-cell At the Root Used For Skin Panel Sizing

By inspection, q_3 is equal to q_1.

$\Sigma M_1 : q_o = \frac{2019 \cdot lb \cdot in - 40.42 \cdot in^2 \cdot q_4}{67.9 \cdot in^2}$

$$\phi_1 = \phi_2 : q_o = \frac{4049.5 \cdot lb \cdot in^{-1} - \left(\frac{18.5 \cdot in}{t} + 32.5\right) \cdot q_4 + \frac{1208 \cdot lb}{t}}{\left(\frac{5.3 \cdot in}{t} + 32.5\right)}$$

If a sheet thickness of 0.02 inches is tested, the results are as follows.

$q_o = -13.83 \cdot lb \cdot in^{-1}$ $q_1 = -7.53 \cdot lb \cdot in^{-1}$ $q_2 = -66.83 \cdot lb \cdot in^{-1}$ $q_3 = -7.53 \cdot lb \cdot in^{-1}$ $q_4 = 71.6 \cdot lb \cdot in^{-1}$

$K_s = 10.2$ (this is for a 15.0" by 9.25" sheet - see Appendix 6 for graph) $E = 10 \cdot 10^6 \cdot lb \cdot in^{-2}$

$f_{crit} = K_s \cdot E \cdot \left(\frac{t}{b}\right)^2$ $f_{crit} = 476.8 \cdot lb \cdot in^{-2}$ $f_{q_1} = 376.5 \cdot psi$

$MS = 0.266$

Therefore, 0.02" is the skin and rib thickness since all panels are the same size.

Sizing the Lightening Holes in the Spars and Ribs

For the front spar at 7.0 inches to 37.0 inches along the half-span:

(see Appendix 7)

$q = q_4$ $t = .072 \cdot in$ $h = 2.68 \cdot in$ $f_s = \frac{q}{t}$ $f_s = 994.4 \cdot psi$ $F_o = 24000 \cdot psi$

$K_1 = \frac{f_s}{F_o}$ $K_1 = .1$ Using the optimum K_1 curve: $d = .76 \cdot h$ $d = 2.0 \cdot in$ $b = \frac{d}{.75}$ $b = 2.67 \cdot in$

For the front spar at 37.0 inches to 67.0 inches along the half-span.

$q = q_4$ $t = 0.032 \cdot in$ $h = 1.98 \cdot in$ $f_s = 2237.5 \cdot psi$ $F_o = 18500 \cdot psi$ $K_1 = .121$

$d = .76 \cdot h$ $d = 1.50 \cdot in$ $b = \frac{d}{.75}$ $b = 1.88 \cdot in$

The same analysis was used for the rear spar and the ribs. The results of these ananlyses are shown in the table below. (Note these are the allowed values and not necessarily the values actually used.)

Structure	Length Affected	Hole Diameter	Spacing
Front Spar	7.0" - 22.0"	2.00"	2.67"
Front Spar	22.0" - 52.0"	1.50"	1.88"
Front Spar	67.0"	1.25"	1.53"
Rear Spar	7.0" - 22.0"	1.50"	2.00"
Rear Spar	22.0" - 37.0"	1.20"	1.60"
Rear Spar	37.0" - 52.0"	1.00"	1.40"
Rear Spar	67.0"	0.50"	0.87"
Ribs	7.0" - 22.0"	1.50'	1.88"
Ribs	22.0" - 37.0"	1.35"	2.00"
Ribs	37.0" - 52.0"	1.00"	1.40"
Ribs	67.0"	0.60"	0.90"

The lengths are with respect to the center line of the aircraft

Sizing the Fuselage Interface

Front Spar: $R_1 := 1.64 \cdot in \quad R_2 := 1.95 \cdot in$

$M := 11947 \cdot lb \cdot in \quad R_1 := 0.841 \cdot R_2 \quad P_1 := 0.841 \cdot P_2$

$\Sigma P_i R_i = M \quad P_1 := 754.0 \cdot lb \quad P_2 := 897 \cdot lb \quad FF := 1.5$

$f_{brgy} := 88000 \cdot psi \quad P := 717.0 \cdot lb \quad f_{brg} := \frac{P \cdot FF}{t \cdot d}$

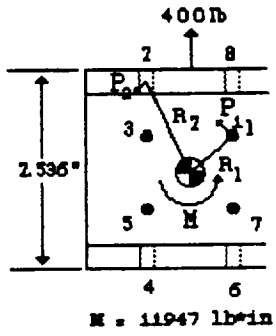

Load Diagram of the Front Interface

If a bolt of 0.25" in diameter is selected, and f_{brg} equals f_{brgy}, then the channel thickness is required to be 0.049". However, after fatigue analysis, it was determined that 0.25" bolts must be used with a plate thickness of 0.082" in addition to the spar.

$MS_{fatigue} := 0.074$

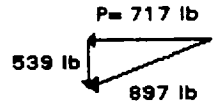

X-Y Components of the Maximum Bearing Force

Rear Spar: The same analysis was used for the fuselage interface at the rear spar. Before, fatigue analysis, the channel thickness required if 0.25" diameter bolts were used was 0.049". However, after fatigue analysis, it was determined that the rear interface structure have 0.25" bolts in a thickness of 0.082" sheet in addition to the rear spar.

Sizing the Hinges On the Horizontal Stabilizer

$P := 84.0 \cdot lb$ (maximum hinge load) $FF := 2.0$

$f_{brg} := 11000 \cdot psi$ $f_{brg} = \frac{P \cdot FF}{A_{bolt}}$

Therefore, the minimum required area of the bolt is 0.0153 in2. If a 0.25" bolt is chosen, then the minimum required length, L, is:

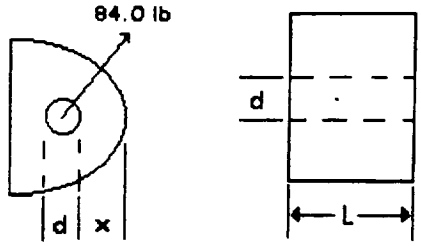

Side and Front Views of A General Elevator Hinge

$L = \frac{A_{bolt}}{d}$ $L := 0.0612 \cdot in$ Therefore, a length of 0.1" was chosen.

$f_{tearout} := 26000 \cdot psi$ $f_{tearout} = \frac{P \cdot FF}{2 \cdot x \cdot L}$ $x := 0.032 \cdot in$ Therefore, an x value of 0.1" was chosen.

$f_{tensiony} := 47000 \cdot psi$

$f_{tension} = \frac{P \cdot FF}{x \cdot L}$ $f_{tension} := 16800 \cdot psi$ $MS := 1.798$

4.2 SIZING THE VERTICAL STABILIZER

The first step in stabilizer design was sizing of the front spar. 2024-T3 aluminum with a yield strength of 42 ksi was chosen for the entire fin structure. The worst case bending for the spar was evaluated to determine the necessary moment of inertia, which then determined the required flange areas for the spar as shown.

$\sigma_{yld}=42ksi$
$M_{cr}=1206ftlb$
$y=2.1inches$
$\sigma=\frac{My}{I} \therefore I=0.7236inche$
$I=\Sigma A_f y^2 \therefore A_f=0.083inch$

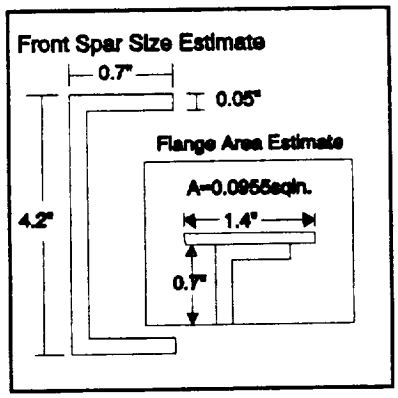

Judging from what other aircraft manufacturers used, a thickness of 0.05" was chosen for the spars. The flange length is then usually about twenty thicknesses, which would be 0.4". However, 0.7" was used for the flange length to allow ample space for riveting. Skin thickness was chosen as 0.02" to be within the 3:1 spar to skin ratio. The flange area was then estimated according to the diagram on the above right. The shear flows in the skin and the webs of the spars were then calculated by the same method shown in the section titled Sizing the skin thickness on the horizontal stabilizer. To obtain

representative values for the stabilizer, the shear flows were calculated at water lines 46, 59.5, and 77, with the results given in the following table in units of pounds per inch.

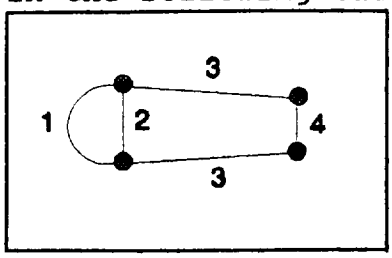

#	W.L. 46	W.L.59.5	W.L. 77
1	29.57	16.90	5.72
2	61.13	36.90	14.60
3	14.92	8.10	2.33
4	37.40	24.20	10.91

Each of the shear panels and spars was then checked for buckling using the equations below. The table on the right shows the critical stress , the stress in each panel, as well as the margin of safety.

$$K_s=75$$
$$E=10E6 lb/inch^2$$
$$t=0.02 inches$$
$$b=12 inches$$
$$q=29.6 lb/inch$$
$$F_{cr}=K_s E(\frac{t}{b})^2=2083 lb/inch^2$$
$$F_{panel}=\frac{q}{t}=1480 lb/inch^2$$

Section	F_{panel} psi	F_{cr} psi	M.S.
Root nose	1480	2083	0.41
Root main	745	586	-.21
Mid nose	845	1920	1.27
Mid main	405	360	-.11
Tip nose	286	3109	9.87
Tip main	119	718	5.03
Spar root	1678	12755	6.60
Spar mid	895	14168	14.8
Spar tip	333	21852	64.6

As the table shows, the panel stress exceeds the critical stress in the main panels of the root and mid-section. A stringer that runs through the middle of the main panels from the root to the mac was added to prevent this buckling. Because the spars undergo considerable cyclic loading, calculations were performed to confirm the required 10^7 cycles. The values for f_{max} and f_{mean} were checked against the fatigue graph (Appendix 5) to insure the proper life. The spar as previously designed failed before the required number

$$f_{limit}=27.47ksi$$
$$f_{max}=\frac{f_{limit}}{2}=13.74ksi$$
$$f_{mean}=\frac{f_{limit}}{3.8}=7.23ksi$$

of cycles. Therefore, two L-doublers were added to the top and bottom of the main spar. With the doublers, the limit load on the spar is 27470 psi which gives a margin of safety for cyclic loading of 0.13. The L-doublers run approximately 26 inches along the spar starting at the fuselage. The stabilizer-fuselage interface pieces were designed to rivet to bottom portion of each spar and extend several inches down into the fuselage where each would be bolted to a former.

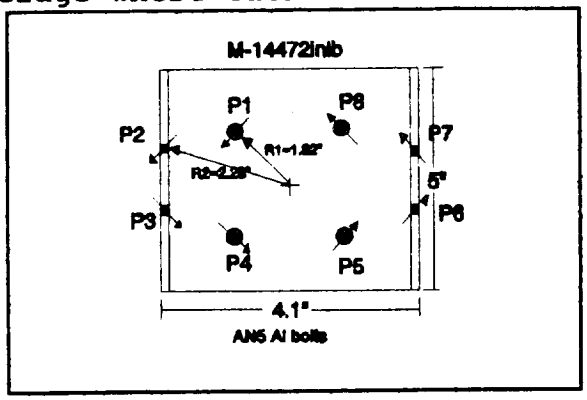

$$\frac{P_1}{R_1}=\frac{P_2}{R_2}=\ldots$$
$$\frac{P_1}{P_2}=\frac{R_1}{R_2}=\frac{1.82}{2.28}=0.8$$
$$\Sigma P_i R_i=M=14472inchlb$$
$$4P_oR_o+4P_nR_n=14472$$
$$P_n=968.4lb$$
$$P_o=774.7lb$$

$$f_{brg}=\frac{P(FF)}{tD}=\frac{(968.4)1.5}{(0.15)(0.3125)}$$
$$f_{brg}=30.9ksi$$
$$f_{mean}=\frac{30.9}{3.8}=8.16ksi$$
$$f_{max}=\frac{30.9}{2}=15.5ksi$$

4.3 Sizing the Rudder

The sizing of the rudder front spar proceeded just as the calculations for the vertical stabilizer. The same material was used for simplicity and reduced manufacturing costs. However, 0.02" sheet with a 0.5" flange width was sufficient for the spar because of the relatively small loads. The tables below show the shear flows (lb/in) in the skin and spars, the critical stresses for buckling, and the corresponding margins of safety. Three evenly spaced ribs in combination with the main spar were

sufficient for the rudder structure.

Location	W.L.51.9	W.L.72.9
Skin	0.449	0.639
Spar	15.81	20.06

Section	F_{panel}(psi)	F_{cr}(psi)	M.S.
Skin inboard	31.95	204.1	5.39
Skin outboard	22.45	284.3	11.7
Spar root	1003	4784	3.77
Spar tip	1003	7269	6.25

The rudder hinges were designed following the same procedure as that shown for the horizontal stabilizer hinges. The hinge is made of two 0.02" sheets plus two doublers (0.032" each) on the outside to give l=0.104". The x distance is 0.2" and the bolt diameter is 0.25". The critical factor in the hinge design was the bearing strength of the oillite bearing. With a load of 90 lb, the hinge with the doublers yielded a margin of safety of 0.59. The mate hinge on the stabilizer is essentially two rudder hinges side by side. However, the doublers were placed on the hinge inner walls for the smallest possible tolerance between the mating hinges.

4.4 Sizing the Elevator

Elevator sizing was similar to the rudder analysis. The same size spar was used to produce the following results for shear flows (lb/in) and buckling stresses. Cyclic loading was not critical.

Location	B.L.22	B.L.52
Skin	6.6	5.95
Spar	18.14	41.65

Section	F_{panel}(psi)	F_{cr}(psi)	M.S.
Skin inboard	330	202	-.39
Skin outboard	297	805	1.71
Spar root	2083	6351	2.05
Spar tip	2083	23333	10.2

The inboard skin panel made it necessary to add an auxiliary spar to prevent that panel from buckling. The elevator hinges have the same critical dimensions as the stabilizer hinges.

4.5 Sizing the Tail Cone

In order to simplify the analysis of the empennage, the tail cone was assumed to be a right circular cone and thus the stringer taper angles were constant in all planes. The analysis was then divided into seven areas: skin sizing for torsion, stringer design and former location, stringer fatigue, control surface interface former design, fuselage interface connection, tie down provision, and access panel location.

Skin Sizing:

The skin was chosen to be aluminum 2024-T3 to minimize weight and cost. The skin panels were chosen to be semicircular for easy manufacturing and assembly to the frame. Panel dimensions were determined by former locations based on the preliminary structural design. The initial 0.032" thick aluminum sheet was reduced to 0.025" due to sufficient critical buckling strength. Both the calculated and critical shear stresses for each section were determined as follows.

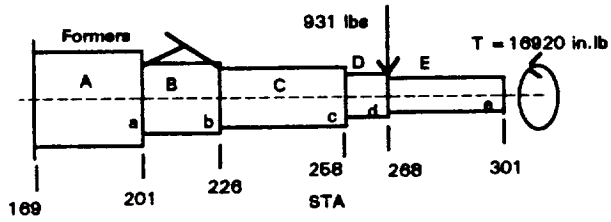

Shear flow equation for Panel A:

$q = T / (2A) = 16920 \text{ in.lb} / (2)(380.133 \text{ in}^2) = 22.3 \text{ lb/in}$

Shear stress for panel: $f_{shear} = q / t = 22.3 / 0.025 \text{ in.} = 892 \text{ psi}$

Allowable shear stress in Panel A given by:

$f_{critical} = K_S E (t / b)^2 = 1831 \text{ psi}$

Where: $K_S = 300$ (panel stiffness factor from Niu Figure 5.4.8)

$E = 10 \times 10^6$ psi (modulus of elasticity)

$t = 0.025$ in. (skin thickness)

$b = 32$ in. (panel length)

Skin Panel Shear Stress Results

Panel	Length, in	Shear flow, q lb/in	Ks	f shr actual psi	f shr critical psi	Margin of Safety
A	32	22.3	300	892	1831	1.05
B	25	29.8	250	1192	2500	1.09
C	32	47.9	250	1916	2473	0.29
D	10	63.8	90	2552	5625	1.20
E	28	89.1	200	3564	3830	0.07

Stringer Design and Former Location:

The bending moment was first calculated at the left of each stringer length from the preliminary former locations. Since the 931 lb resultant load could be produced by four flight conditions, four stringers were used. The final configuration positioned the stringers at 45° to the aircraft axes as shown in figure below.

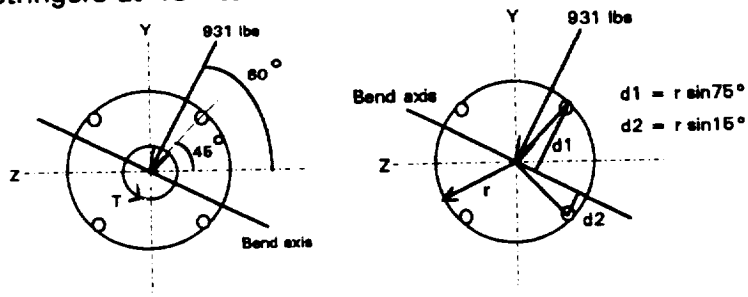

A stringer moment of inertia, I_{str} , of 0.02 in^4 was assumed. By equating the bending stress formula, $f_{bend} = My / I$, and the critical buckling formula, $f_{crit} = (\pi^2 E I) / (A l^2)$, the equation below was derived to determine the maximum stringer length, L, using the assumed I value.

$$L = \sqrt{\frac{(1.97x10^8)(d_1 + d_2) I_{str}}{My}}$$

Where: d_1 and d_2 = see figure above
M = bending moment (in.lb)
I_{str} = 0.02 in^4 estimated stringer property
y = distance to outermost stringer (same as d_1)

The stringer length dictated former placement. The stringer cross section was then designed using the skin thickness of 0.025" and the I value. This cross section can be seen in Drawing 421S9303B206. Below are the results from the above length equation applied to the same stringer/former locations used during skin sizing .

Critical Stringer Lengths and Former Locations

STA	Moment, in/lb	d1 = y in	d2, in	Length, L in	Former STA (Fig ref)
169	93100	11.1	3	22.4	191.4 (a)
191.4	72245	10.2	2.74	24.4	215.8 (b)
215.8	49530	9.2	2.4	28	243.8 (c)

The lengths indicated that another former must be placed between b and c of the initial design. Since the data showed that formers a, b, and the new former could be spaced 20 inches apart without affecting the critical length or skin buckling, this was done to move weight closer to the aircraft c.g.. The stringer between the new former and former c was then checked for buckling using the 20-inch former spacing.

STA	Moment, in/lb	d1 = y in	d2, in	Length, L in	Former STA (Fig ref)
229 (new)	37240	8.2	2.2	30.5	259.5 (c)

Former c was not moved since it was initially located at STA 258 and the critical length exceeds that location. This shows that the stringer between the new former and c will not buckle.

The curved, skin panels D and E were then analyzed for their buckling resistance to compressive loads without stringer reinforcement. Niu Figure 5.4.4 provided the equation for the critical buckling stress, f_{crit}. This value was compared to the actual bending stress.

For Panel D: $$f_{crit} = k_c \frac{\pi^2 E}{12(1-\mu^2)}\left(\frac{t}{b}\right)^2 = 15182 \text{ psi}$$

Where: k_C = 1300 (from Niu Figure 5.4.4)
E = 10×10^6 psi for aluminum
μ = 0.301 (Poisson's ratio for aluminum)
t = 0.025 in (skin thickness)
b = 22 in (panel circumference)

Actual bending stress for Panel D: $$f_{actual} = \frac{Mr_1}{\frac{\pi}{4}\left(r_1^2 - r_2^2\right)} = 1222.6 \text{ psi}$$

Where: M = (931 lbs) (10 in) = 9310 in.lb
r_1 = 7 in (outside radius)
r_2 = 6.95 in (inside radius)

Curved Panel Buckling Analysis Results

Panel	Length in	b, in	OD rad r1, in	ID rad r2, in	Momen t in.lb	Kc	fcrit psi	factual psi	M.S.
D	10	22	7	6.95	9310	1300	15182	1222.6	11.41
E	28	20.4	6.5	6.45	10472	1950	26486	1596.2	15.59

These results show that no stringers are necessary after STA 258.

After the sizing calculations, the new empennage configuration was developed and is shown in Drawing 421S9303B206. A simplified version used in future calculations is shown in the figure below.

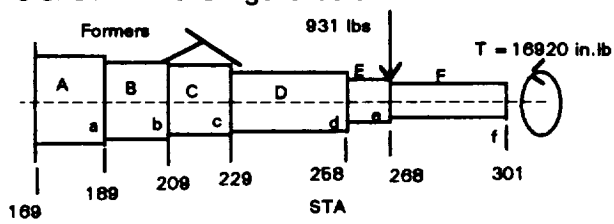

Stringer Fatigue Life:

Fatigue analysis for each stringer section was determined per the requirements in the statement of work. This was done by finding the limit bending stress, $f_{bend\ LL}$, the maximum cyclic stress, f_{cycmax}, and the mean stress, f_{mean}. These values were then compared in Niu Figure 15.4.5 at 10^7 cycles.

For Section A: $I = 2A(d_1^2 + d_2^2) = 26.44\ in^4$

Where: A = 0.1 in^2 (stringer area - constant in all sections)
d_1 and d_2 = 11.1 in and 2.97 in (see Figure xxxxxxxxxx)

I was used to find the limit bending stress for Section A:

$f_{bend\ LL} = Mr / I = 40490$ psi

Where: M = (931 lbs) (100 in) = 93100 in.lb
r = 11.5 in (section radius)

Maximum cyclic stress was then: $f_{cycmax} = f_{bend\ LL} / 2 = 20245$ psi

Mean stress calculated from: $f_{mean} = f_{bend\ LL} / n = 10655$ psi

Where: n = 3.8 (aircraft load factor)

Niu Figure 15.4.5 indicates that 10^7 cycles is acceptable for this stringer. The fatigue stresses for the other sections are listed below.

Stringer Fatigue Analysis and Stresses

Section	d1, in	d2, in	r, in	I, in^4	M, in.lb	f bend LL, psi	f cycmax, psi	f mean, psi	M.S.
A	10.7	2.87	11.5	26.44	93100	40490	20245	10655	1.0
B	10.6	2.84	11.0	24.2	74480	33854	16930	8908	1.0
C	10.1	2.71	10.5	22.0	55860	26600	13300	7000	1.0
D	8.2	2.20	8.5	14.45	37240	21900	10952	5764	1.0

All stringers are capable of 10^7 life cycles.

Interface Former Design:

The formers at STA 258, 268, 278, and 301 (Drawing 421S9303B206) are located where the C-channel spars of the control surfaces mate with empennage. The forces in the bolts of the interface connections for both the stabilizer and vertical fin were designed according to the control surfaces loads. Each interface has eight bolts, two at each spar flange and four in the web. The flange bolts attach to an L-bracket riveted to the former, while the center bolts pass through the former. Since the former is made of 0.025" aluminum sheet, a doubler plate behind the spar interface was necessary to provide sufficient material through which to rivet the L-brackets.

The rivets mentioned above were the sized to withstand the bolt shear transferred to the L-bracket, the vertical shear imposed by the lift of the control surface, and the resulting bearing stress developed under cyclic loading. The L-brackets and doubler plates were sized according to rivet requirements for material thickness. After the analysis of all four interface formers, the size of the rivets, L-brackets, and doubler plates did not change from those of the first. The analysis of the bolt loads at the first interface former (STA 258) is given on the next page.

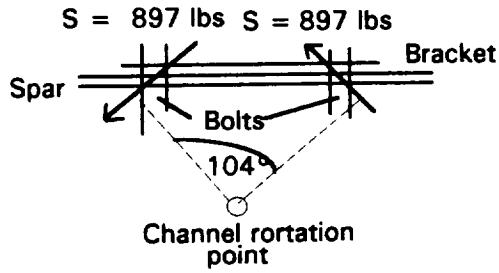

Resultant load of the S shears: R = 2 (897 lbs) cos (104 / 2) = 1104.5 lbs

Min. number of 1/8" dia. rivets in L-bracket: 1104.5 lbs / (368 lbs / rivet) = 3 rivets

The L-bracket is 0.1" aluminum. Using 7, 1/8" dia. rivets spaced between 0.75 and 1 inches, rivet bearing stress under cyclic loading is as follows:

Bearing stress per rivet:

$$f_{bng} = \frac{(11045 lbs / 7 rivets)}{(0.1 in)(0.125 in)} = 12662.8 \text{ psi}$$

Maximum cyclic stress: fcycmax = fbng / 2 = 6311.4 psi

Mean stress: fmean = fbng / 3.8 = 3321.8 psi

From Niu Figure 15.4.5 these rivets will not fail under 10^7 cycles.

The maximum rivet spacing distance was computed by finding the shear flow in half the former. The 400-lb vertical shear from one side of the horizontal stabilizer was used along with geometric information from the former.

Shear flow: q = VQ / I = 63.61 lb/in

Where: V = 400 lb
Q = 15.46 in^3 (at the first row of rivets in the L-bracket)
I = 97.21 in^4 (for the area above the first rivet row)

Maximum rivet spacing: d = (368 lb/rivet) / q = 5.78 inches

Since this distance is much greater than the actual spacing, the rivets, L-brackets, and former will handle all forces imposed by the control surface. The last column in the table below is the number of 1/8" dia. rivets per L-bracket.

Interface Former Statistics

STA	Bolt Ld. (lb)	Resltnt (lb)	q (lb/in)	fbng (psi)	fcycmx (psi)	fmean (psi)	V (lb)	M.S.	# Rivets
258	897	1104.5	63.61	12623	6311	3321	400	1.0	7
268	629	774.5	82.02	8851	4425	2329	400	1.0	7
278	968	1747.4	46.41	19970	9985	5242	476	1.0	7
301	932	1682.4	45.77	16824	8412	4427	476	1.0	8

Fuselage Interface Design:

The empennage is attached to the aft section of the fuselage by overlapping the skins of each section and joining two identical formers (STA 169). This can be seen in Drawing 421S9303B206. The rivets joining the two formers were sized and spaced to withstand the vertical shear and torsional loads developed by the control surfaces. The external rivets joining the skin were sized according to the bending moments imposed at the outer radius of the empennage.

Ninety-six, 3/32" dia. rivets spaced 0.75 inches apart join the formers. This was calculated using circumference and maximum allowable rivet spacing. Vertical shear and torsional analysis would also determine the maximum spacing as follows.

Shear flow in interface former: $q = VQ / I = 51.63$ lb/in

Where: $V = 931$ lbs (worst case resultant load from surfaces)

$Q = 13.16$ in^3 (from former geometry)

$I = 237.3$ in^4 (from former geometry)

Maximum rivet spacing: $d =$ (206 lb/rivet) / 51.63 lb/in $= 4$ in.

The torsional moment about the former was divided by the number of rivets and the section radius yielding the shear force in each rivet in pounds:

Shear force = (16900 in.lb) / [(96 rivets) (11 in.)] = 16.0 lb/rivet

Both the shear flow and the shear force were combined to determine the loading for the former rivets.

(16.0 lb/rivet) + [(0.75 in/rivet) (51.63 lb/in)] = 54.72 lb/rivet

Since this loading is much less than the allowable shear force for a 3/32" dia. rivet (206 lb), one row of 96 rivets joining the interface formers is acceptable (M.S. = 2.76).

The external skin rivets were then analyzed in bending. The maximum bending moment, M, of 93100 in.lb (acting at STA 169) is also developed from the worst case control surface loads. This moment was broken into a couple with a shearing force of 4047 lbs on the rivets. Dividing this force by the max. allowable rivet shear of 206 lbs determined that 20 rivets were required per rivet group. This was made into 4 rows of 96 rivets spaced at 0.75 inches circumscribing the interface. Any group of 20 rivets is capable of withstanding the moment.

Tie Down Provision:

The tie down provision (Drawing 421S9303B206) is a 7/16" dia., forged, eye bolt that is connected to the STA 268 former and protrudes from the bottom of the empennage. The tie down force of 775 lbs produces 1288.8 psi of pure tensile stress which is far below the allowable 9800 psi for this type of bolt (M.S. = 6.6). Since the tie down force is less than the 931 lb resultant and is applied at the same location, the stringers and/or skin will not deform. A skin doubler plate at the bottom of the former provides sufficient material through which to fasten the bolt.

5. Manufacturing and Maintenance

5.1 General Assembly

The aft empennage tail surfaces will be assembled in the following order. The elevator will be attached to the horizontal stabilizer. The horizontal tail will then be attached to the empennage. The vertical stabilizer will be mounted to the empennage, and, finally, the rudder to it. (See Appendix 1)

5.2 Horizontal Stabilizer and Elevator

The C-channel spars and L-shaped doublers are brake formed. The lightening holes are cut from the sheets used to make the spars before they are brake formed. The interface structures are cast from aluminum, and then machined for bolt holes and trim by-pass holes (See Figure 02). The ribs are sheared and hydropressed. The patterns for the lightening holes in the ribs are made into the blank. The skin panels are sheared. The hinges are made of two sheared sheets which are riveted together and press fitted with oillite bearings. (See Figure 08).

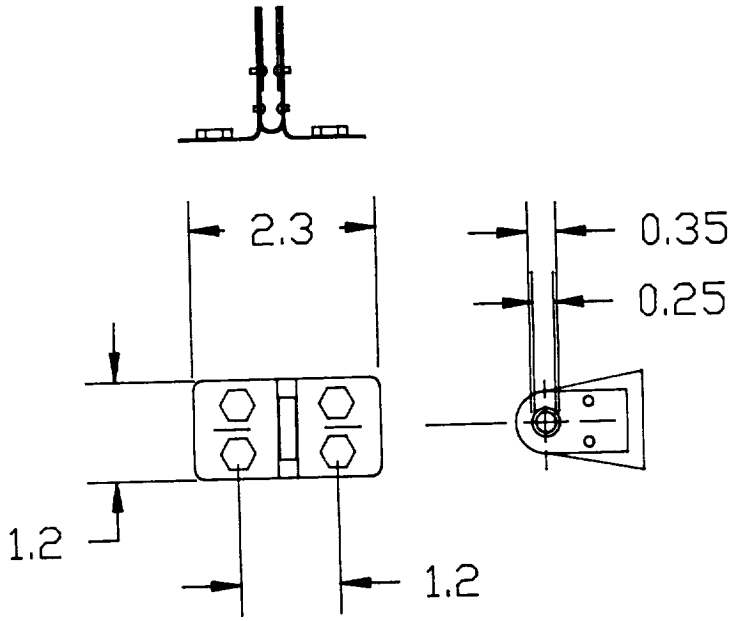

Figure 08 Elevator Hinge Detail

There is an oval access panel which is centered 13.8" from the center line of the empennage to allow for maintenance of the trim screwjack and pulley in the horizontal stabilizer. The elevator also has an access panel for maintenance of the trim tab. There are numerous water drains in each half span of the tail surfaces. In the stabilizer, these drains are located near the 30 percent chord which is the location of maximum thickness, allowing water to pool. The elevator drains are located forward and aft of the front spar.

5.3 Vertical Stabilizer and Rudder

The manufacturing processes for these tail surfaces are identical to those used for the horizontal stabilizer and elevator. There are no drains specifically manufactured for these surfaces. Drains are automatically provided by the lightening holes in the bottoms of the stabilizer and rudder. These lightening holes also provide space to house the electrical systems which supply power to the navigational lights on top of the tail surface.

5.4 Tail Cone

The empennage skin is flat-wrapped aluminum sheet consisting of two, semicircular panels that cover the structure up to the former at the first interface (STA 258). One edge of the skin panel is break formed to construct the stringer. The panels are attached to the formers by riveting the bent edge of one panel to the clean edge of the other, forming the complete stringer (Refer to Formal Drawing 421S9303B206). The other two stringers are break formed C-channels which are riveted to the inside of the skin. The formers are stamped from blanks of aluminum sheet and rubber block pressed into a C-channel cross section. The skin along the top of the interface formers is a single panel cut to form around the surfaces and attached to the interface formers before the surfaces are connected.

There are three removable panels on the empennage. Two, round inspection panels are located on the sides of the empennage just aft of the STA 229 former, and the third panel is located just behind the last horizontal stabilizer interface (STA 268) on the underside of the empennage. Two smaller panels serve to provide inspection and maintenance of the control system fairlead assembly. A skin doubler plate around the hole inside the airframe provides panel reinforcement and a base for the fasteners. The large panel allows access to the control cables, elevator torque tube, torque tube bearings, and interface connections. The hole for this panel is reinforced by continuing the two bottom stringers to the last former. Each panel is fastened to the skin using several Camloc^{R} fasteners (Refer to Formal Drawing 421S9303B206).

6. Weight Summary

Table 2 Estimated Weight Summary

Part No. (Dwg. #)	Title	Number Used	Weight per Part (lb)	Total Weight (lb)
1 (02)	Front Spar (HS)	2	1.45	2.90
2 (02)	Rear Spar (HS)	2	1.13	2.26
5-9 (02)	Ribs (HS)	10	0.06	.60
13 (02)	Skin (HS)	N/A	7.94	7.94
3 (02)	Front Fus. Inter. (HS)	2	1.81	3.62
4 (02)	Rear Fus. Inter. (HS)	2	1.60	3.20
1 (03)	Front Spar (Elev)	2	0.34	0.68
2 (03)	Rear Spar (Elev)	2	0.20	0.40
3-6 (03)	Ribs (Elev)	6	0.03	0.18
16 (03)	Skin (Elev)	N/A	5.06	5.06
1 (04)	Front Spar (VS)	1	1.11	1.11
2 (04)	Rear Spar (VS)	1	0.77	0.77
7-12 (04)	Ribs (VS)	4	0.22	0.88
25 (04)	Skin (VS)	N/A	6.25	6.25
5 (04)	Front Fuselage Interface (VS)	1	1.03	1.03
6 (04)	Rear Fuselage Interface (VS)	1	1.03	1.03
1 (05)	Front Spar (Rudder)	1	0.33	0.33
2 (05)	Rear Spar (Rudder)	1	0.18	0.18
3-7 (05)	Ribs (Rudder)	4	.047	0.19
14 (05)	Skin (Rudder)	N/A	3.35	3.35
7(03), 9(05)	Con. Surf. Hinges (Female)	6	.083	.50
10(02), 13(03)	Con. Surf. Hinges (Male)	6	.065	.39
1 (06)	Stringers	4	0.62	2.48
12 (06)	Formers	8	0.40	3.20
1 (06)	Skin	N/A	27.06	27.06
N/A	Fasteners	N/A	6.00	6.00

Table 3 Target Weight Comparison

Parameter	Target Value	Actual Value	Percent Difference
Horizontal Tail Weight	28.0 lb	27.29 lb	-2.54%
Vertical Tail Weight	14.0 lb	15.57 lb	11.21%
Aft Fuselage Weight	Less Than 130.0 lb	41.02 lb	N/A
Moment About Zero Station	Less Than 35,000 lb*in	Less than 28,184 lb*in	N/A

7. Conclusions

The design presented illustrates the detailed design of the aft empennage, vertical stabilizer and rudder, and horizontal stabilizer and elevator as well as integration of the subsystems. All requirements set forth in the statement of work are met by the final design.

7.1 Horizontal Stabilizer

The ribs were first sized by assuming that they carried all of the applied moments. However, this caused the sizes to be unacceptably large. Therefore, the portion of the moments carried by each spar was determined. This resulted in acceptable spar sizes. After performing a fatigue analysis, L-shaped triplers had to be integrated into the design. The skin was first sized using a single cell, i.e. the front spar was removed for the analysis. This resulted in an abnormally thick skin. When the front spar was replaced and multi-cell analysis performed, the skin thickness was significantly reduced. The sizes of both the front and rear interfaces had to be increased once the fatigue analysis was applied. Increasing the length of the interfaces from 2.0" to 4.0" resulted in decreased bolt loads and, in turn, a smaller required thickness.

7.2 Vertical Stabilizer

After performing a fatigue analysis on the front spar, it was determined that a larger value for the moment of inertia was required. Therefore, L-shaped doublers were added. In the initial analysis, the buckling forces in the skin panels exceeded the critical value. In order to solve this problem, stringers were added between the front and rear spars. In order to integrate the rear interface structure, the bottom hinge had to be moved further away from the root of the stabilizer.

7.3 Tail Cone

The empennage assembly design was only modified once from the original concept. This modification required changing the former spacing to every 20 inches.

Appendix 1

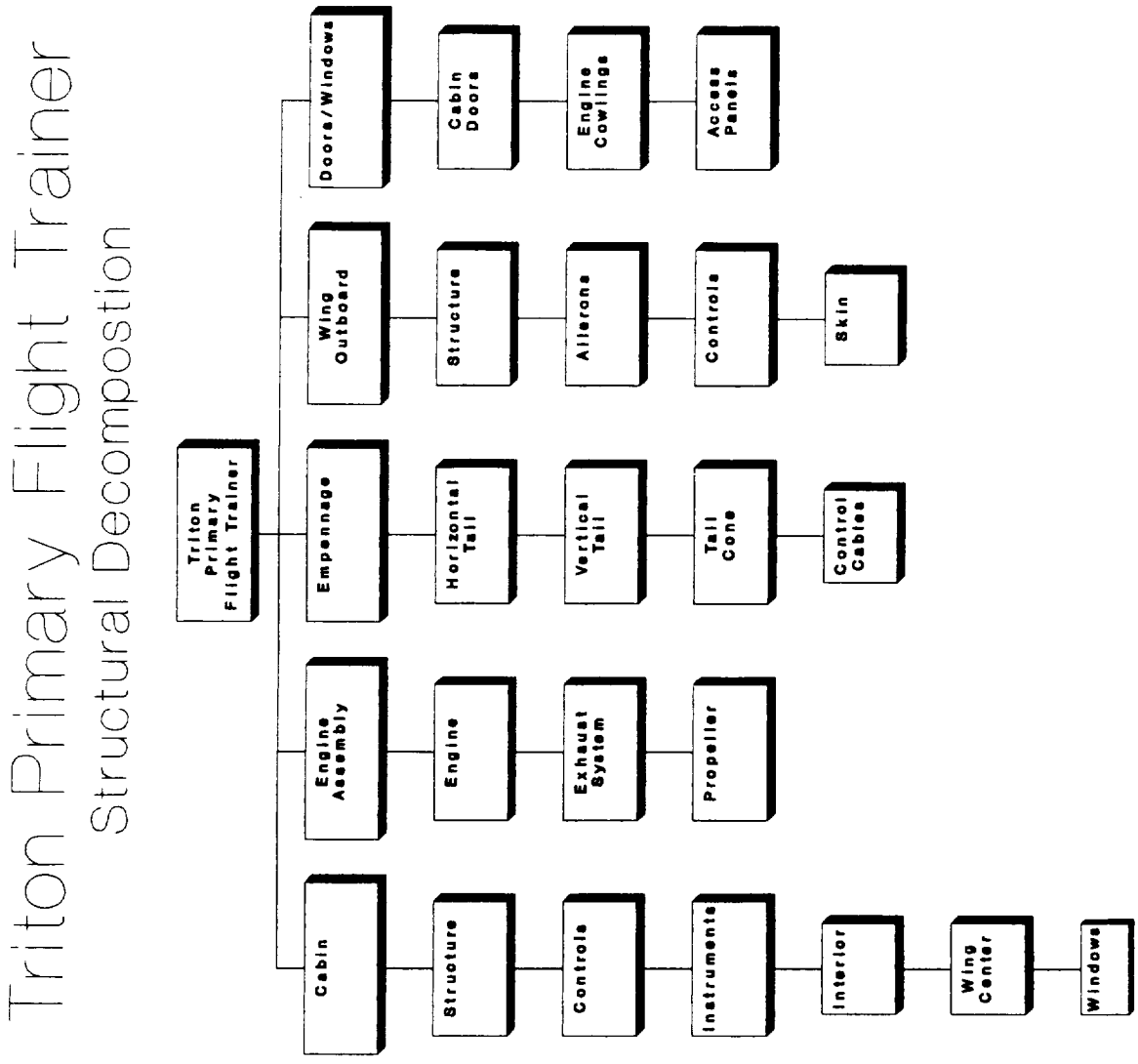
Triton Primary Flight Trainer
Structural Decompostion
Triton Primary Flight Trainer
Cabin
Structure
Controls
Instruments
Interior
Wing Center
Windows
Engine Assembly
Engine
Exhaust System
Propeller
Empennage
Horizontal Tail
Vertical Tail
Tail Cone
Control Cables
Wing Outboard
Structure
Ailerons
Controls
Skin
Doors/Windows
Cabin Doors
Engine Cowlings
Access Panels

SURFACE	DIRECTION OF LOADING	MAGNITUDE OF LOADING	CHORDWISE DISTRIBUTION
ORIZONTAL TAIL I	a) Up and Down	Figure A5 Curve (2)	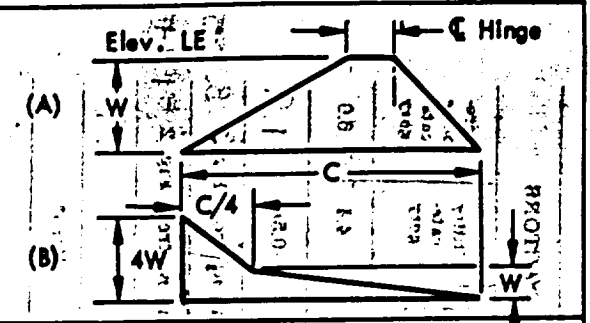
	b) Unsymmetrical loading (Up and Down)	100% $\bar{w}$ on one side airplane ℄ 65% $\bar{w}$ on other side airplane ℄ for normal and utility categories. For acrobatic category see A23.11(C)	
VERTICAL TAIL II	a) Right and Left	Figure A5 Curve (1)	Same as (A) above
	b) Right and Left	Figure A5 Curve (1)	Same as (B) above

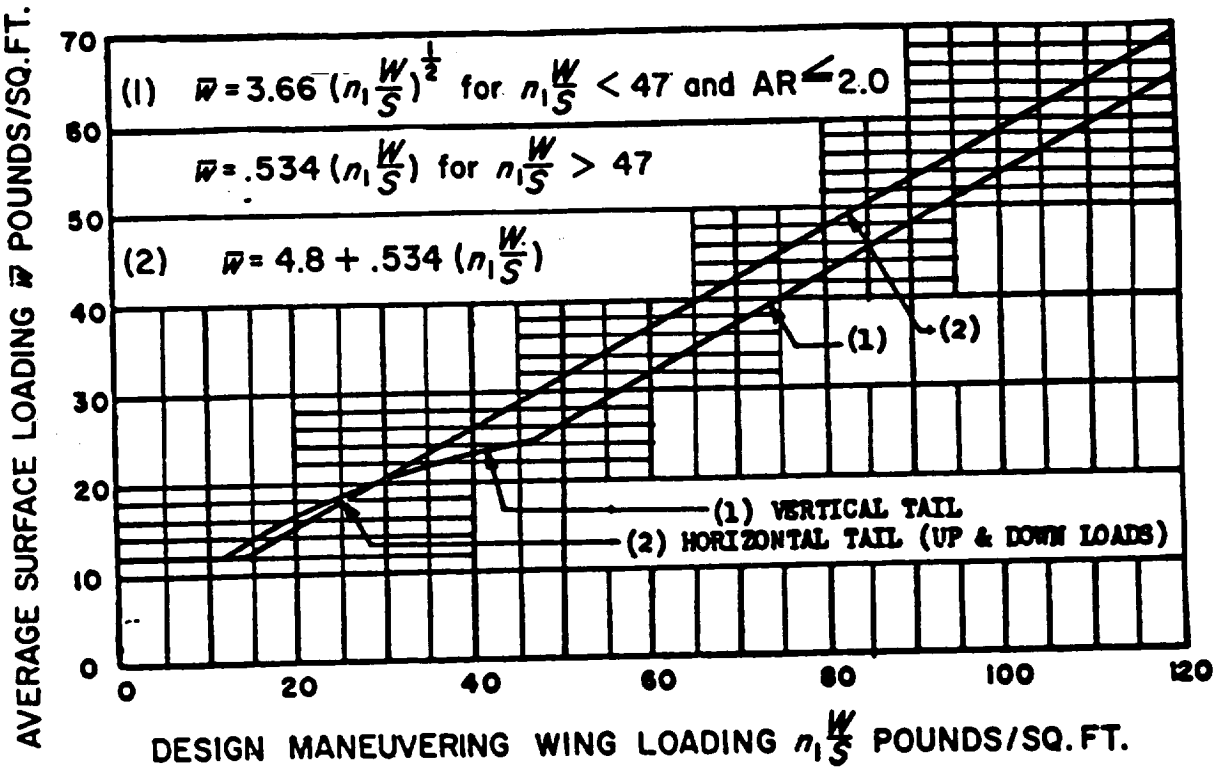

FIGURE A5—Average limit control surface loading.

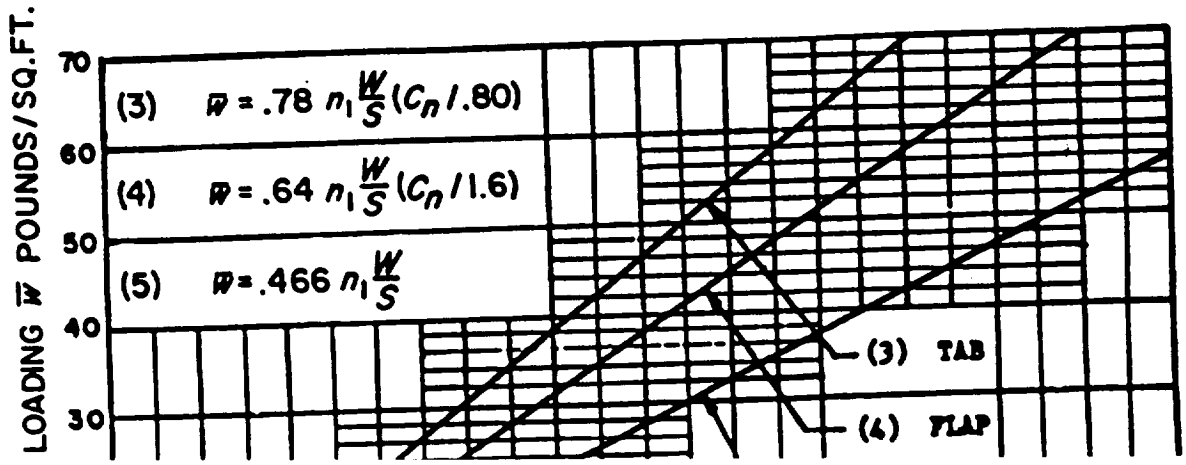

TABLE 3.2.3.0(b_1). *Design Mechanical and Physical Properties of 2024 Aluminum Alloy Sheet and Plate*

Specification	QQ-A-250/4																			
Form	Sheet					Plate												Sheet		Plate
Temper	T3					T351												T361		
Thickness, in.	0.008-0.009	0.010-0.128		0.129-0.249		0.250-0.499		0.500-1.000		1.001-1.500		1.501-2.000		2.001-3.000		3.001-4.000		0.020-0.062	0.063-0.249	0.250-0.500
Basis	S	A	B	A	B	A	B	A	B	A	B	A	B	A	B	A	B	S	S	S
Mechanical properties:																				
F_{tu}, ksi:																				
L	64	64	65	65	66	64	66	63	65	62	64	62	64	60	62	57	59	68	69	67
LT	63	63	64	64	65	64	66	63	65	62	64	62	64	60	62	57	59	67	68	66
ST	...	...	...	...	...	...	...	...	...	...	...	...	...	52	54	49	51	...	...	...
F_{ty}, ksi:																				
L	47	47	48	47	48	48	50	48	50	47	50	47	49	46	48	43	46	56	56	54
LT	42	42	43	42	43	42	44	42	44	42	44	42	44	42	44	41	43	50	51	49
ST	...	...	...	...	...	...	...	...	...	...	...	...	...	38	40	38	39	...	...	...
F_{cy}, ksi:																				
L	39	39	40	39	40	39	41	39	41	39	40	38	40	37	39	35	37	47	48	46
LT	45	45	46	45	46	45	47	45	47	44	46	44	46	43	45	41	43	53	54	52
ST	...	...	...	...	...	...	...	...	...	...	...	...	...	46	48	44	47	...	...	...
F_{su}, ksi	39	39	40	40	41	38	39	37	38	37	38	37	38	35	37	34	35	42	42	41
F_{bru}[a], ksi:																				
(e/D = 1.5)	104	104	106	106	107	97	100	95	98	94	97	94	97	91	94	86	89	111	112	109
(e/D = 2.0)	129	129	131	131	133	119	122	117	120	115	119	115	119	111	115	106	109	137	139	135
F_{bry}[a], ksi:																				
(e/D = 1.5)	73	73	75	73	75	72	76	72	76	72	76	72	76	72	76	70	74	82	84	81
(e/D = 2.0)	88	88	90	88	90	86	90	86	90	86	90	86	90	86	90	84	88	97	99	96
e, percent (S-basis):																				
LT	10	b	...	b	...	12	...	8	...	7	...	6	...	4	...	4	...	8	9	9[c]
E, 10^3 ksi	10.5					10.7												10.5		10.7
E_c, 10^3 ksi	10.7					10.9												10.7		10.9
G, 10^3 ksi	4.0					4.0												4.0		4.0
μ	0.33					0.33												0.33		0.33
Physical properties:																				
ω, lb/in.^{3}	0.101																			
C, K, and α	See Figure 3.2.3.0																			

[a] See Table 3.1.2.1.1. Bearing values are "dry pin" values per Section 1.4.7.1.
[b] See Table 3.2.3.0(c).
[c] 10% for 0.500 inch.

Appendix 4

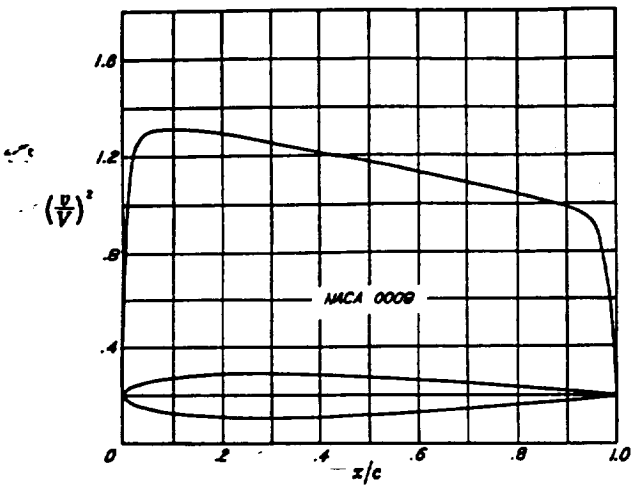

x (per cent c)	y (per cent c)	$(v/V)^2$	v/V	$\Delta v_a/V$
0	0	0	0	0.595
0.5	.....	0.750	0.866	1.700
1.25	1.420	1.083	1.041	1.283
2.5	1.961	1.229	1.109	0.963
5.0	2.666	1.299	1.140	0.692
7.5	3.150	1.310	1.145	0.560
10	3.512	1.309	1.144	0.479
15	4.009	1.304	1.142	0.380
20	4.303	1.293	1.137	0.318
25	4.456	1.275	1.129	0.273
30	4.501	1.252	1.119	0.239
40	4.352	1.209	1.100	0.188
50	3.971	1.170	1.082	0.151
60	3.423	1.126	1.061	0.120
70	2.748	1.087	1.043	0.095
80	1.967	1.037	1.018	0.070
90	1.086	0.984	0.982	0.046
95	0.605	0.933	0.966	0.030
100	0.095	0	0	0
L.E. radius: 0.89 per cent c				

NACA 0009 Basic Thickness Form

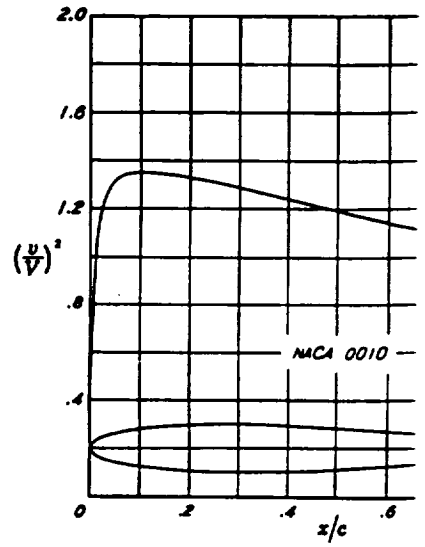

x (per cent c)	y (per cent c)	$(v/V)^2$
0	0	0
0.5	.....	0.712
1.25	1.578	1.061
2.5	2.178	1.237
5.0	2.962	1.325
7.5	3.500	1.341
10	3.902	1.341
15	4.455	1.341
20	4.782	1.329
25	4.952	1.309
30	5.002	1.284
40	4.837	1.237
50	4.412	1.190
60	3.803	1.138
70	3.053	1.094
80	2.187	1.040
90	1.207	0.960
95	0.672	0.925
100	0.105	.....
L.E. radius: 1.10 per cen		

NACA 0010 Basic Thickness

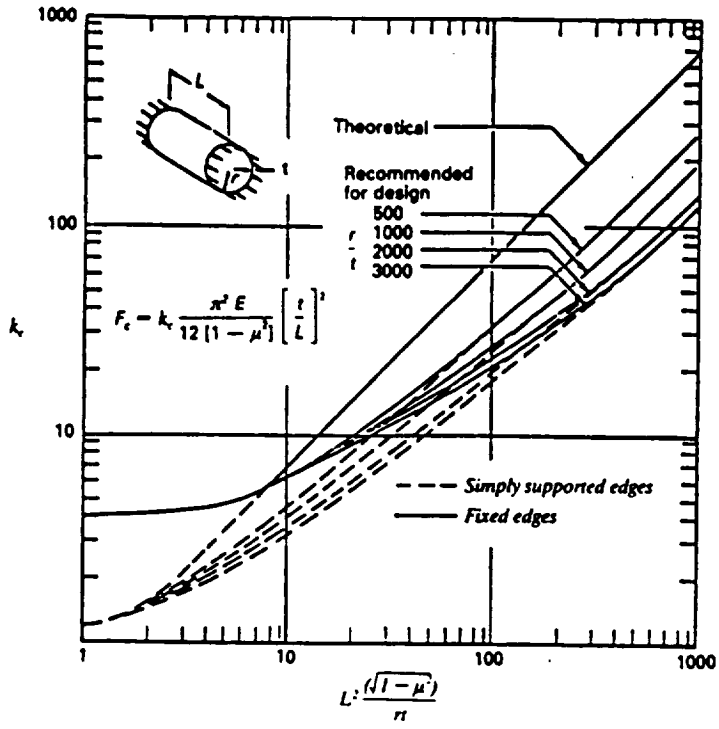

Fig. 5.4.5 Compression buckling coefficients K_c (circular cylinders).

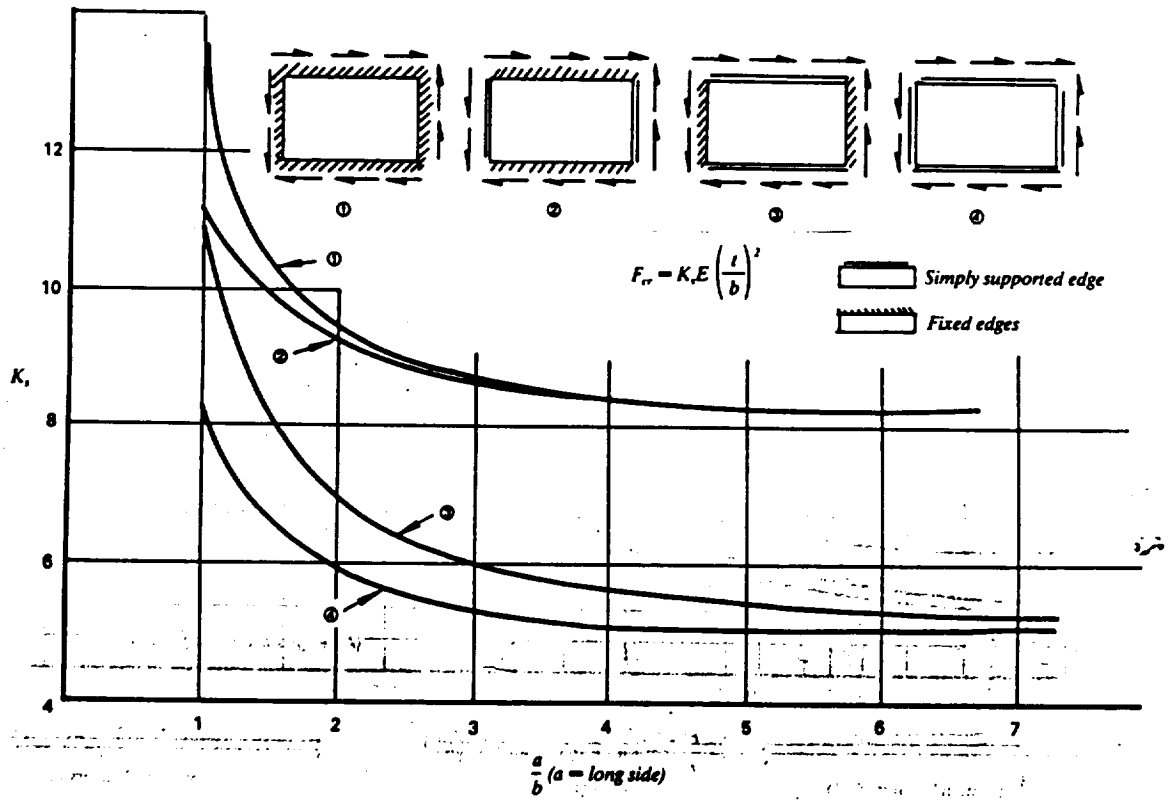

Fig. 5.4.6 Shear buckling coefficients K_s (circular cylinders).

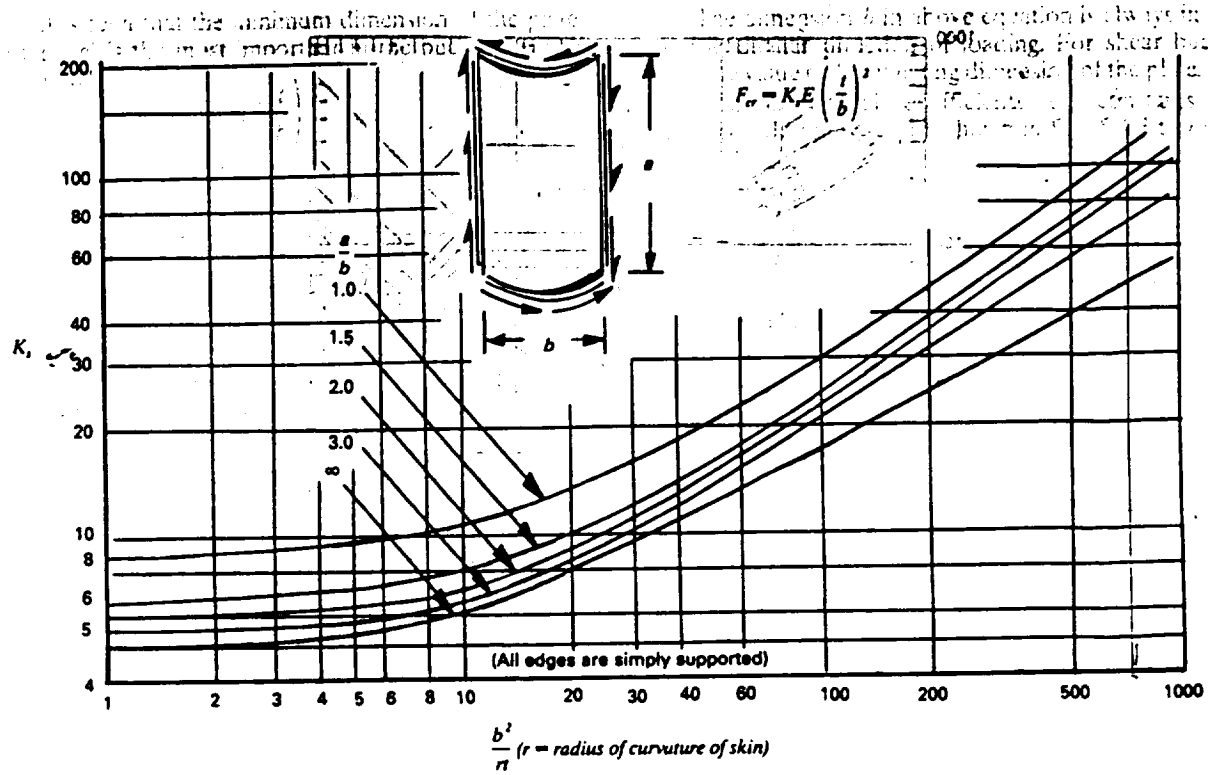

Fig. 5.4.7 Shear buckling coefficients K_s (curved plates, b at curved side).

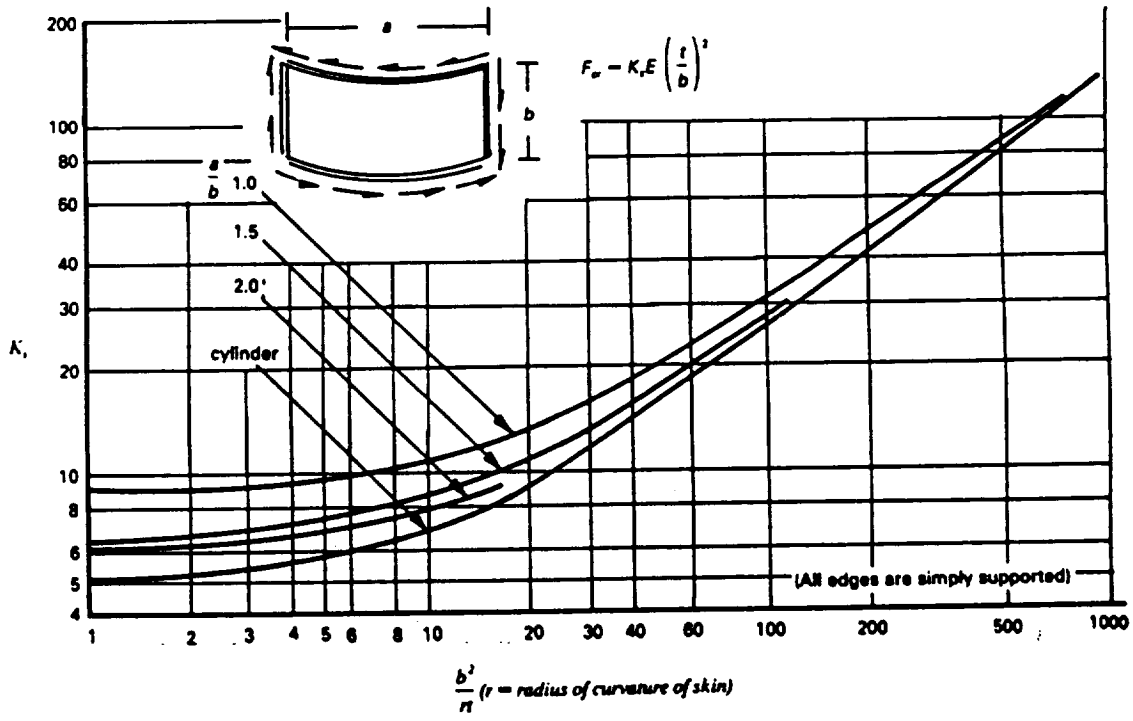

Fig. 5.4.8 Shear buckling coefficients K_s (curved plates, b at straight side).

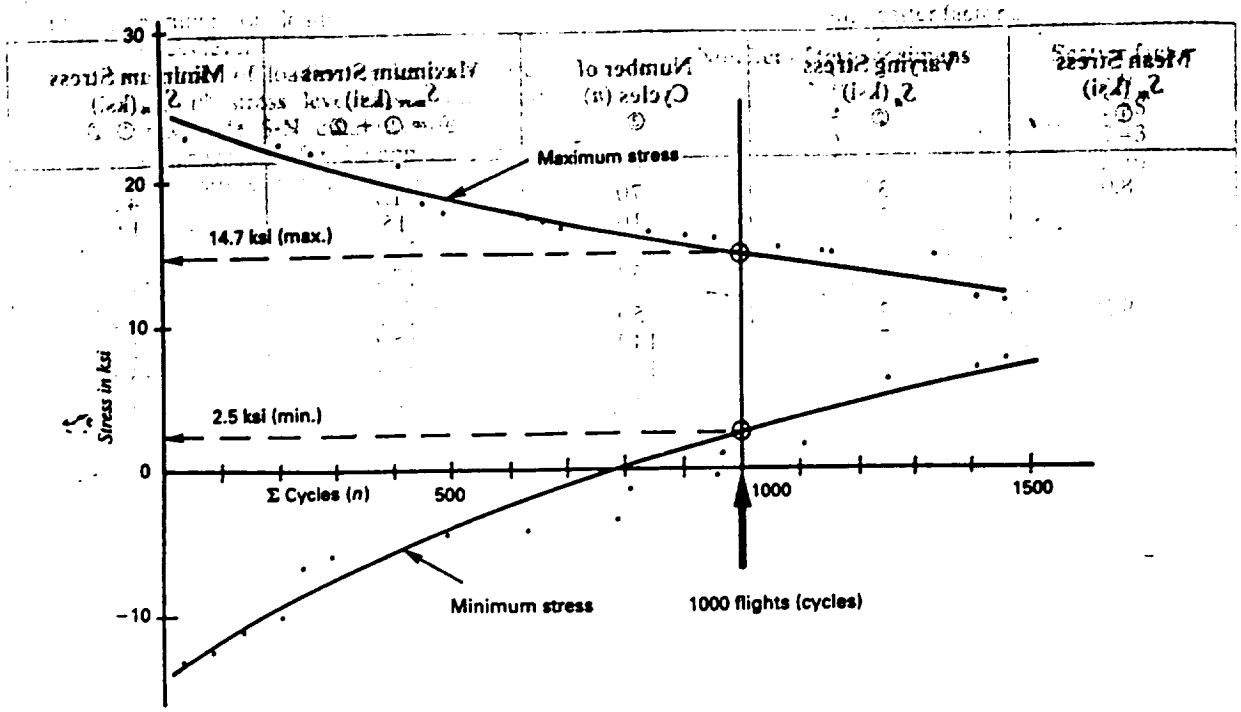

Fig. 15.4.4 Plots of the max. and min. stresses vs. Σ cycles (flights).

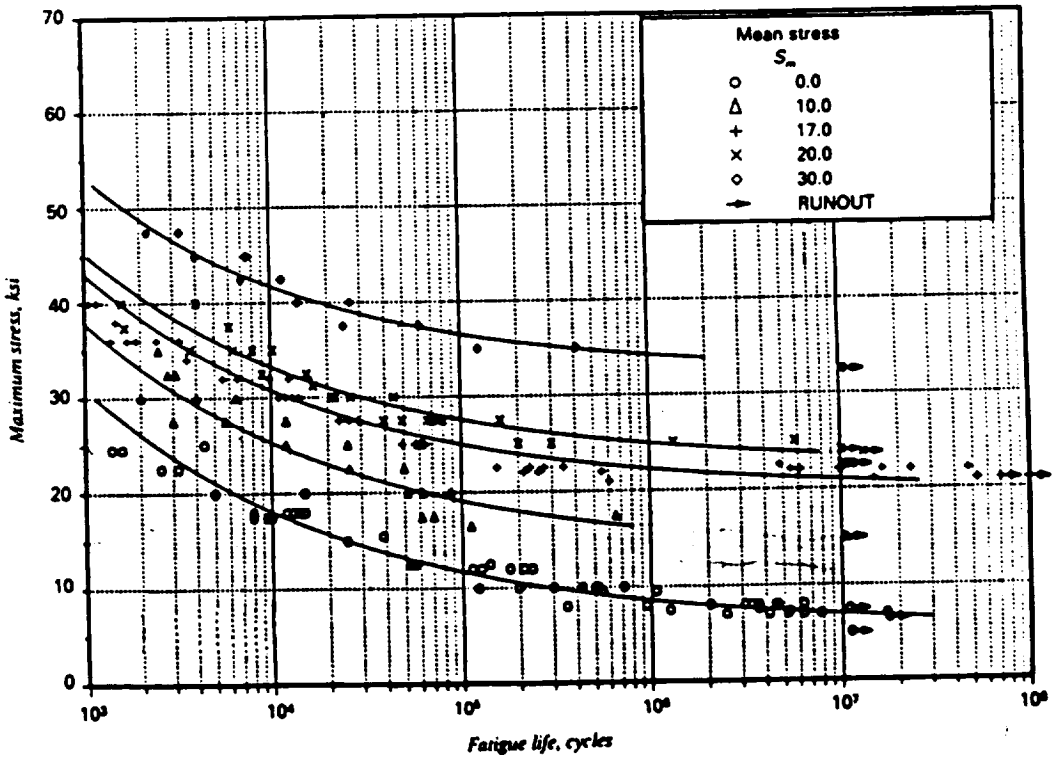

Fig. 15.4.5 Best-fit S-N curves for notched, K = 4.0 of 2024-T3 aluminum alloy sheet, longitudinal direction (Ref. 4.1).

6.2 Lightly Loaded Beams

The ideal construction for most shear-carrying beams is a tension field (or diagonal tension beam per Ref. 6.8). However, in some cases it is advantageous, and in other cases necessary, to incorporate circular, flanged holes in the beam webs. These cases come under two main categories:

- Lightly loaded or very shallow beams. In such cases it may not be practical to construct an efficiently designed tension field beam because of minimum gage considerations and other restrictions due to the small size of the parts involved. It may then be advantageous from a weight standpoint to omit web stiffeners and, instead, introduce a series of standard flanged lightening holes, as shown in Fig. 6.2.1.
- Moderately loaded beams with access holes. Where it is necessary to introduce access holes into the web of a shear-carrying beam, a light, low cost construction is obtained by using a flanged hole with web stiffeners between the holes.

Lightly Loaded or Very Shallow Beams

The following two types of beam construction are considered. The standard flanged lightening holes as shown in fig. 6.2.2 are centered and equally spaced.

- The limiting conditions for the design curves is given in Fig. 6.2.3.

$$0.25 \leq \frac{D}{h} \leq 0.75;$$

web thickness $0.016 \leq t \leq 0.125$

$$0.3 \leq \frac{D}{b} \leq 0.7; \qquad 40 \leq \frac{h}{t} \leq 250$$

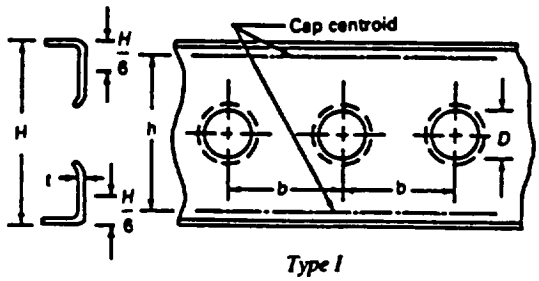

Type I

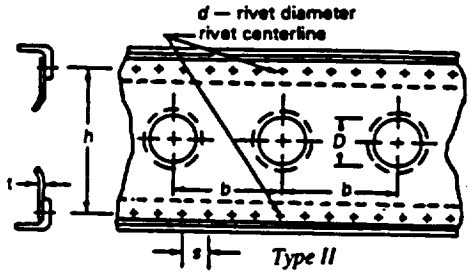

Type II

(Note: $\frac{H}{6}$ is the assumed effective depth of beam cap)

Fig. 6.2.2 Lightly loaded or very shallow beams.

D (inch)	2.0	2.5	3.0	3.5	4.0	4.5	5.0	6.0
f (inch)	.25	.3	.4	.45	.5	.5	.5	.55

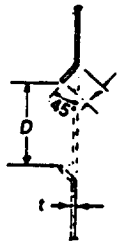

(a) Lightening holes of typical flanged holes (45° flanged)

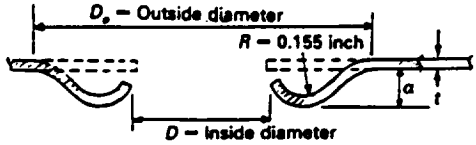

D_0 (Inch)	D (Inch)	α (Inch)
1.7	0.8	0.2
1.95	1.05	0.2
2.65	1.7	0.25
3.0	2.05	0.25
3.65	2.7	0.25
3.9	2.95	0.25
4.95	3.8	0.4
5.95	4.8	0.4
6.95	5.8	0.4
7.44	6.3	0.4
7.95	6.8	0.4
8.95	7.8	0.4
9.45	8.3	0.4

(b) Lightening holes with beaded flanged

Fig. 6.2.1 Common flanged lightening holes. ($t = 0.032$ in $- 0.125$ in)

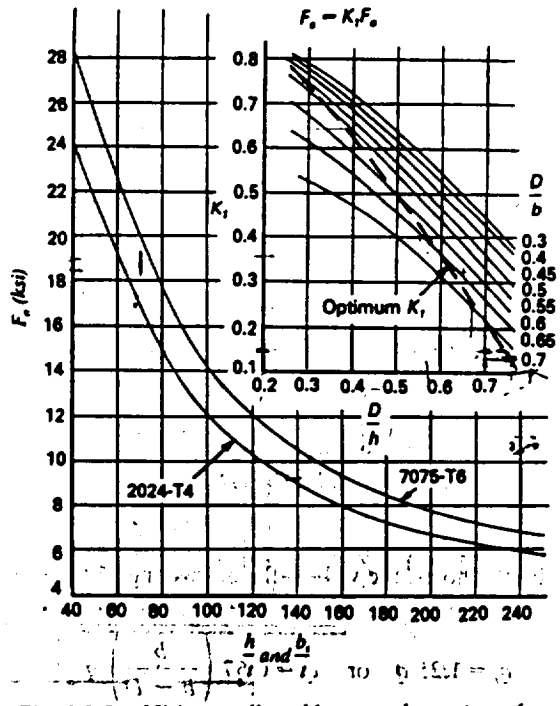

Fig. 6.2.3 Ultimate allowable gross shear stress for aluminum alloy webs with flanged holes as shown in Fig. 6.2.1(a).

FOLDOUT FRAME

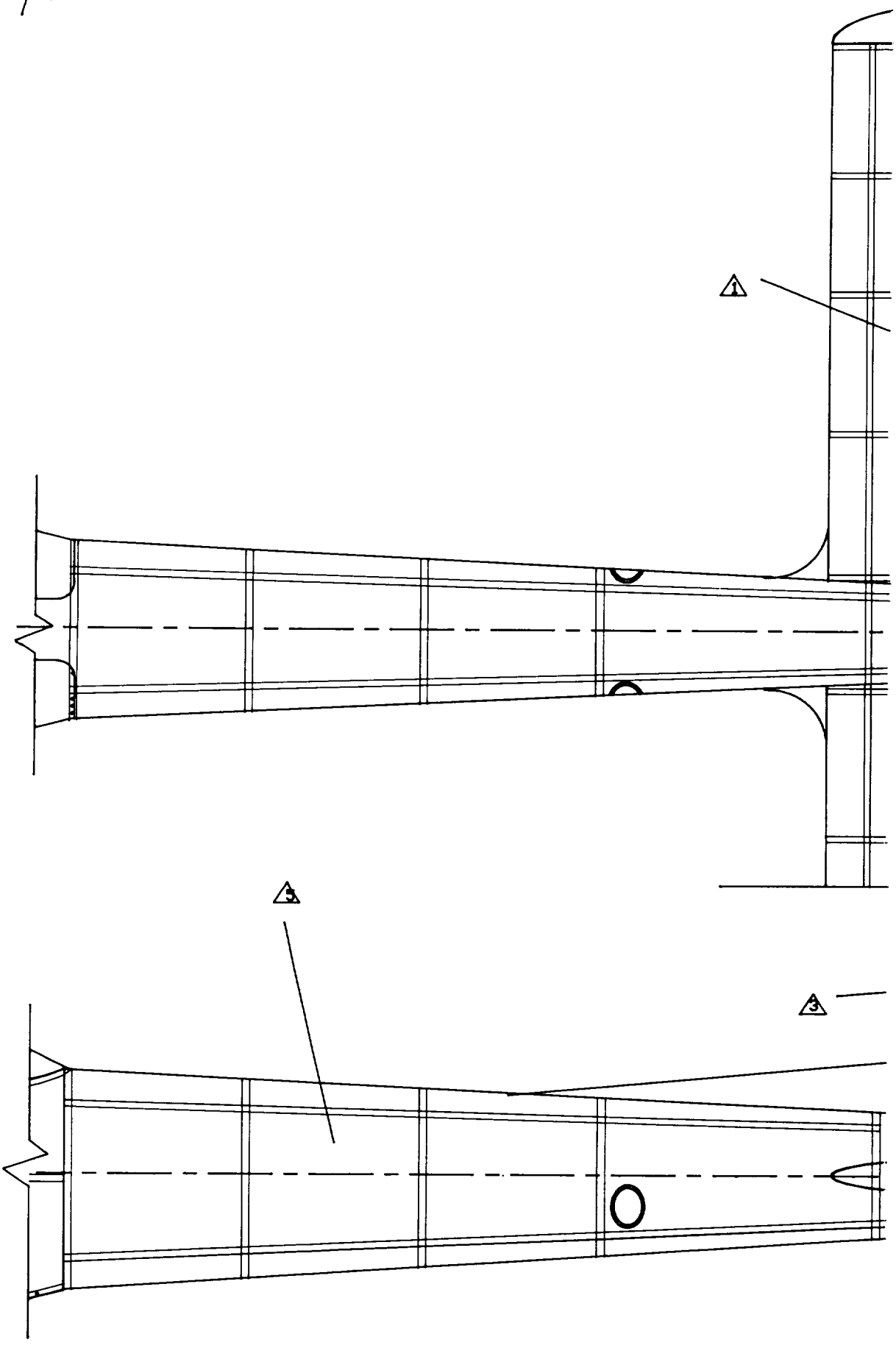

FOLDOUT FRAME 2

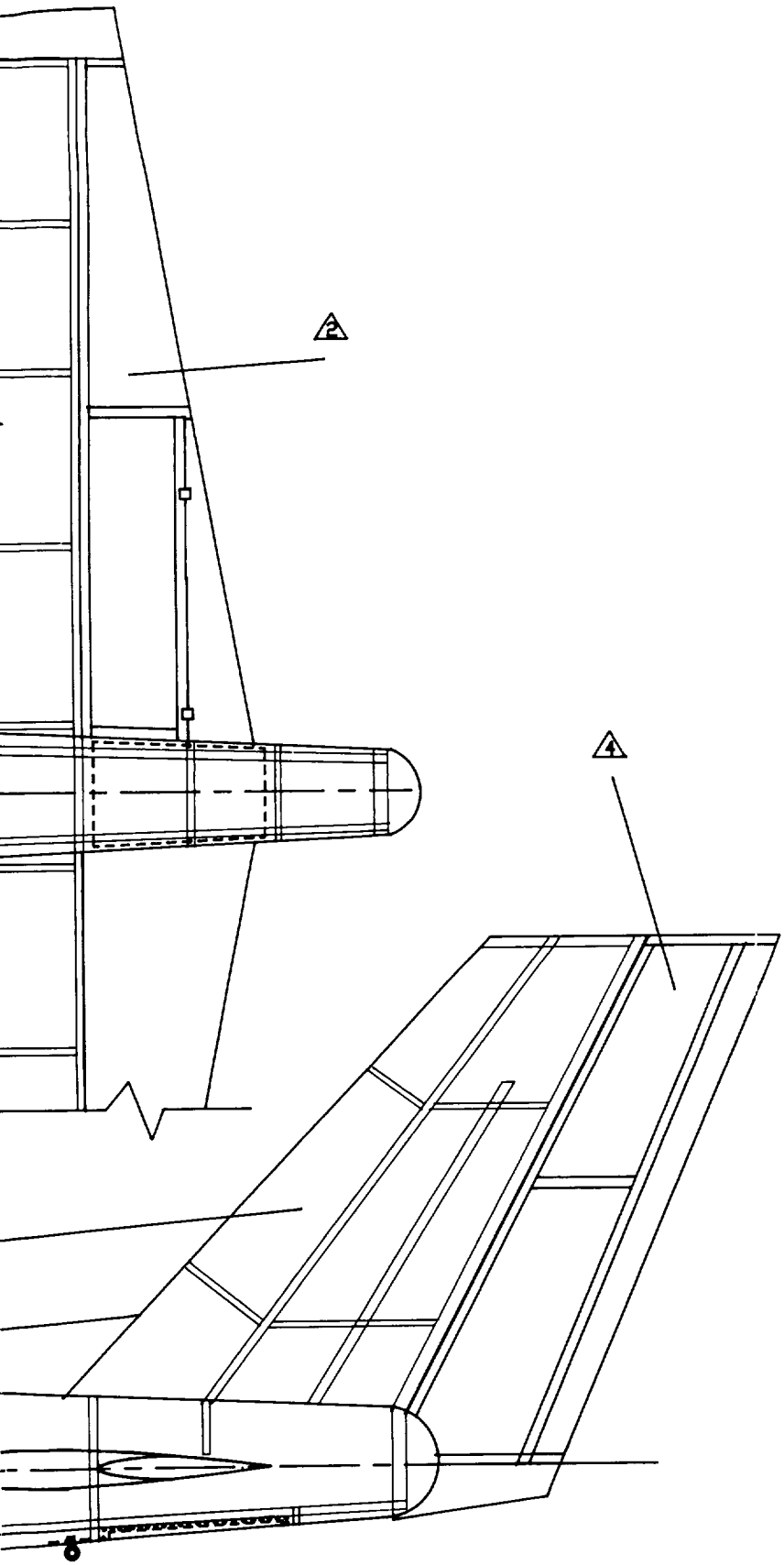

ITEM	DESCRIPTION	421S9303B2xx
5	EMPENNAGE ARRANGEMENT	06-01 THRU 0
4	RUDDER STRUCTURE	05-01
3	VERTICAL STABILIZER STRUCTURE	04-01 THRU 0
2	ELEVATOR STRUCTURE	03-01
1		02-01 THRU 0

DRAWING LIST

UNLESS OTHERWISE SPECIFIED DIMENSIONS ARE IN INCHES	EMBRY-RIDDLE AERONAUTICAL UNIVERSITY DAYTONA BEACH FLORIDA			
.XX ± .01	SIZE D	DATE 4/19/93	SCALE 1:10	DRAWN BY G. TELLA
.XXX ± .001	TITLE AFT FUSELAGE ASSEMBLY			
ANGLES ± 1/2°	DRAWING NO. 421S9303B201			SHEET 01

FOLDOUT FRAME

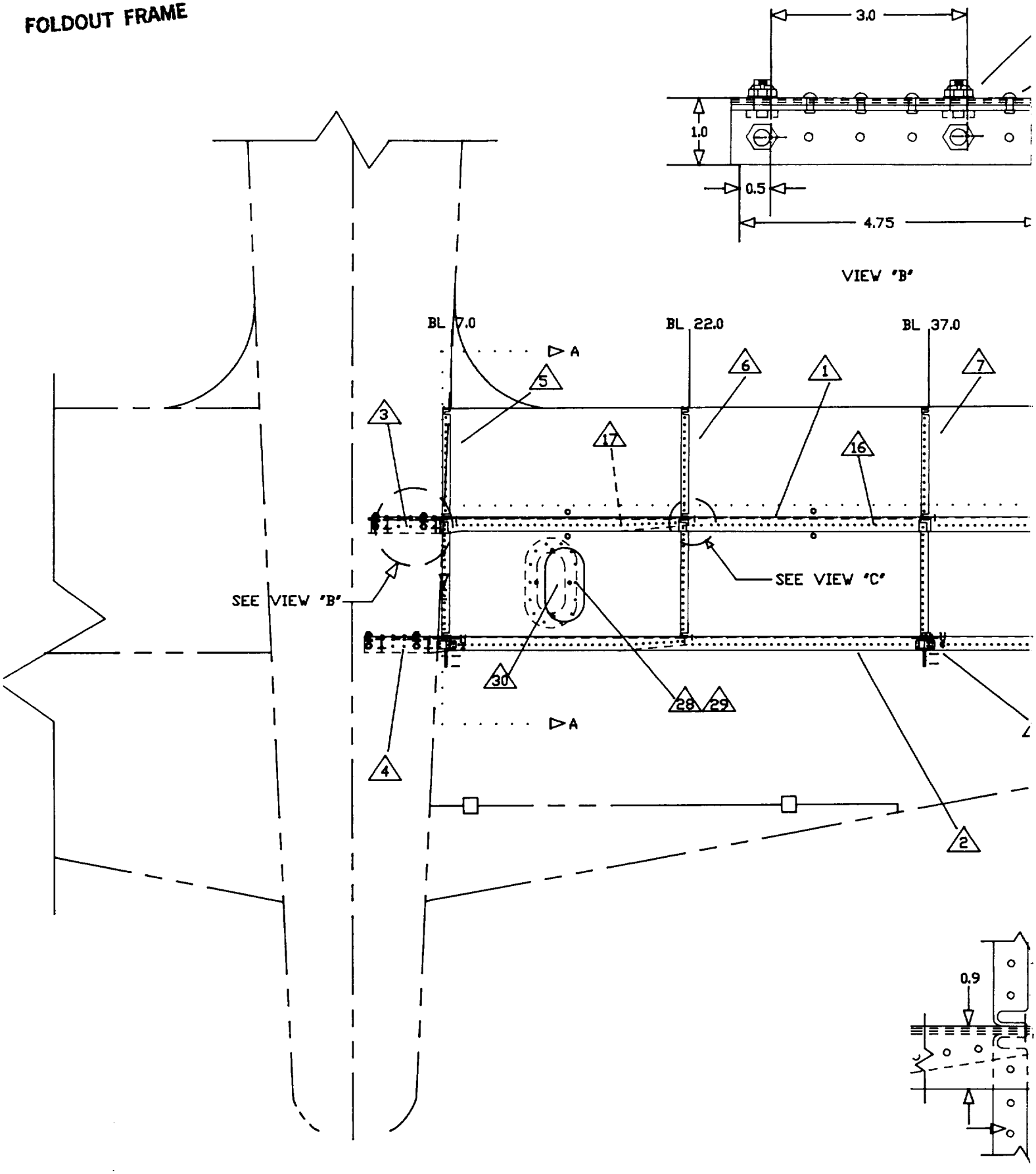

2.

FOLDOUT FRAME

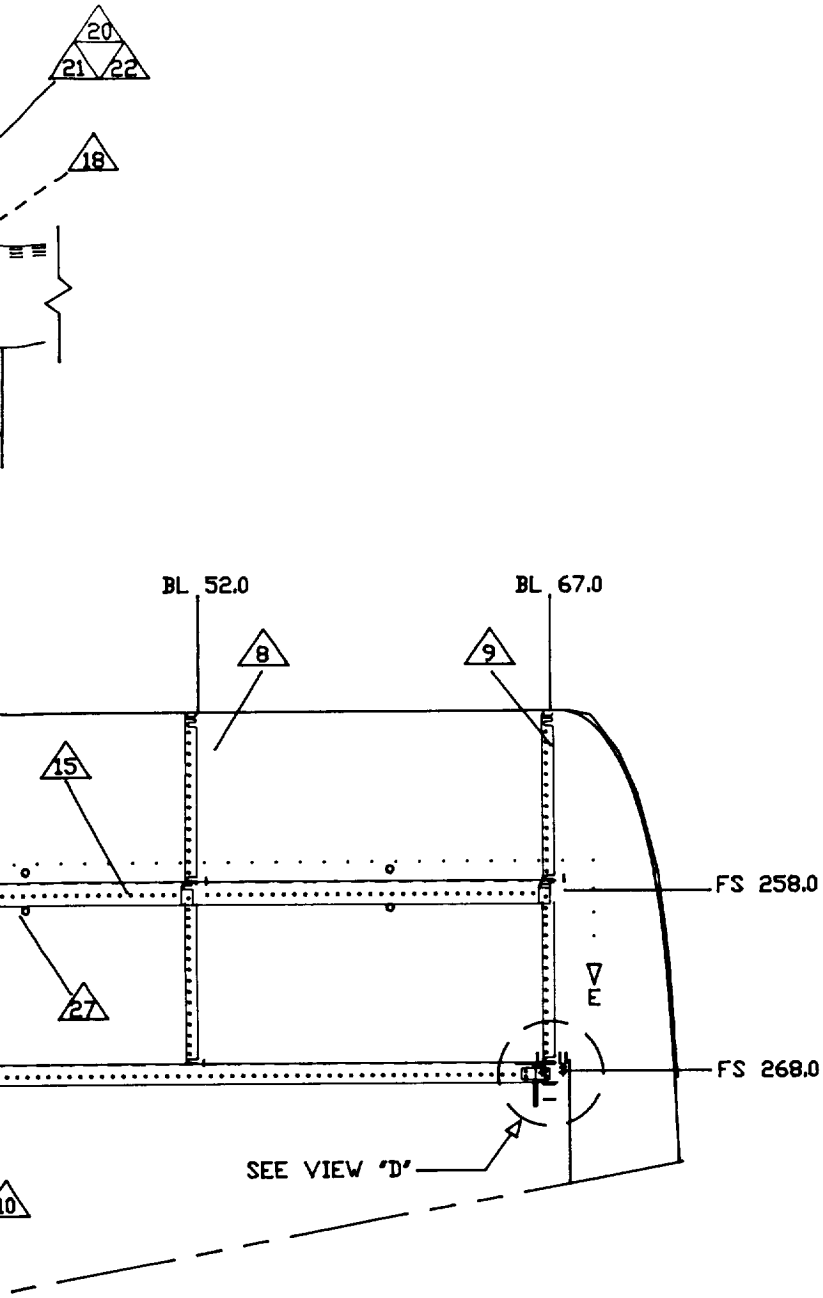

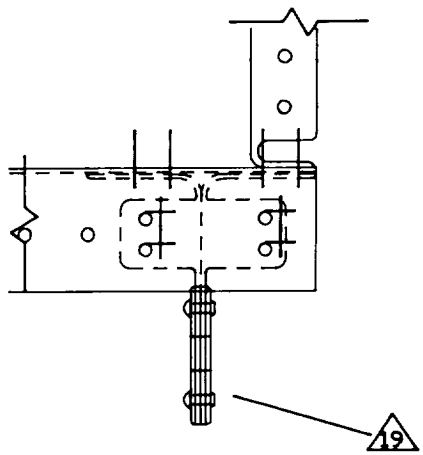

VIEW "D"

ITEM	QTY	DESCRIPTION	IDENTIFICAT
30	1	ACCESS PANEL	2024-T3 (0
29	4	BLIND NUTS	AN362-F62
28	4	MACHINE SCREWS	AN500-6-3
27	8	DRAIN HOLE	--
26	2	REAR SPAR TRIPLER	2024-T3 (
25	1	REAR SPAR DOUBLER	2024-T3 (
24	2	FRONT SPAR TRIPLER	2024-T3 (
23	1	FRONT SPAR DOUBLER	2024-T3 (
22	16	WASHER (FLAT)	AN960PD41
21	16	BOLT	AN4K-6
20	16	NUT (CASTELIATED)	AN310-D4
19	24	HINGE RIVET	MS20430D3
18	28	INTERFACE RIVET	MS20430D3
17	124	INBOARD SPAR/SKIN RIVET	MS20426D3
16	124	MID SPAR/SKIN RIVET	MS20426D3
15	528	OUTBOARD SPAR/RIB RIVET	MS20426D3
14	53	LIGHTENING HOLE	--
13	1	SKIN	2024-T3 (
12	1	OILLITE BEARING	--
11	3	NUT, BOLT (NOT SHOWN)	AN3-3/362F
10	3	ELEVATOR HINGE	2024-T3 (0
9	1	RIB #5	2024-T3 (0
8	1	RIB #4	2024-T3 (0
7	1	RIB #3	2024-T3 (0
6	1	RIB #2	2024-T3 (0
5	1	RIB #1	2024-T3 (0
4	1	FUSELAGE INTERFACE (RS)	2024-T3 (0
3	1	FUSELAGE INTERFACE (FS)	2024-T3 (0
2	1	REAR SPAR	2024-T3 (0
1	1	FRONT SPAR	2024-T3 (0

PARTS LIST

UNLESS OTHERWISE SPECIFIED DIMENSIONS TOLERANCES

.XX ± .01

.XXX ± .001

ANGLES ± 1/2°

EMBRY-RIDDLE AERONAUTICAL UNIVERSITY
DAYTONA BEACH FLORIDA

SIZE D | DATE 4/19/93 | SCALE 1/20 | DRAWN BY M. SINGE

TITLE HORIZONTAL TAIL STRUCTURE

DRAWING NO. 421S9303B202 | SHE

FOLDOUT FRAME

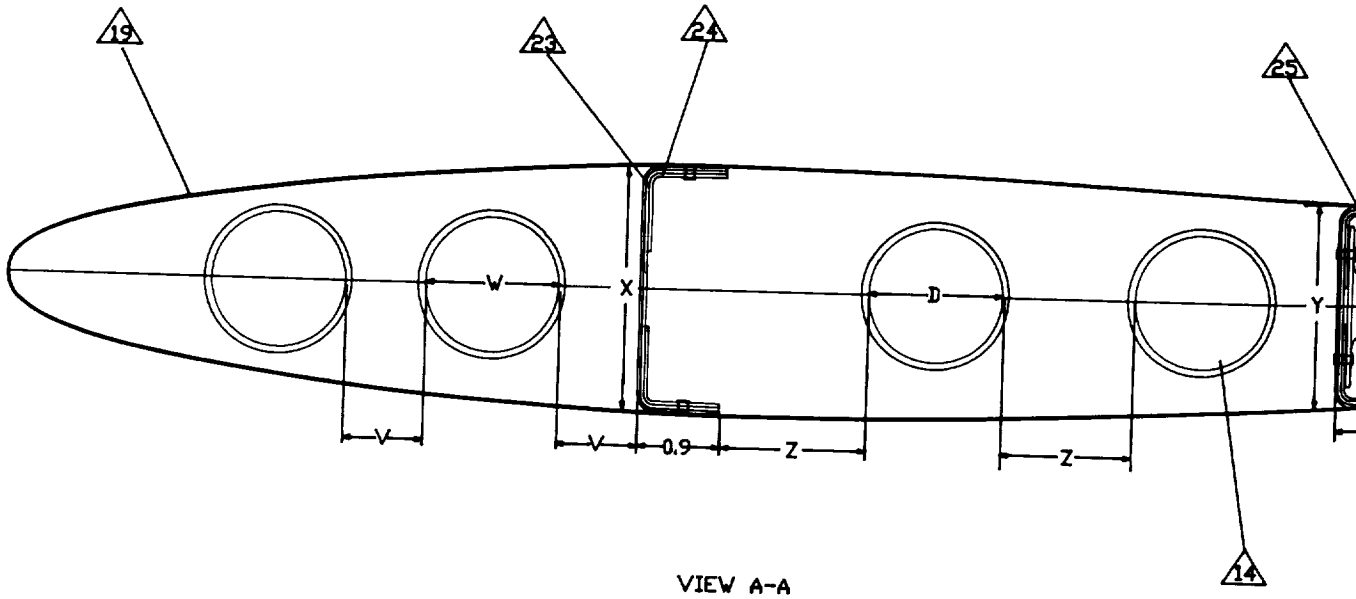

VIEW A-A

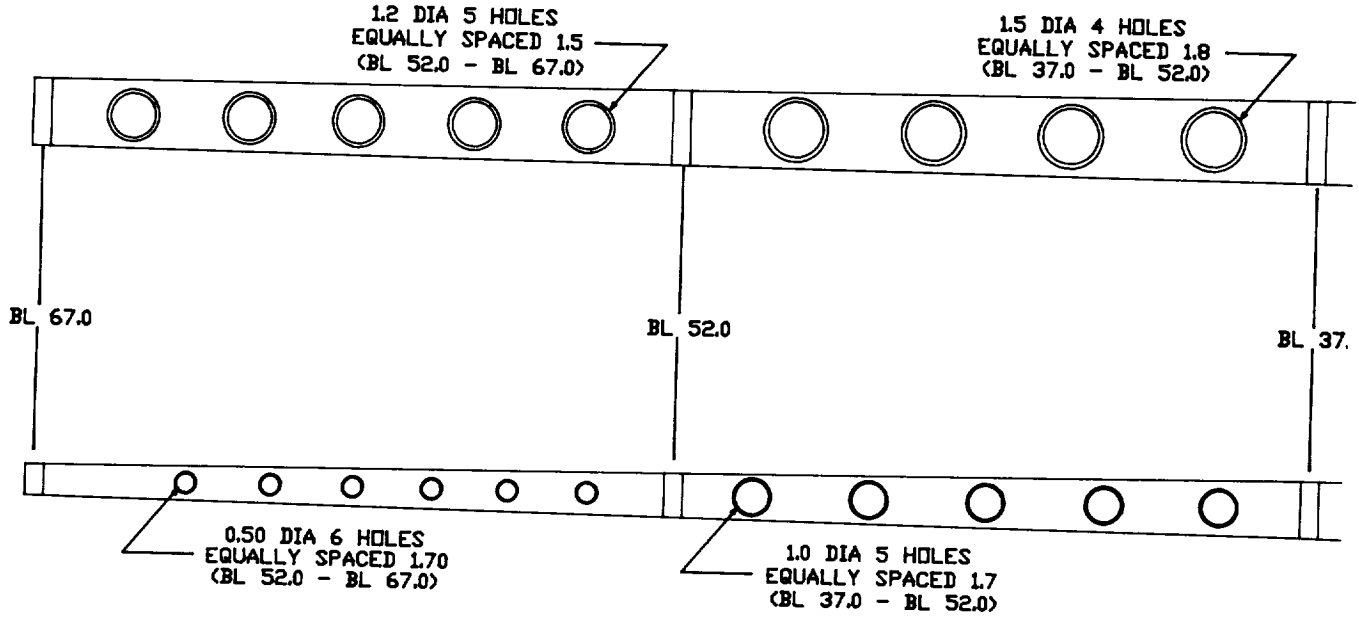

VIEW E-E
FRONT SPAR
REAR SPAR

2.

FOLDOUT FRAME

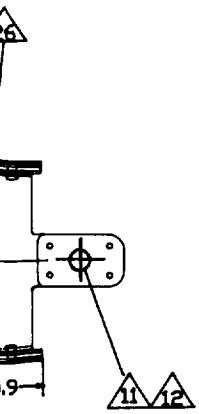

RIB SPECIFICATION WITH RESPECT TO BUTTLINE

BL	X	Y	D	Z	W	V	M	N
7.0	2.68	2.19	1.5	1.5	1.5	0.38	2	2
22.0	2.44	2.02	1.35	0.4	1.5	0.38	4	2
37.0	2.20	1.58	1.35	0.4	1.5	0.38	4	2
52.0	1.98	1.20	1.00	0.7	1.5	0.38	4	2
67.0	1.80	0.84	0.6	1.0	1.5	0.38	4	2

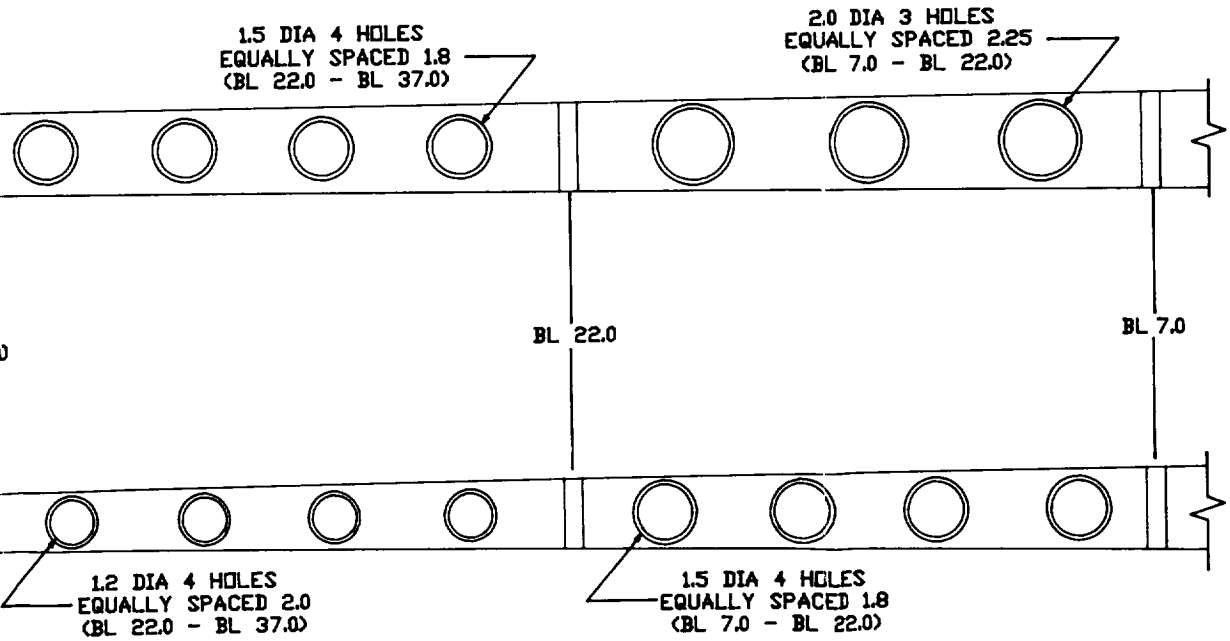

UNLESS OTHERWISE SPECIFIED	EMBRY-RIDDLE AERONAUTICAL UNIVERSITY DAYTONA BEACH FLORIDA			
.XX ± .01	SIZE D	DATE 4/19/93	SCALE 1/20	DRAWN BY M. SINGER
.XXX ± .001	TITLE HORIZONTAL TAIL STRUCTURE			
ANGLES ± 1/2°	DRAWING NO. 421S9303B202			SHEET 02

FOLDOUT FRAME

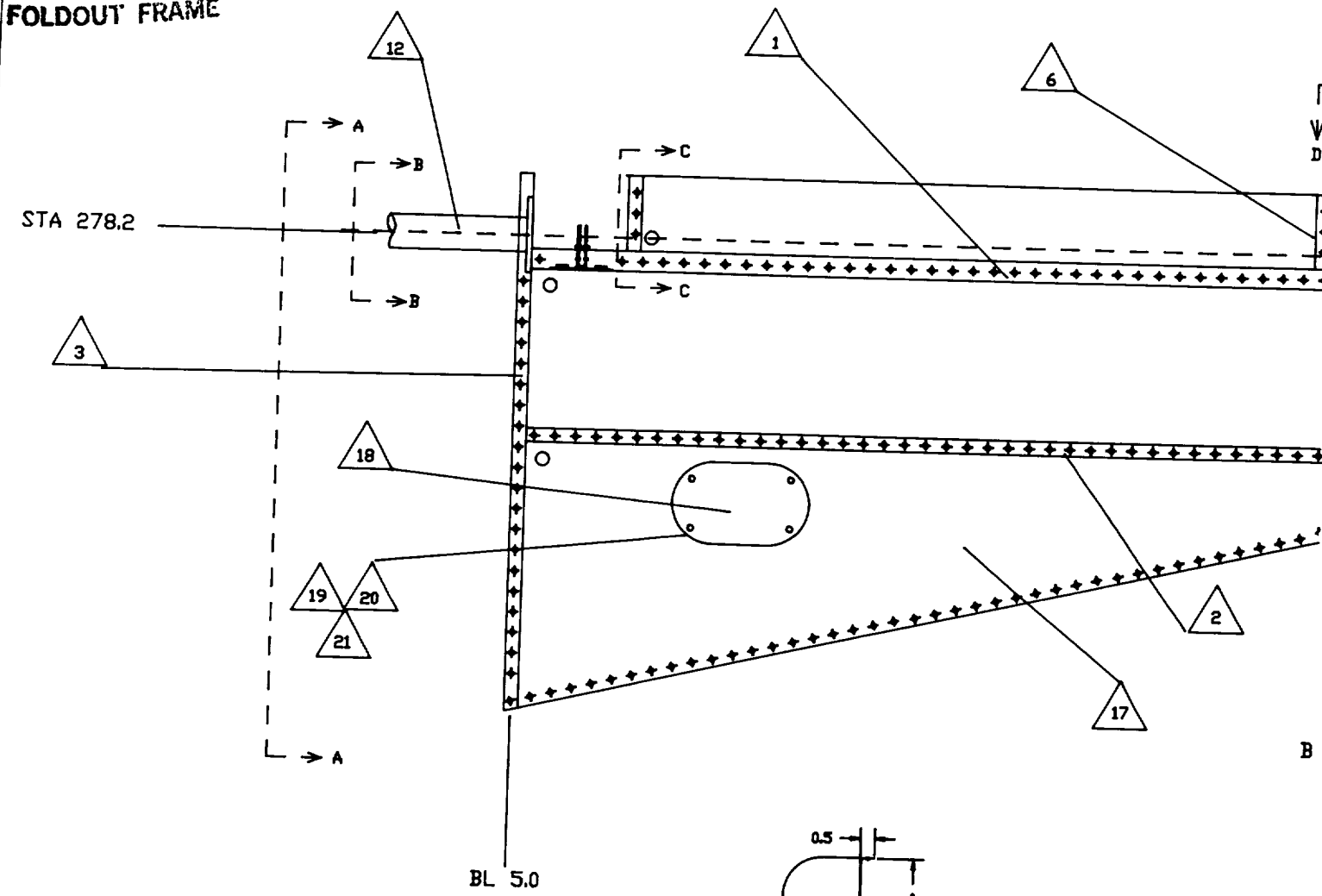

BL	A
8.5	2.8
30.5	1.75
58.5	.65

VIEW C-C

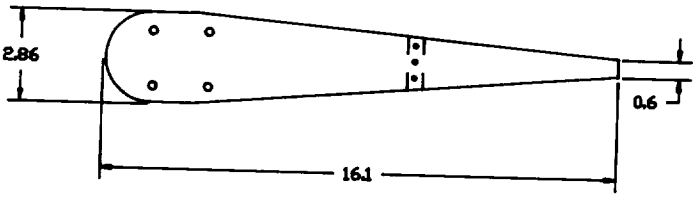

VIEW A-A

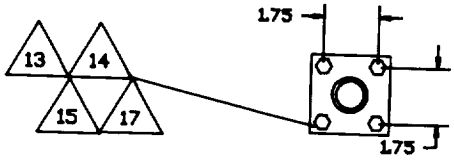

VIEW B-B

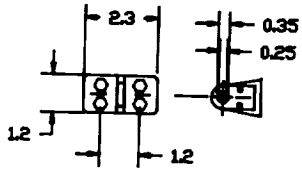

VIEW D-D

1.75

2.

FOLDOUT FRAME

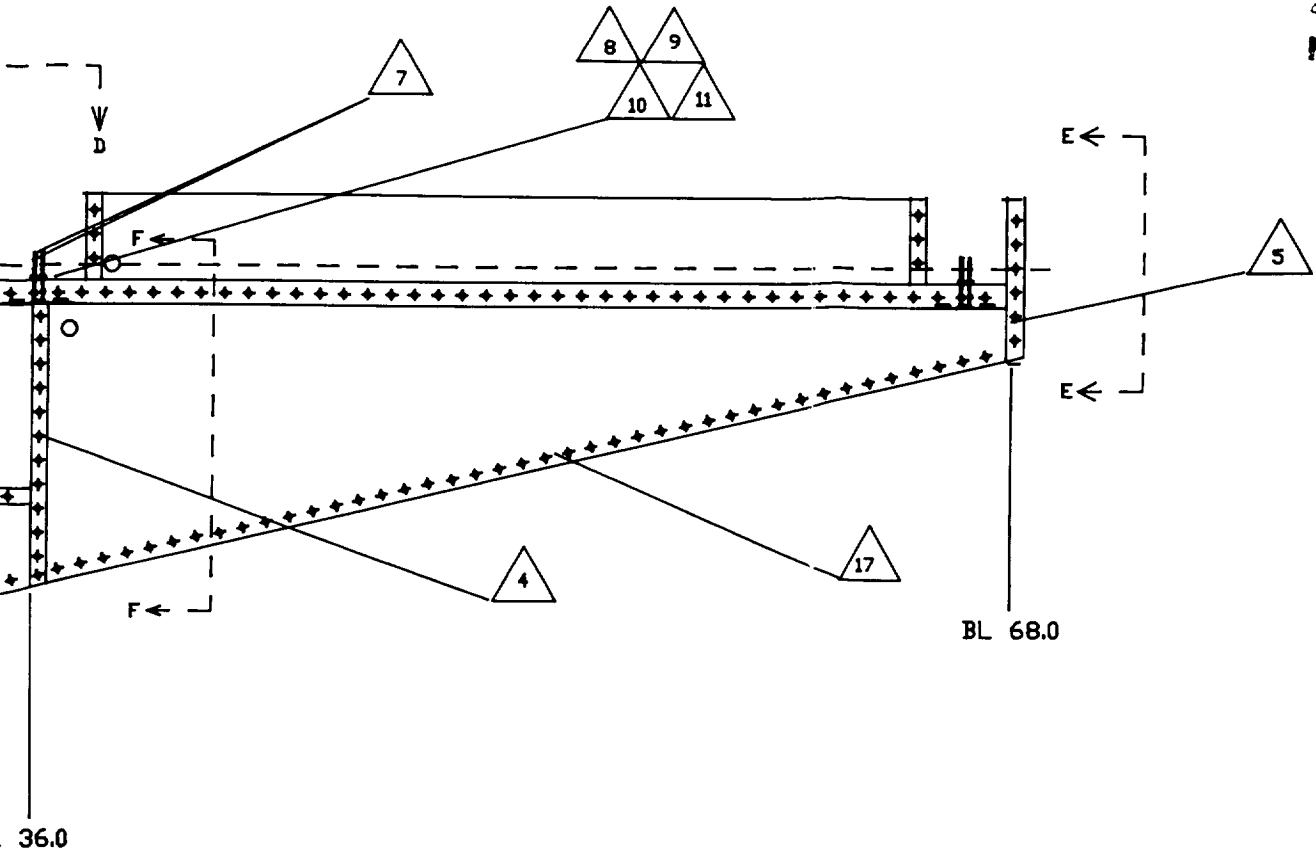

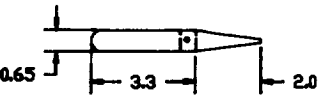

VIEW E-E

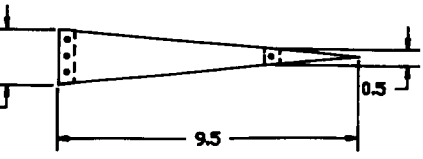

VIEW F-F

20	4	NUT, HIDDEN	AN362-F624
19	4	SCREW, MACHINE	AN500-6-3
18	1	ACCESS PANEL, TRIM TAB T=.02	2024-T3 SHEE
17	400	RIVETS, STANDARD	MS20455DD3-4
16	-	SKIN (FLAT WRAPPED PANELS)T=.02	2024=T3 SHEE
15	4	NUT, HIDDEN	AN362-F428
14	4	WASHER	AN960-C416
13	4	BOLTS, STEEL	AN4H5A
12	1	ELEVATOR TORQUE TUBE	AL TUBE&SHEE
11	32	RIVETS, COUNTERSUNK	MS20426DD4-6
10	12	NUT, CASTELIATED	AN362-F1032
9	12	WASHER	AN960-3
8	12	BOLT, STEEL	AN3-3
7	3	HINGE, ELEVATOR (RITETED SHEET)	2024-T3 SHEE
6	4	RIB, LEADING EDGE T=.02	2024-T3 SHEE
5	1	RIB, TIP (HYDRO-PRESSED) T=.02	2024-T3 SHEE
4	1	RIB, MIDDLE(HYDRO-PRESSED)T=.02	2024-T3 SHEE
3	1	RIB, ROOT (HYDRO-PRESSED)T=.02	2024-T3 SHEE
2	1	SPAR, REAR (BREAK-FORMED)T=.02	2024-T3 SHEE
1	1	SPAR, FRONT (BREAK-FORMED)T=.02	2024-T3 SHEE
ITEM	QTY	DESCRIPTION	MATERIAL OR PART #

UNLESS OTHERWISE SPECIFIED TOLERANCES
.XX ± .01
XXX ± .001
ANGULAR
± 1/2°

EMBRY-RIDDLE AERONAUTICAL UNIVERSITY
DAYTONA BEACH FLORIDA

SIZE	DATE	SCALE	DRAWN BY
D	4-1-93	1/3	ROBERT HARVEY

TITLE
STRUCTURE, ELEVATOR

DRAWING NO.
421S9303B203

SHEET 1 OF

/.

FOLDOUT FRAME

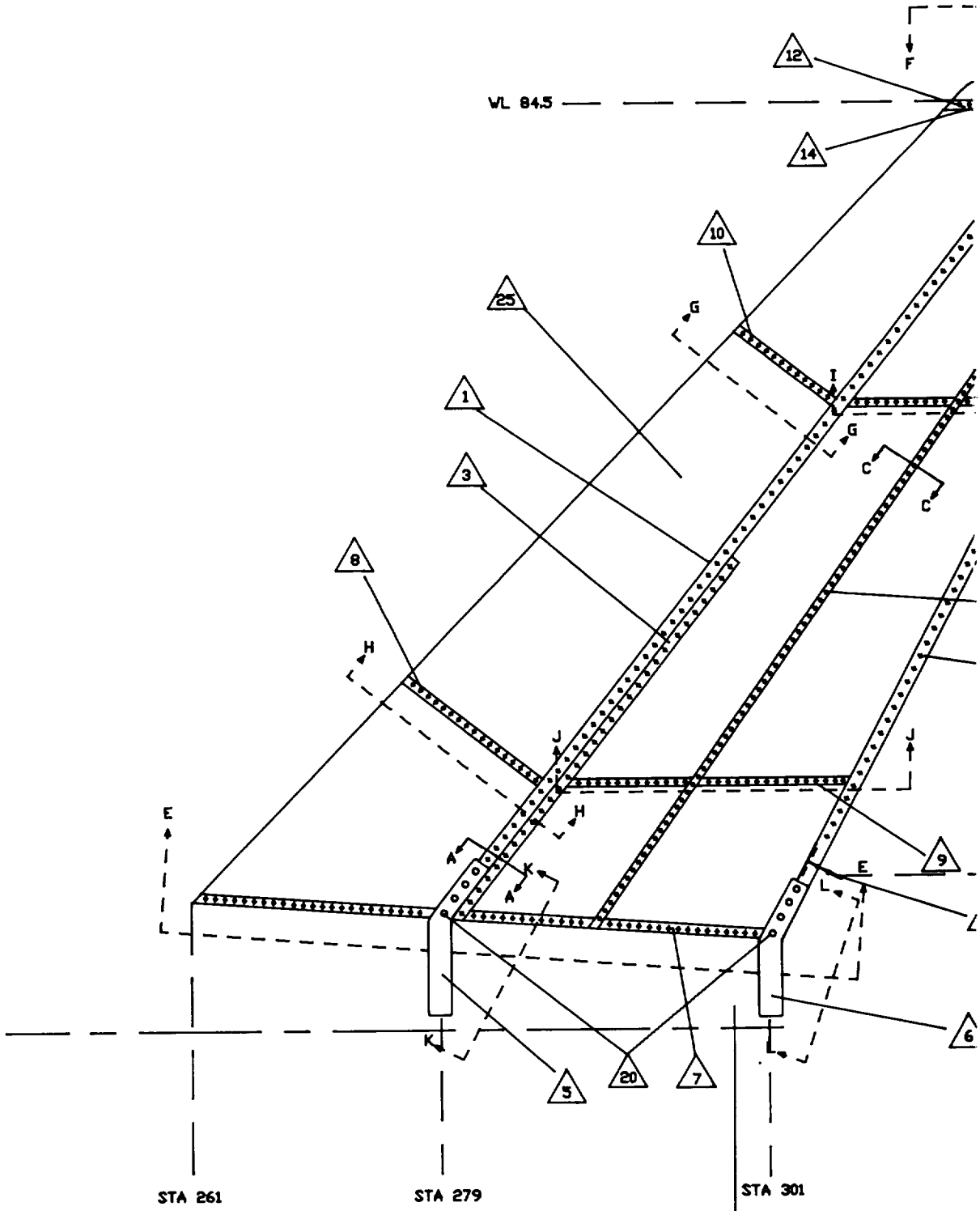

2.

FOLDOUT FRAME

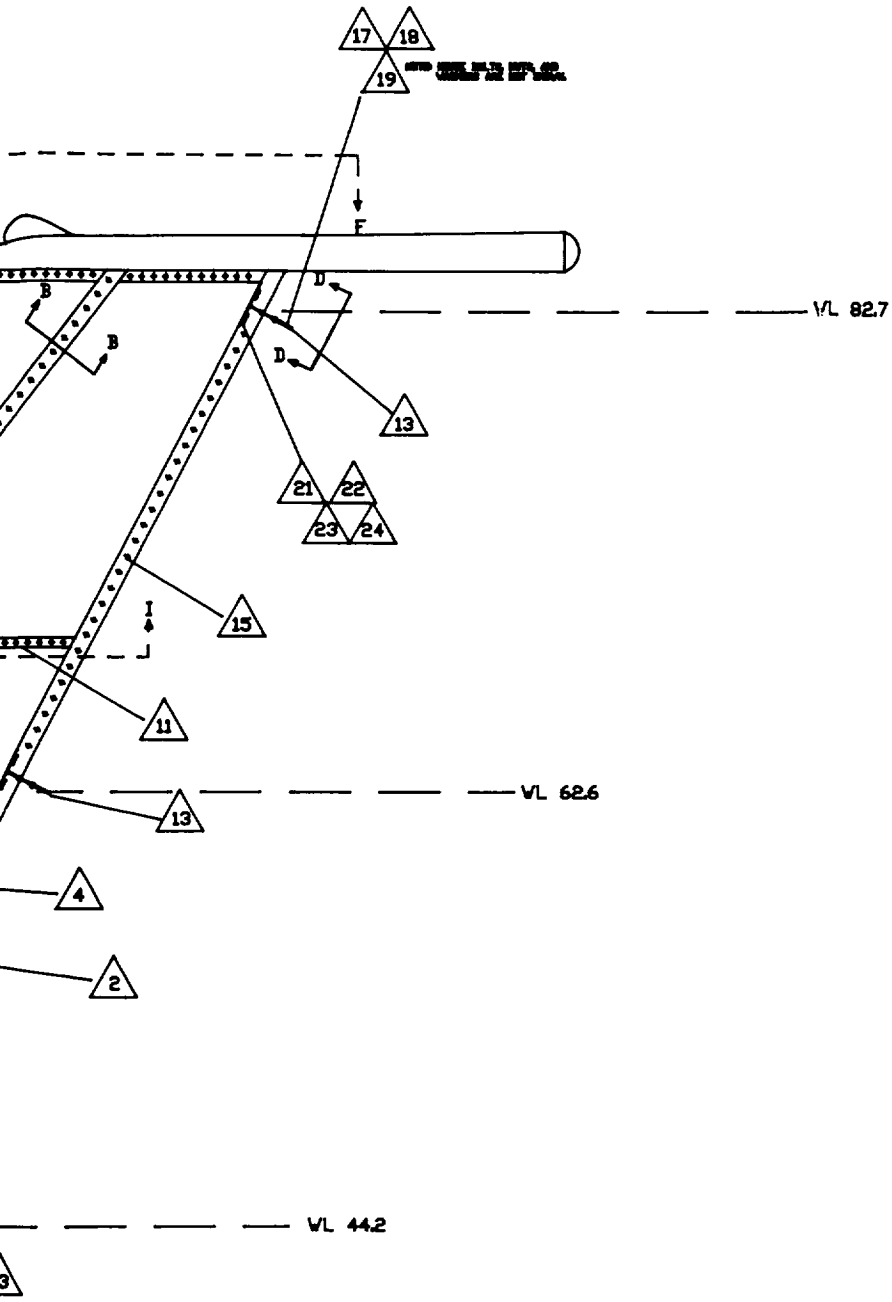

28	32	WASHER	AN960-C416
27	32	NUT, CASTELIATED	AN310-5
26	32	BOLT, STEEL	AN5-6
25	-	STABILIZER SKIN (NOT SHOWN) T=.02	2024-T3 AL
24	24	RIVETS	MS-20426DD4-
23	12	NUT, PLATE, SELF-LOCKING	AN362-F1032
22	12	WASHER, STEEL	AN960-3
21	12	BOLT, STEEL	AN3H3A
20	16	RIVETS 5/32" DIA.	MS20430DD5-7
19	3	WASHER, STEEL	AN960-C416
18	3	NUT, CASTELIATED	AN310-4
17	3	BOLT, STEEL	AN4-C4
16	40	RIVETS 3/32" DIA.	MS20430DD3-
15	275	RIVETS 3/32" DIA.	MS20426DD3-
14	450	RIVETS 1/16" DIA.	MS20426DD2-
13	3	RUDDER HINGE	2024 T3 SHE
12	1	TIP RIB T=.02	2024-T3 SHE
11	1	OUTBOARD CENTER RIB T=.02	2024-T3 SHE
10	1	OUTBOARD TIP RIB T=.02	2024-T3 SHE
9	1	INBOARD CENTER RIB T=.02	2024-T3 SHE
8	1	INBOARD TIP RIB T=.02	2024-T3 SHE
7	1	ROOT RIB T=.02	2024-T3 SHE
6	1	REAR SPAR INTERFRFACE BRACKET	CAST 2024-
5	1	FRONT SPAR INTERFACE BRACKET	CAST 2024-
4	1	L-STRINGER (BREAK FORMED T=.02)	2024-T3 AL
3	1	L-FORMER (BREAK FORMED T=.032)	2024-T3 AL
2	1	REAR SPAR (BREAK FORMED T=.05)	2024-T3 AL
1	1	FRONT SPAR (BREAK FORMED T=.05)	2024-T3 AL
ITEM	QTY	DESCRIPTION	MATERIAL OR PART #

DIMENSIONS TOLERANCES UNLESS OTHERWISE SPECIFIED DECIMAL

.XX ± .01
.XXX ± .001

ANGLES
± 1/2°

EMBRY-RIDDLE AERONAUTICAL UNIVERSITY
DAYTONA BEACH FLORIDA

SIZE	DATE	SCALE	DRAWN BY
D	4-1-93	1/4	ROBERT HARVE

TITLE
STRUCTURE, VERTICAL STABILIZER

DRAWING NO.
421S9303B204

SHE
1 OF

FOLDOUT FRAME

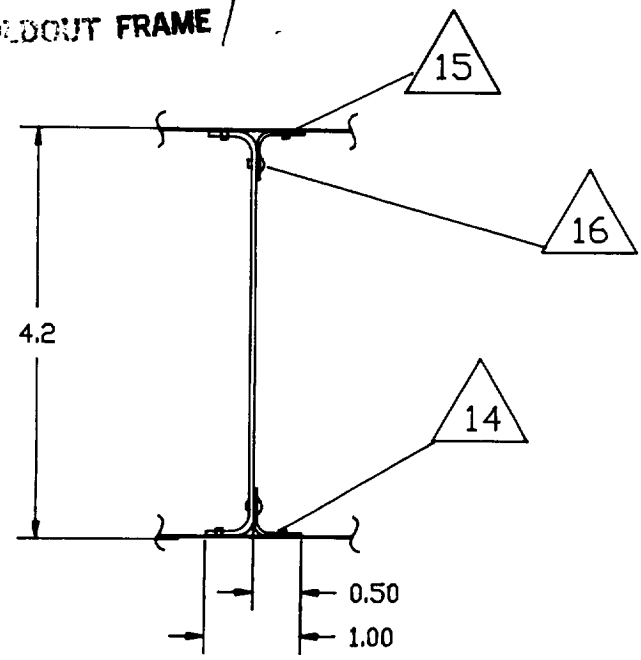

VIEW A-A

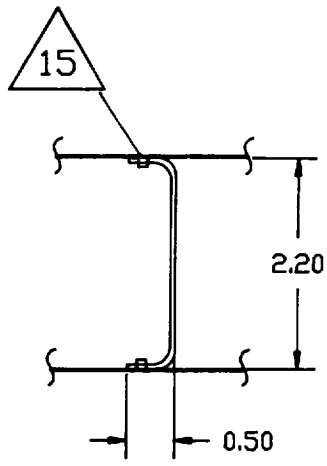

VIEW B-B

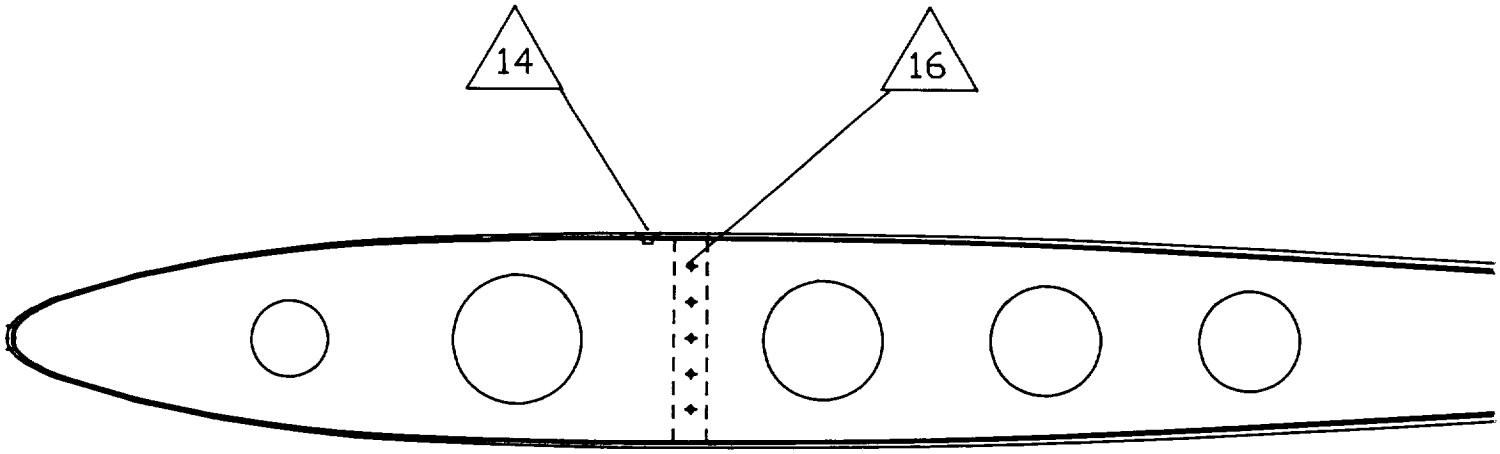

VIEW E-E

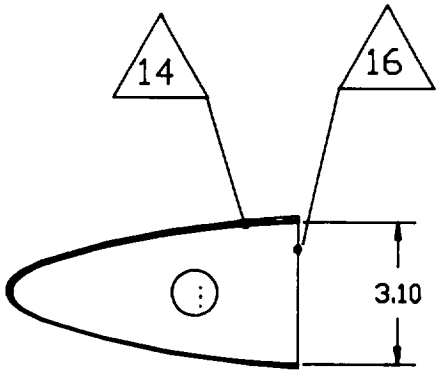

VIEW G-G

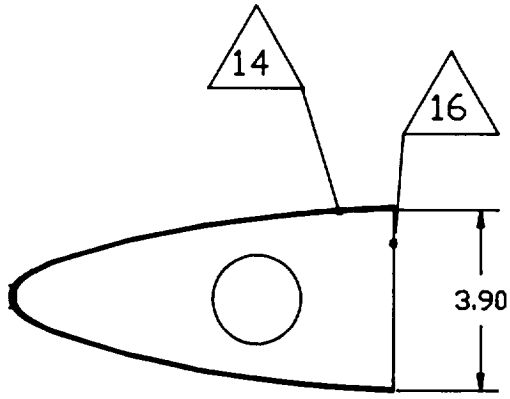

VIEW H-H

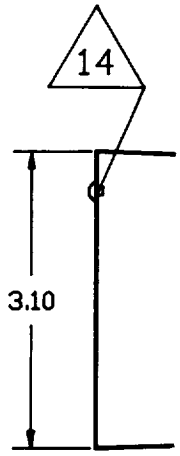

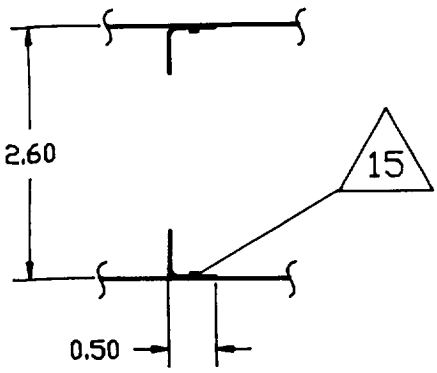

VIEW C-C

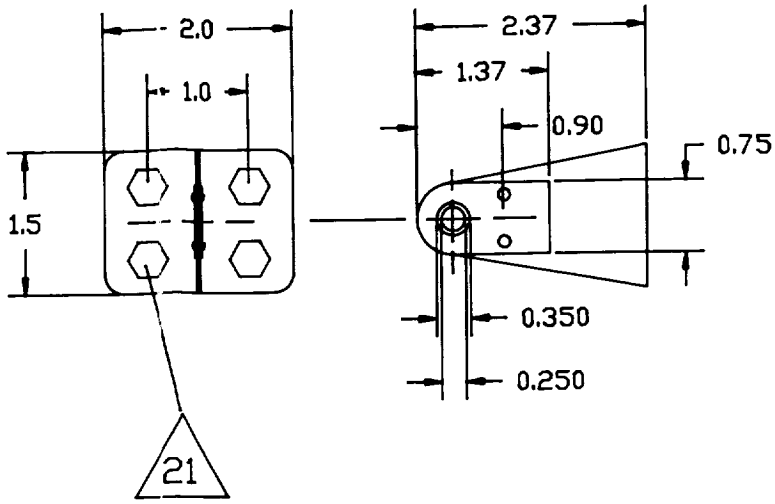

VIEW D-D

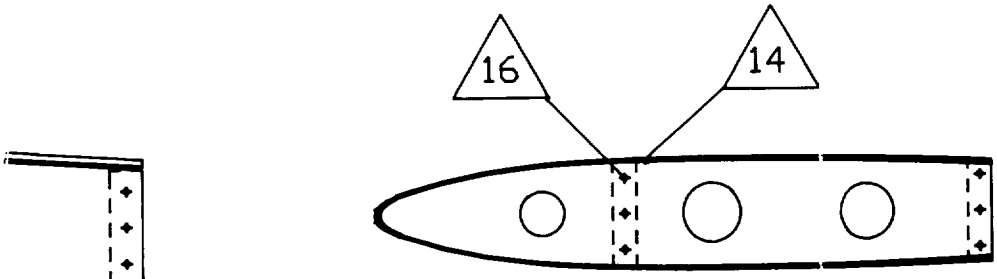

VIEW F-F

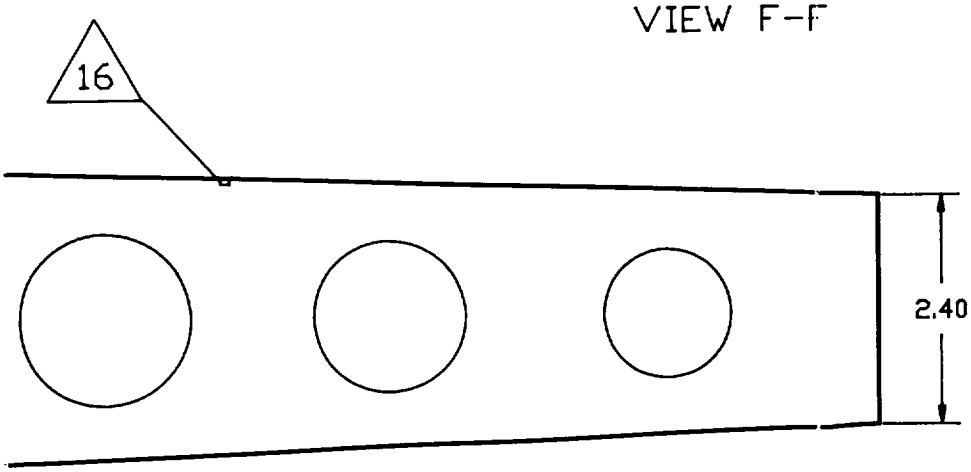

VIEW I-I

NOTE: VIEWS E-E, F-F, G-G, AND H-H ARE DRAWN TO 1/2 SCALE.

UNLESS OTHERWISE SPECIFIED DIMENSION TOLERANCES	EMBRY-RIDDLE AERONAUTICAL UNIVERSITY DAYTONA BEACH FLORIDA		
.XX ± .01	SIZE D	DATE 4-1-93	SCALE 1/1	DRAWN BY ROBERT HARVE
.XXX ± .001	TITLE STRUCTURE, VERTICAL STABILIZER			
ANGLES ± 1/2°	DRAWING NO. 421S9303B204			SHE 2 [

FOLDOUT FRAME

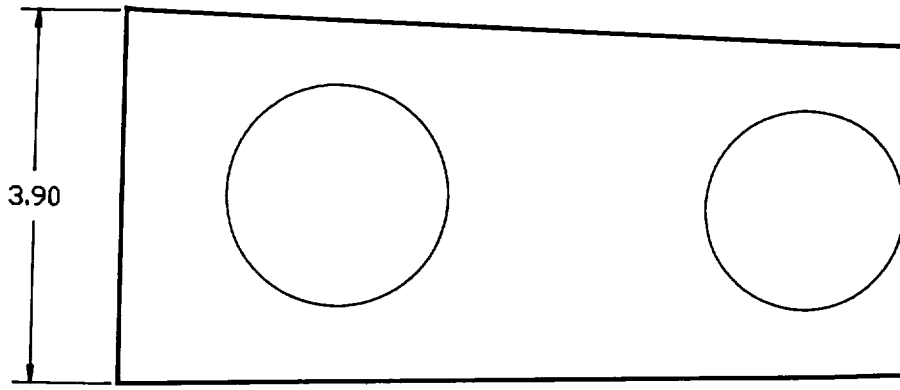

VIEW J-

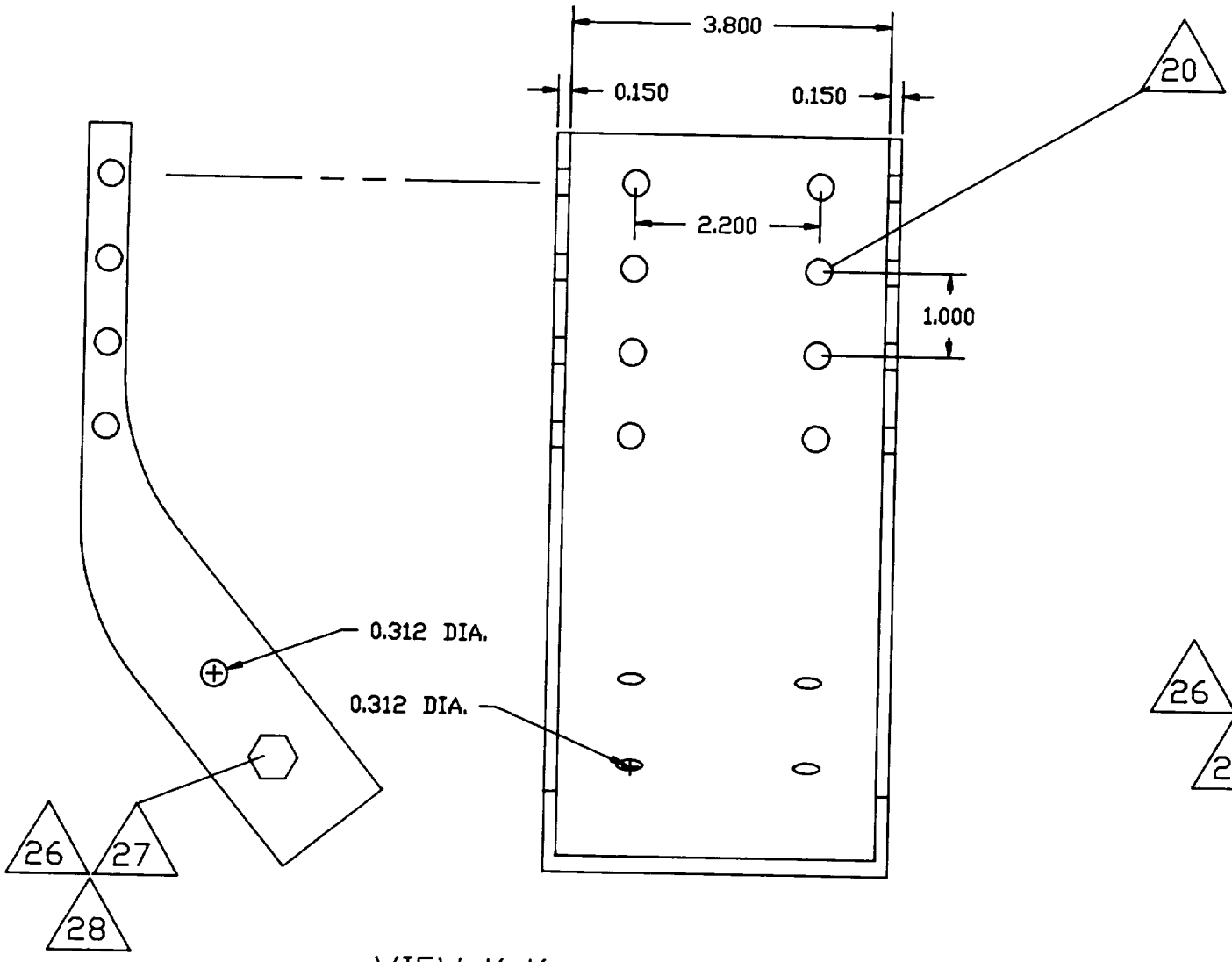

VIEW K-K

2.

FOLDOUT FRAME

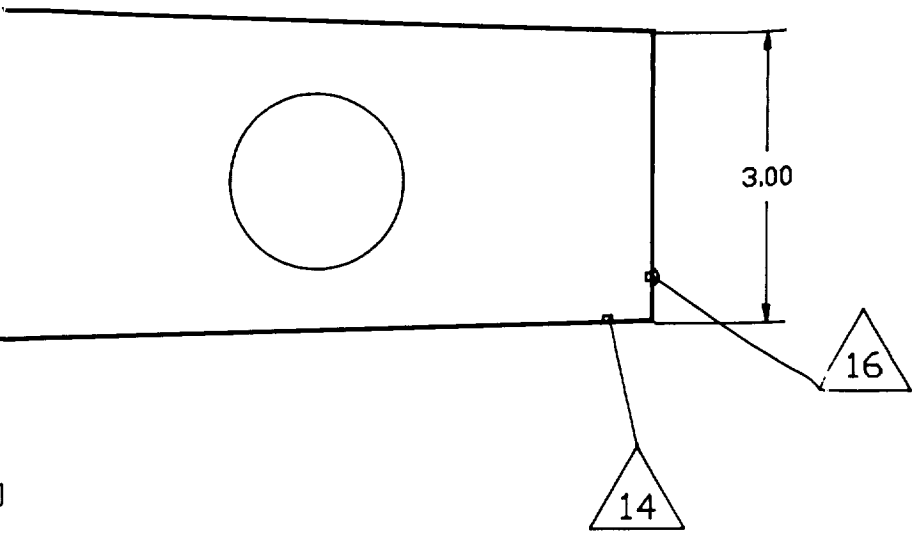

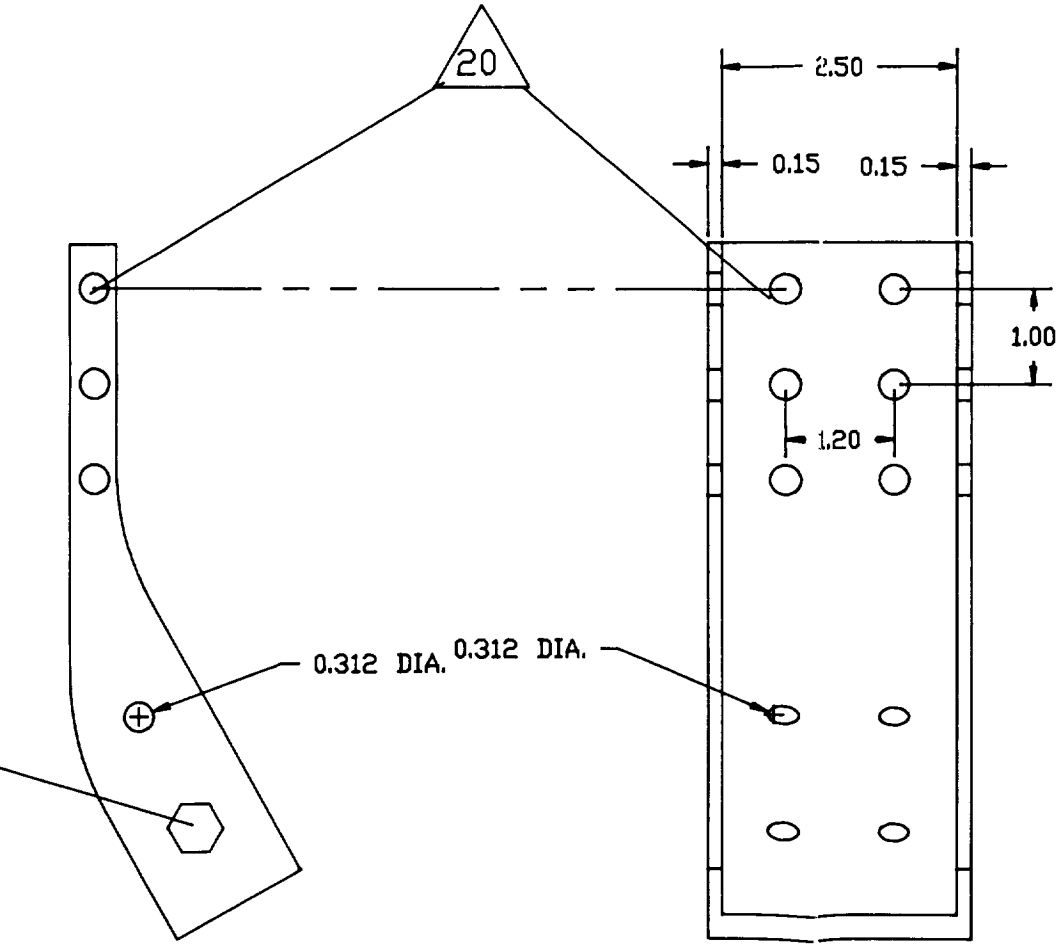

VIEW L-L

.XX ± .01 .XXX ± .001 ANGLES ± 1/2°	EMBRY-RIDDLE AERONAUTICAL UNIVERSITY DAYTONA BEACH FLORIDA			
	SIZE D	DATE 4-1-93	SCALE 1/1	DRAWN BY ROBERT HARVEY
	TITLE STRUCTURE, VERTICAL STABILIZER			
	DRAWING NO. 421S93038204			SHEET 3 OF

FOLDOUT FRAME

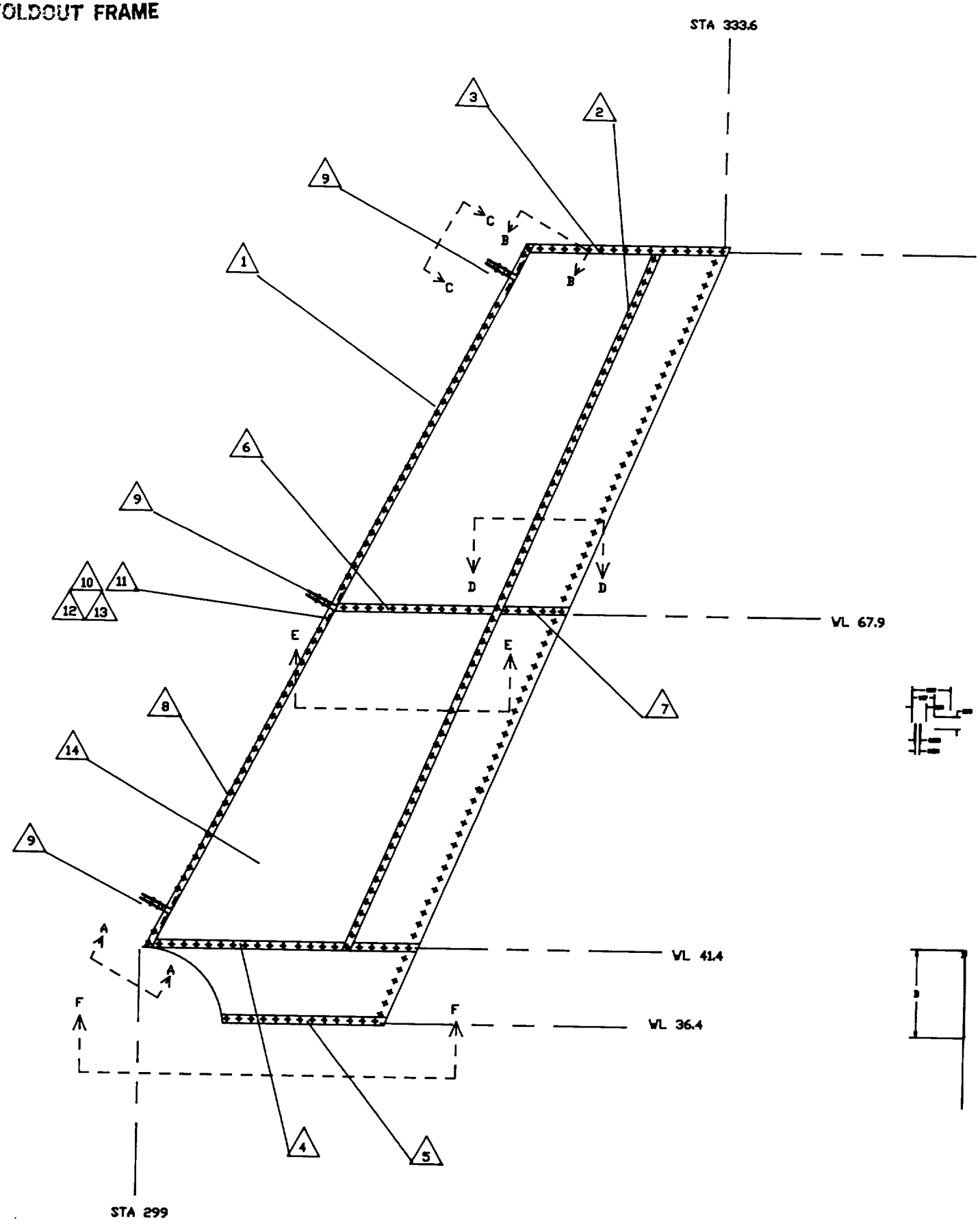

2.

FOLDOUT FRAME

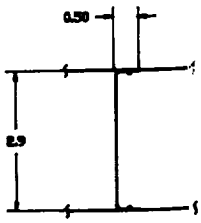

VIEW A-A

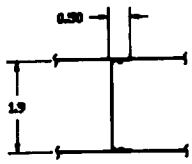

VIEW B-B

VL 89.4

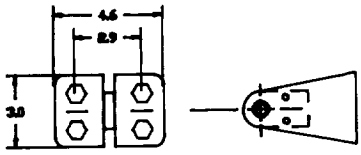

VIEW C-C

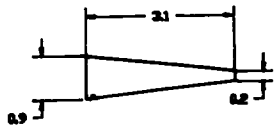

VIEW D-D

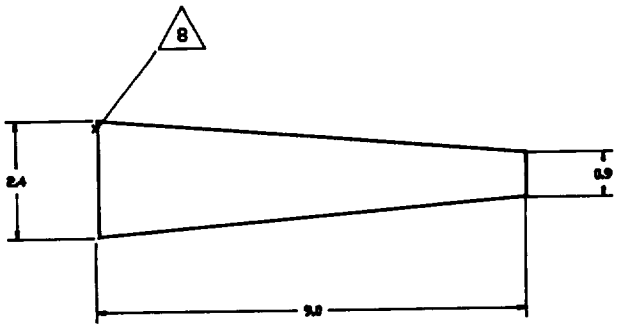

VIEW E-E

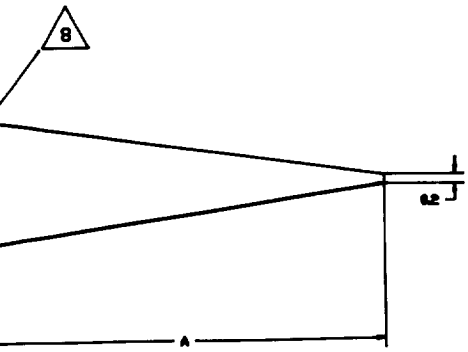

WL	A	B
36.4	1.9	9.5
41.4	2.9	17
89.9	1.9	11

VIEW F-F

NOTE: ALL VIEWS ARE 1/2 SCALE FOR CLARITY

14	-	SKIN, RUDDER (NOT SHOWN) T=.02	2024-T3 SHEE
13	24	RIVETS, COUNTERSUNK	MS-20426DD4-5
12	12	NUT, HIDDEN, SELF-LOCKING	AN362-F1032
11	12	WASHER	AN960-3
10	12	BOLT, STEEL	AN3-3
9	3	HINGE, FEMALE, RUDDER	2024-T3 SHEE
8	470	RIVETS, STANDARD	MS20455DD3-4
7	1	RIB, REAR, CENTER T=.02	2024-T3 SHEE
6	1	RIB, FRONT, CENTER T=.02	2024-T3 SHEE
5	1	RIB, ROOT (HYDRO-PRESSED) T=.02	2024-T3 SHEE
4	1	RIB, BOTTOM (HYDRO-PRESSED) T=.02	2024-T3 SHEE
3	1	RIB, TIP (HYDRO-PRESSED) T=.02	2024-T3 SHEE
2	1	SPAR, REAR (BREAK-FORMED) T=.02	2024-T3 SHEE
1	1	SPAR, FRONT (BREAK-FORMED) T=.02	2024-T3 SHEE
ITEM	QTY	DESCRIPTION	MATERIAL, OR PART #

DIMENSIONS IN INCHES UNLESS OTHERWISE SPECIFIED

.XX ± .01

.XXX ± .001

ANGLES ± 1/2°

EMBRY-RIDDLE AERONAUTICAL UNIVERSITY
DAYTONA BEACH FLORIDA

SIZE	DATE	SCALE	DRAWN BY
D	4-1-93	1/4	ROBERT HARVE

TITLE
STRUCTURE, RUDDER

DRAWING NO.
421S93038205

SHEE 1 1

FOLDOUT FRAME

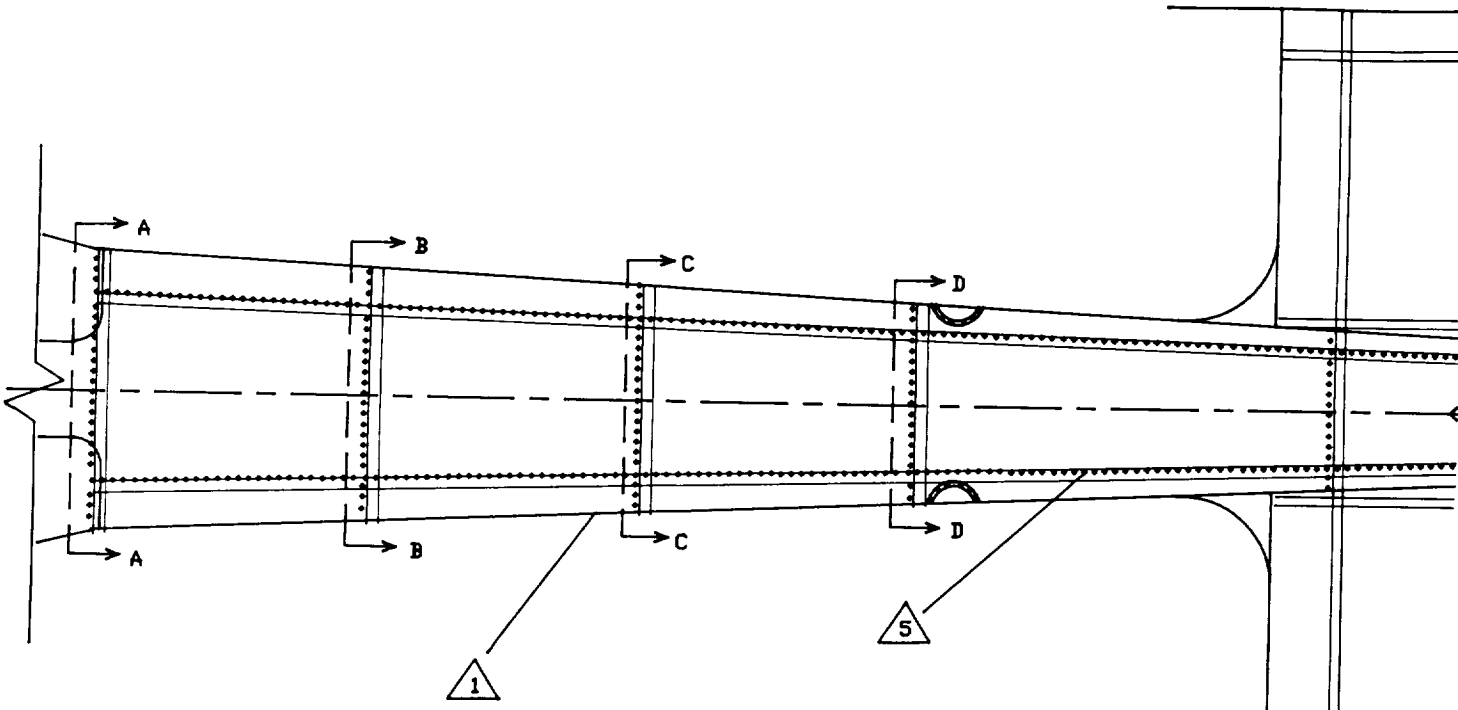

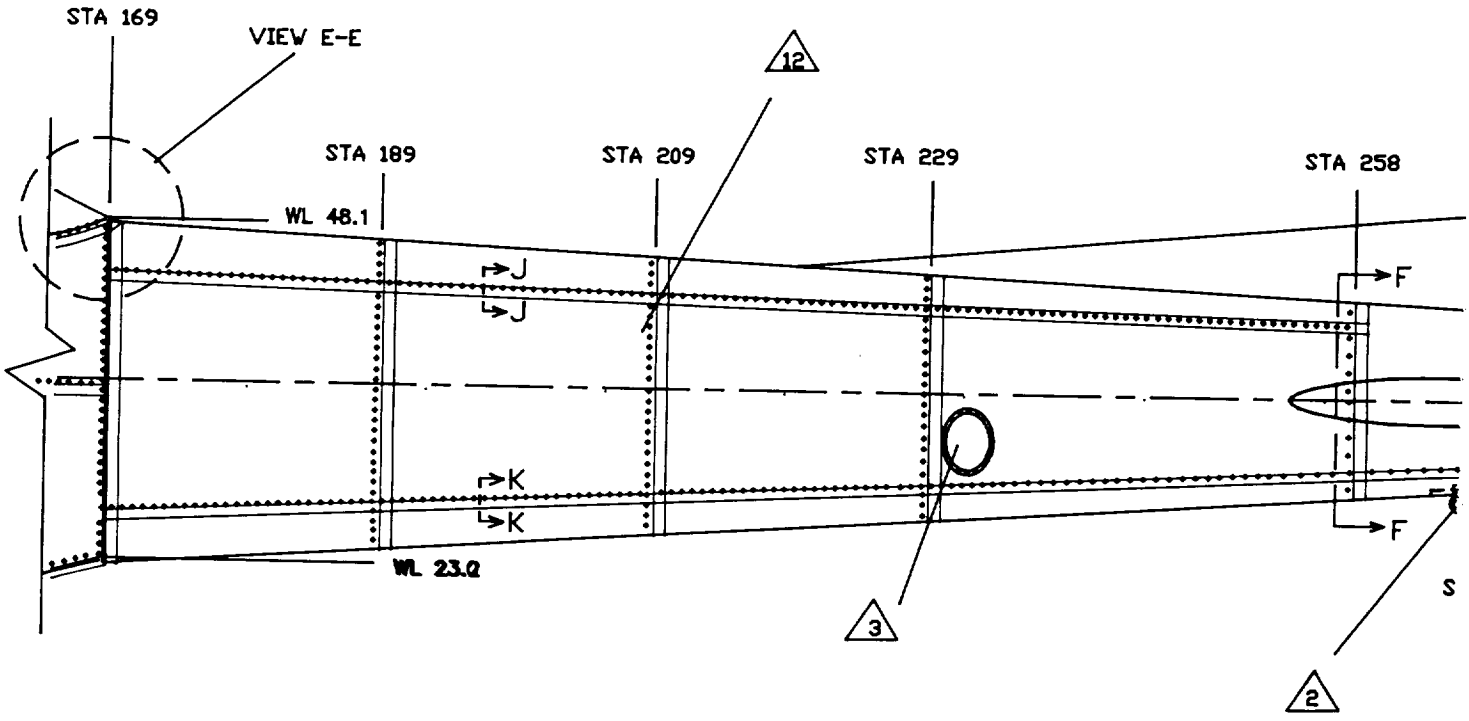

FOLDOUT FRAME 2

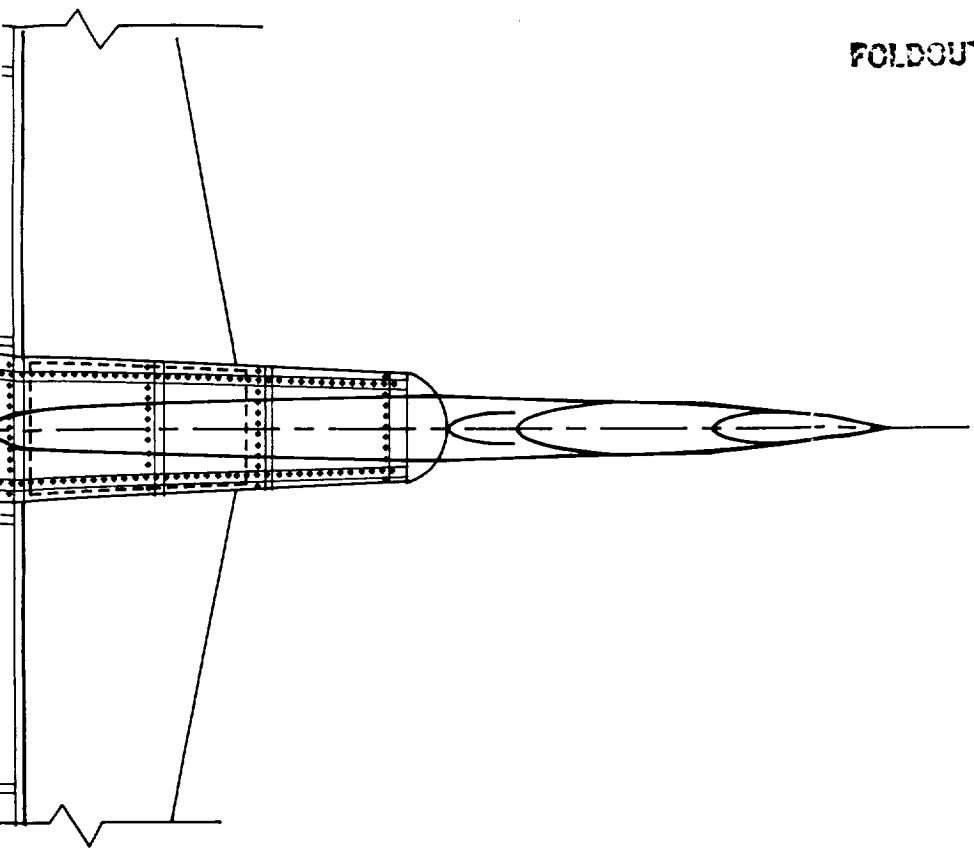

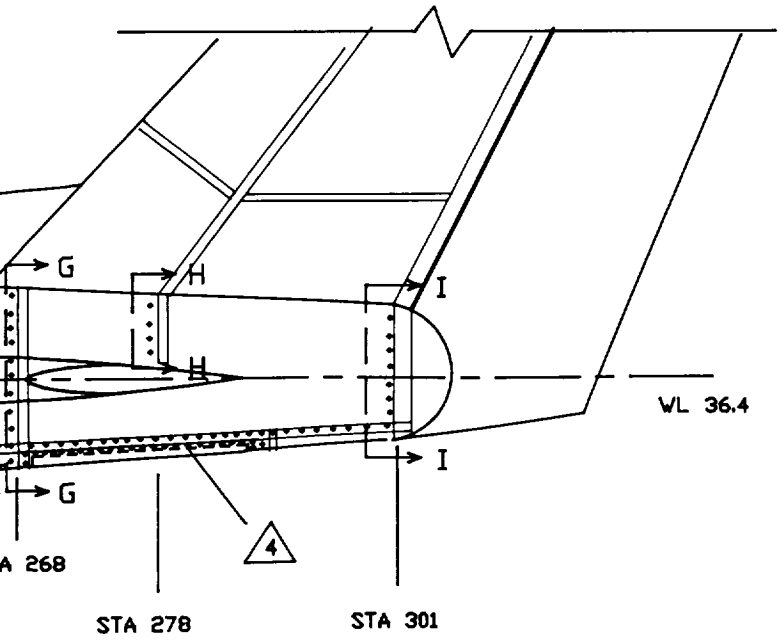

ITEM	QTY.	DESCRIPTION	SIZE OR NO.
14	1	WASHER, TYP.	AN970-7
13	1	NUT, TYP.	AN365-720
12	8	EMPENNAGE FORMER, 2024-T3 SHT.	0.025" THK
11	6	INTERFACE PLATE, 7075 CAST	
10	6	C-CHANNEL SPARS (SIZE VARIES)	ALUMINUM
9	12	MOUNTING BRACKET, 7075 CAST	0.1" THK
8	7	DOUBLER PLATE, 2024 SHT.	0.075" THK
7	64	RIVET, TYP.	MS20455D-4-5
6	116	RIVET, TYP.	MS20455D-4-7
5	1500	RIVET, TYP.	MS20455D-3-4
4	1	UNDERSIDE INSPECTION PANEL	ALUM. SHEET
3	2	SIDE INSPECTION PANELS	ALUM. SHEET
2	1	TIE DOWN BOLT, FORGED EYE	AN7 TYPE
1	1	SKIN, ALUM, 2024-T3 0.025" THK.	

PARTS LIST

UNLESS OTHERWISE SPECIFIED	EMBRY-RIDDLE AERONAUTICAL UNIVERSITY DAYTONA BEACH FLORIDA		
.XX ± .01	SIZE: D	DATE: 4/19/93	SCALE: 1/3	DRAWN BY: G. TELLA
.XXX ± .001	TITLE: EMPENNAGE ARRANGEMENT		
ANGLES ± 1/2°	DRAWING NO. 421S9303B206		SHEET 01

FOLDOUT FRAME

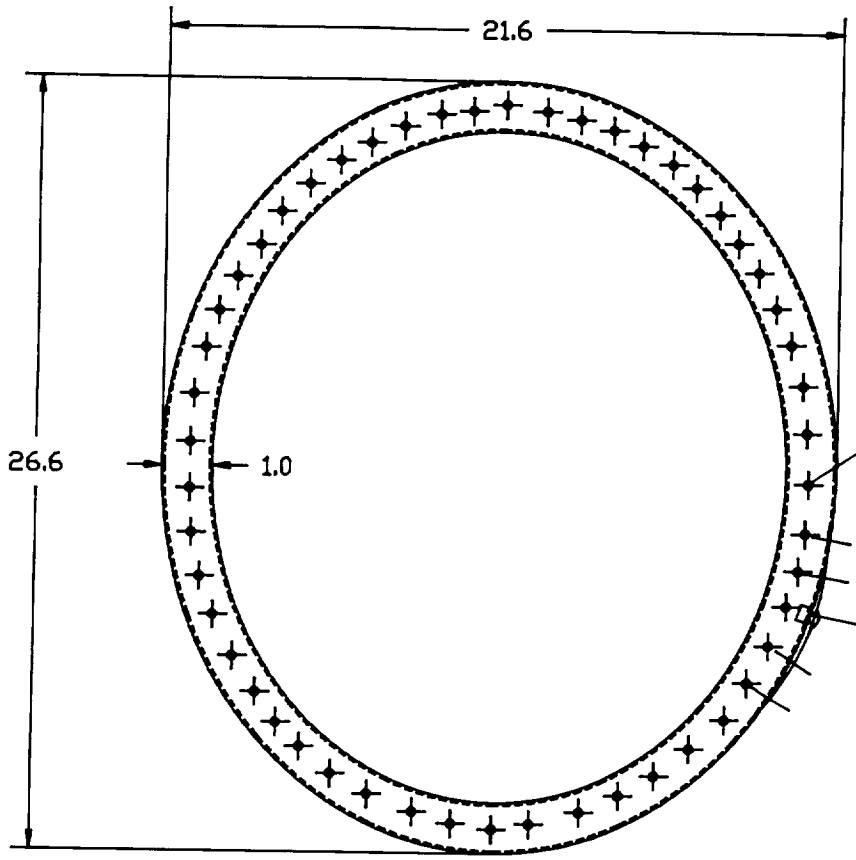

SECTION A-A
STA 169

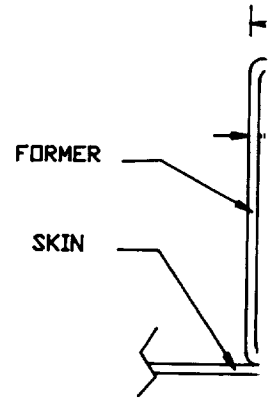

SEC

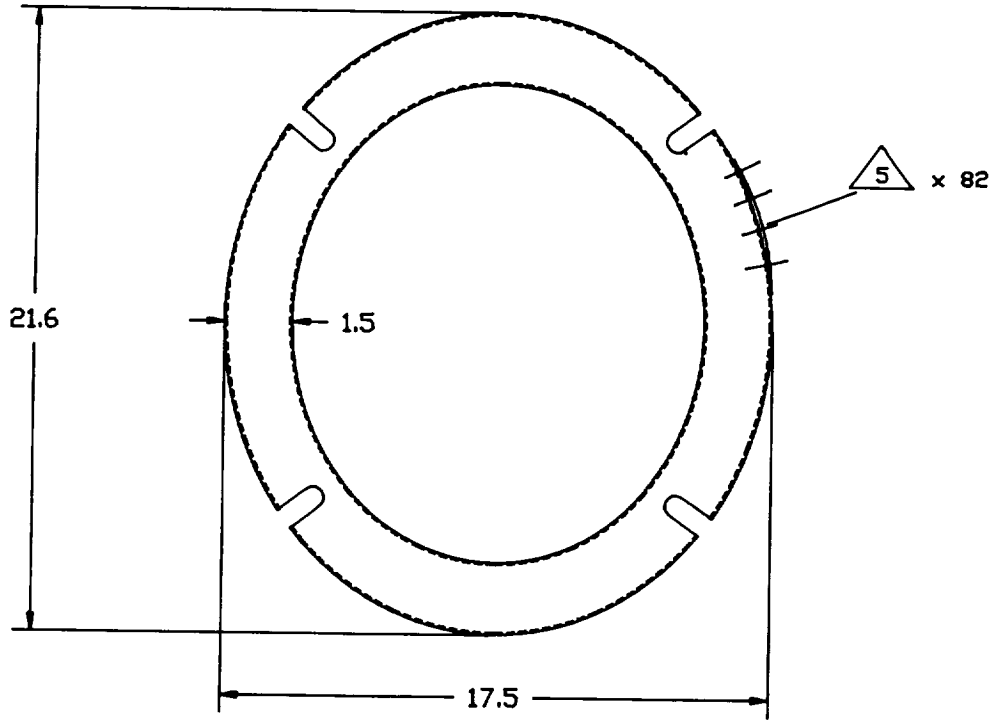

SECTION C-C
STA 209

2.

FOLDOUT FRAME

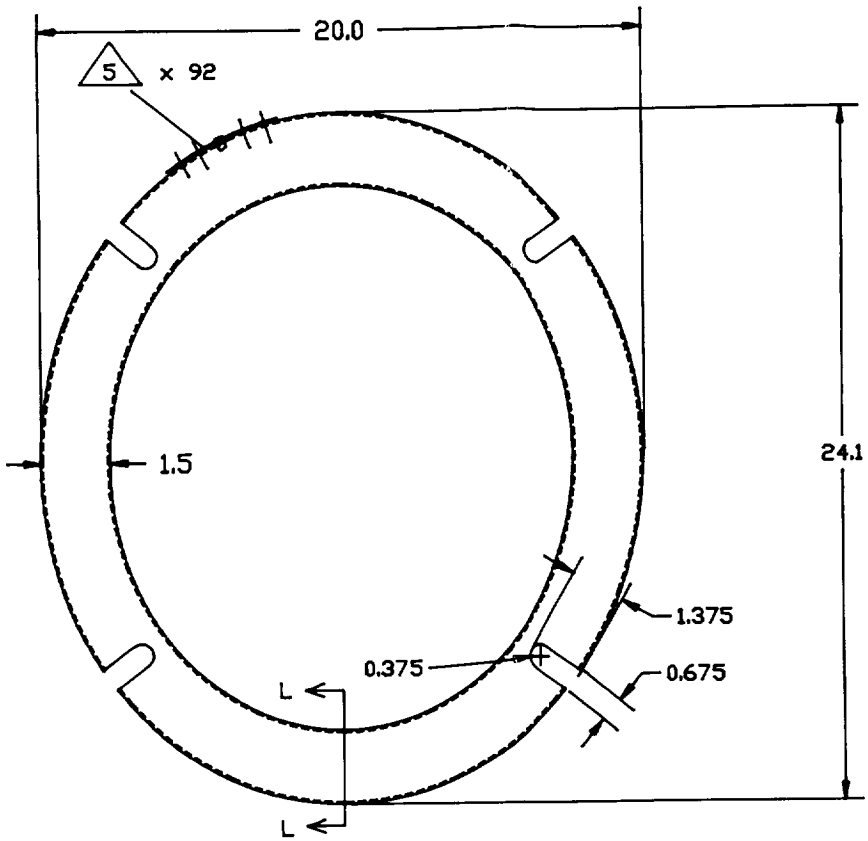

SECTION B-B
STA 189

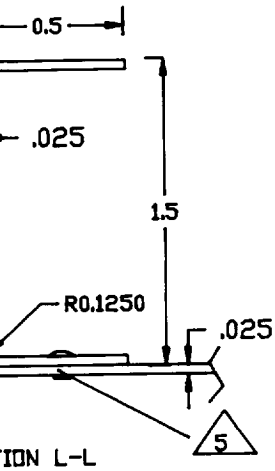

ION L-L

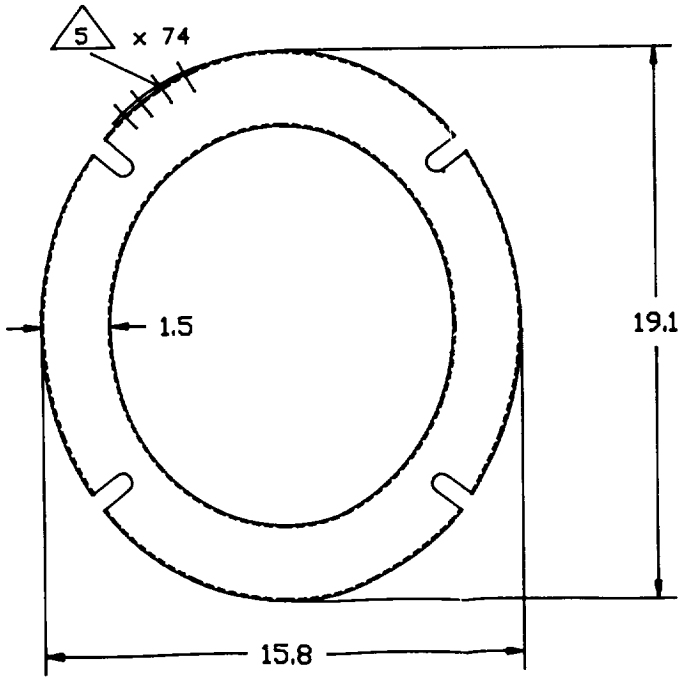

SECTION D-D
STA 229

NOTE: ALL FORMERS 0.025" 2024-T3

UNLESS OTHERWISE SPECIFIED DECIMAL	EMBRY-RIDDLE AERONAUTICAL UNIVERSITY DAYTONA BEACH FLORIDA			
.XX ± .01	SIZE D	DATE 4/19/93	SCALE 1:10	DRAWN BY G. TELLA
.XXX ± .001	TITLE EMPENNAGE FORMERS			
ANGULAR ± 1/2°	DRAWING NO. 421S9303B206			SHEE 02

FOLDOUT FRAME

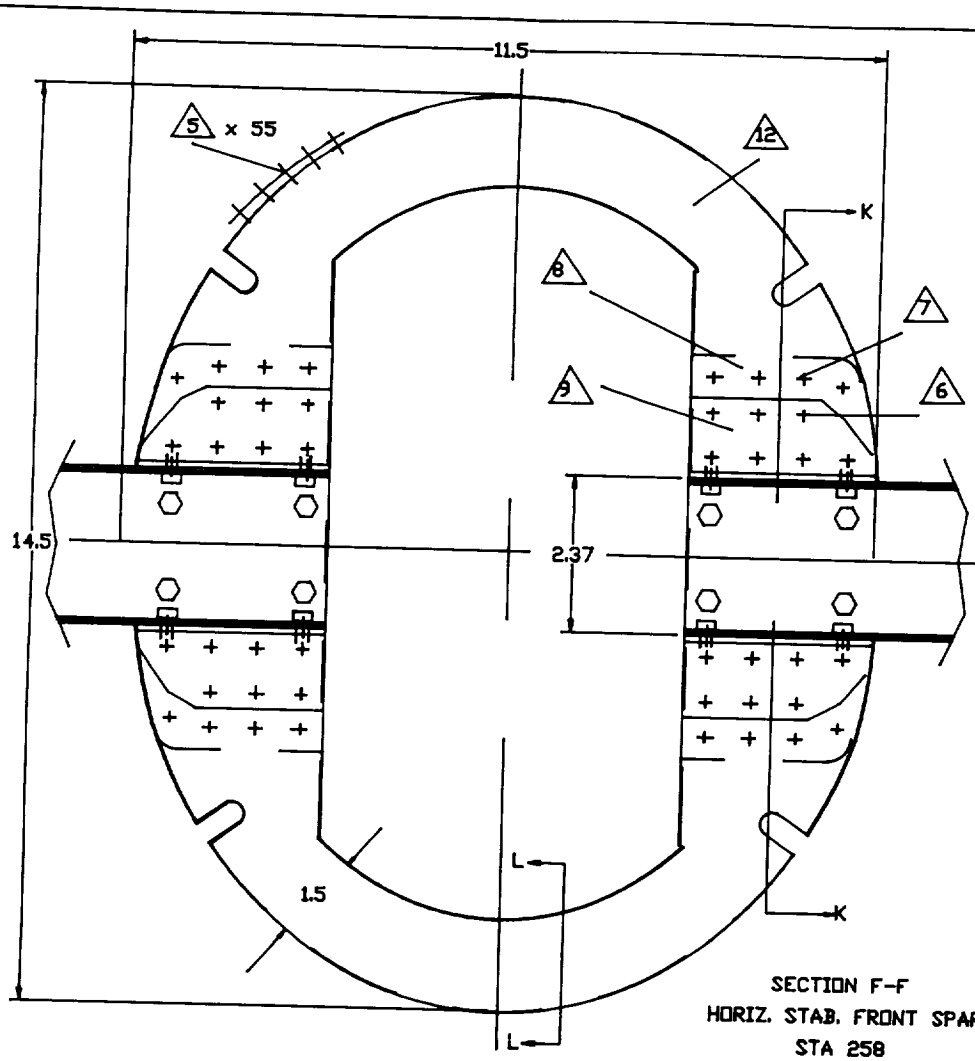

SECTION F-F
HORIZ. STAB. FRONT SPAR
STA 258
(SEE NOTE A)

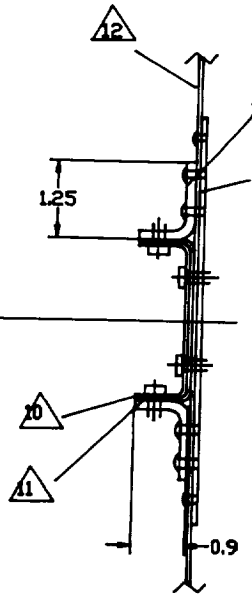

SECTION K-K

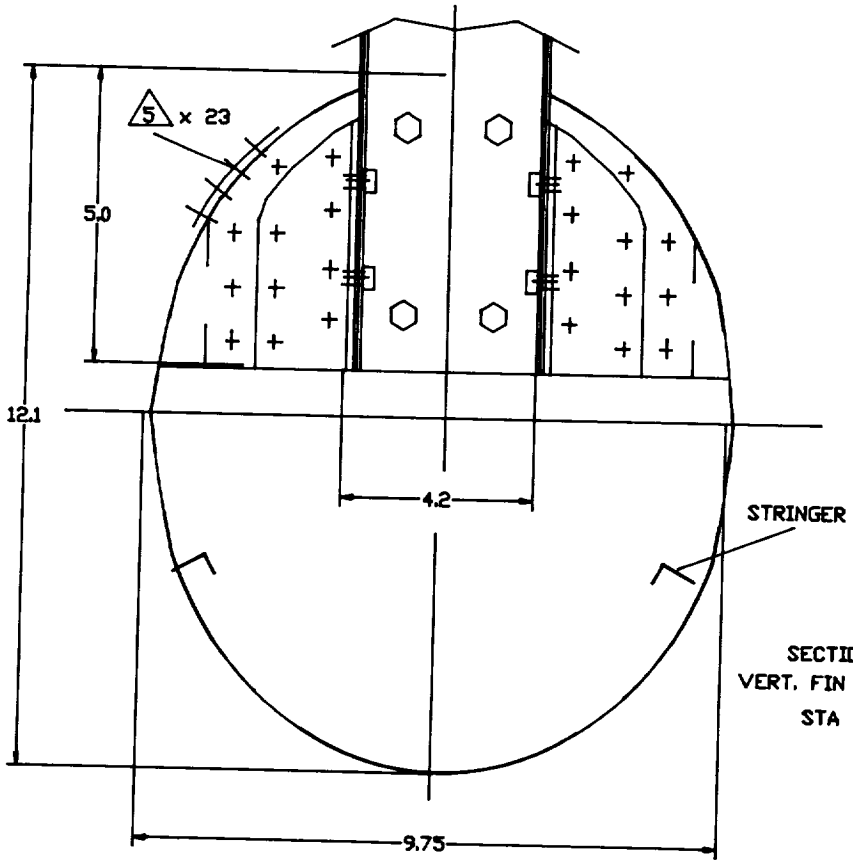

SECTION H-H
VERT. FIN FRONT SPAR
STA 278

SECTION I-I
VERT. FIN REAR SPAR
STA 301

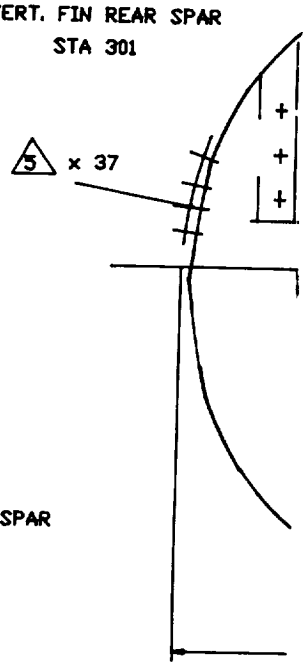

2

FOLDOUT FRAME

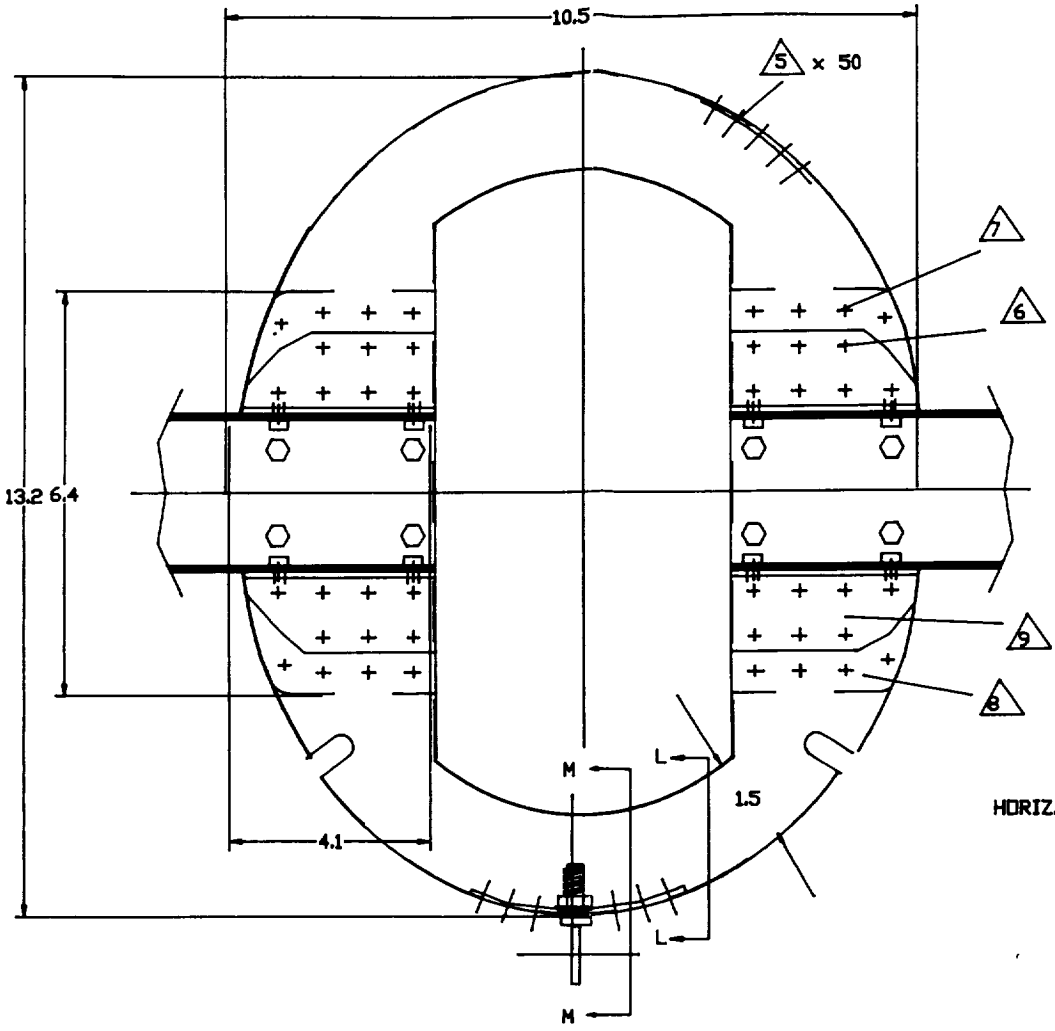

SECTION G-G
HORIZ. STAB. REAR SPAR
STA 268

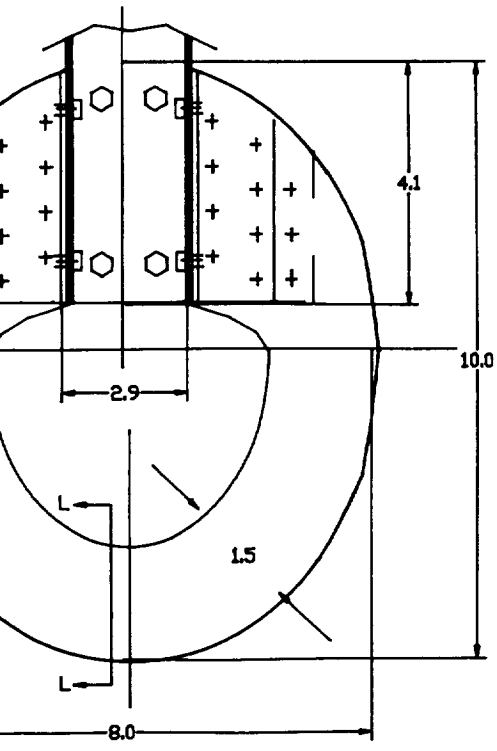

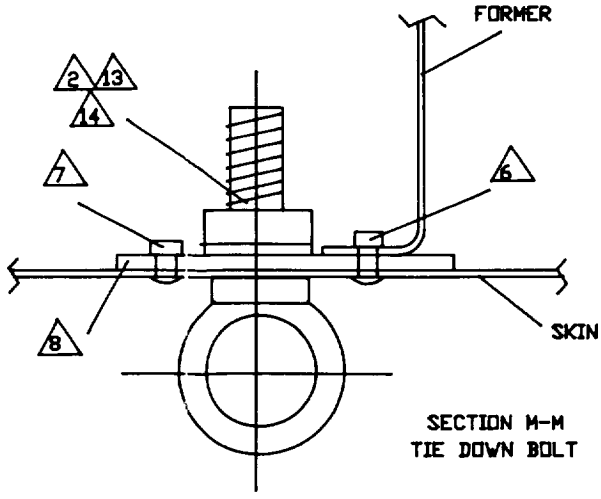

SECTION M-M
TIE DOWN BOLT

NOTE A : SECTIONS F-F AND G-G HAVE THE SAME SPAR DIMENSIONS

DIMENSION TOLERANCES UNLESS OTHERWISE SPECIFIED DECIMAL	EMBRY-RIDDLE AERONAUTICAL UNIVERSITY DAYTONA BEACH FLORIDA			
.XX ± .01	SIZE D	DATE 4/19/93	SCALE 1:10	DRAWN BY G. MEHOLIC
.XXX ± .001	TITLE CONTROL SURFACE INTERFACE FORME			
ANGULAR ± 1/2°	DRAWING NO. 421S9303B206			SHEET 03

FOLDOUT FRAME

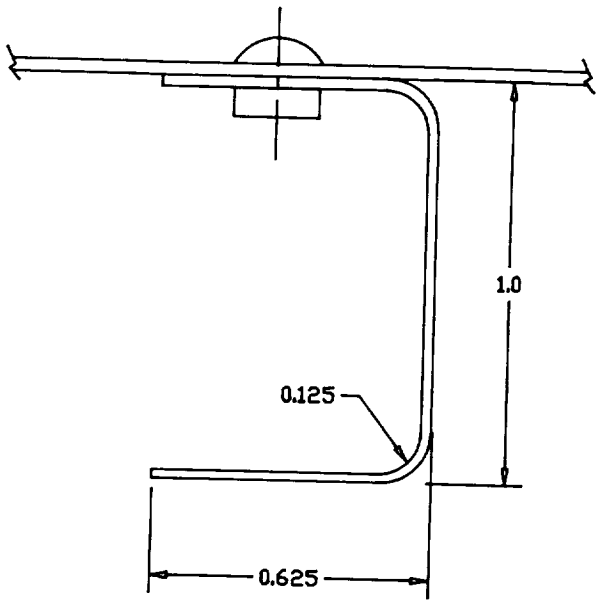

SECTION J-J
CHANNEL-FORMED STRINGER

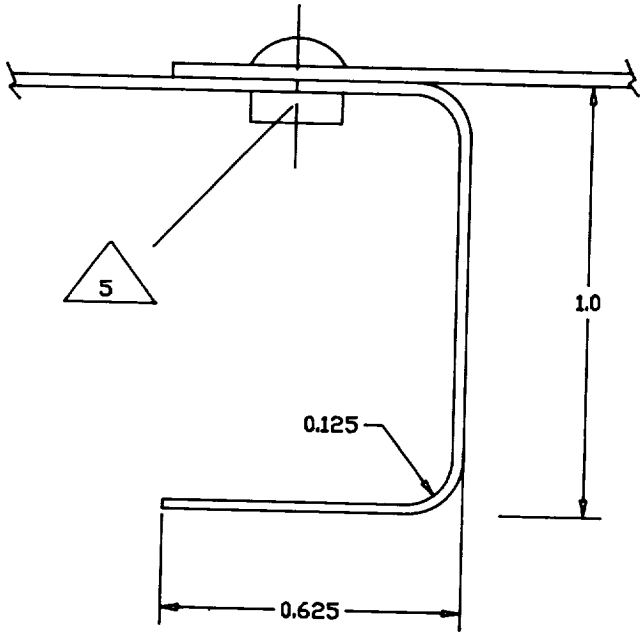

SECTION K-K
SKIN-FORMED STRINGER

2.

FOLDOUT FRAME

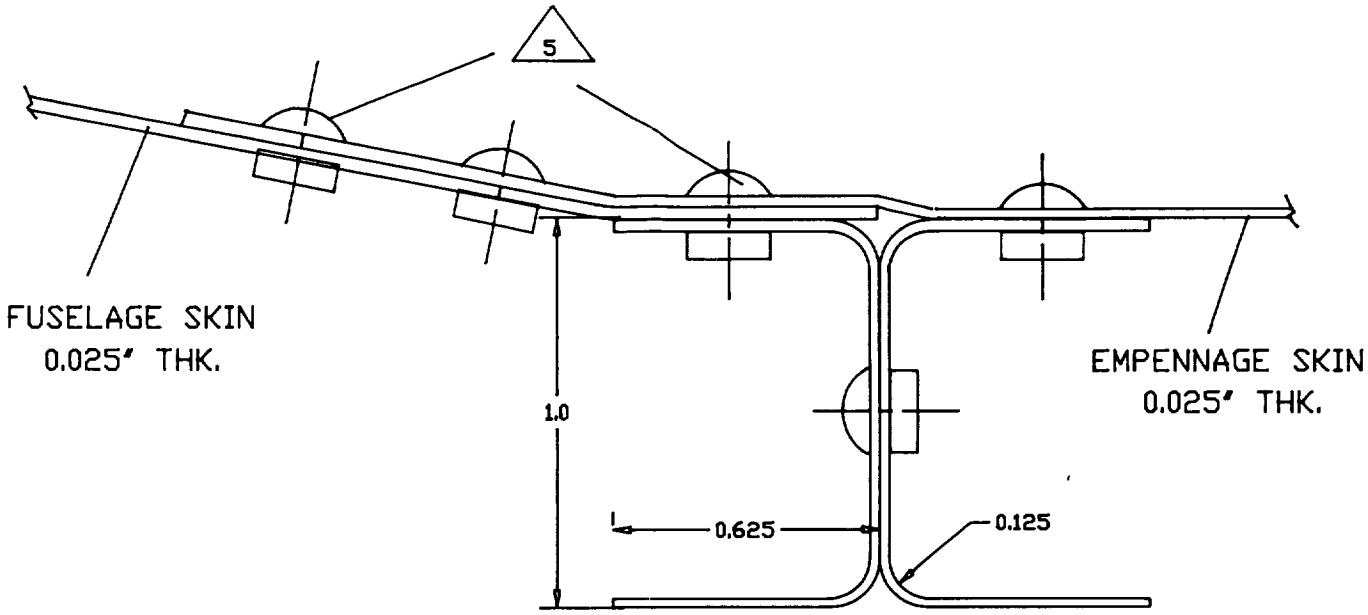

VIEW E-E

FUSELAGE INTERFACE

STA 169

NOTE: ALL MATERIAL IS 0.025" 2024-T3 SHEET.

UNLESS OTHERWISE SPECIFIED	EMBRY-RIDDLE AERONAUTICAL UNIVERSITY DAYTONA BEACH FLORIDA			
.XX ± .01	SIZE D	DATE 4/19/93	SCALE 1:10	DRAWN BY G. MEHOLIC
.XXX ± .001	TITLE STRINGERS AND FUSE INTERFAC			
ANGLES ± 1/2°	DRAWING NO. 421S9303B206			SHEE 04